

**Spontaneous firing rates and anatomical organization of neurons within the
calbindin subnucleus of the hamster suprachiasmatic nucleus**

by

Erin Elizabeth Jobst

A DISSERTATION

Presented to the Department of Physiology and Pharmacology
and the Oregon Health & Science University

School of Medicine

in partial fulfillment of the requirements for the degree of

Doctor of Philosophy

April 2003

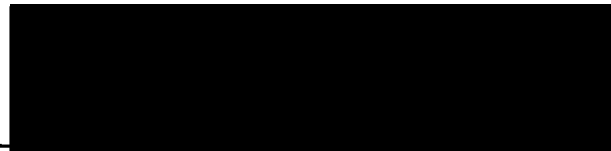
School of Medicine
Oregon Health & Science University

CERTIFICATE OF APPROVAL

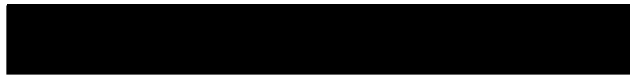
This certifies that the Ph.D. thesis of

Erin Elizabeth Jobst

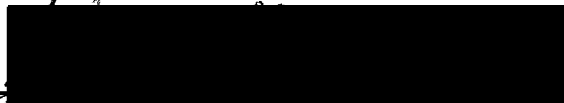
has been approved



Professor in charge of thesis



Member



Member



Member



Member



Member

Table of Contents

List of figures	iii
List of abbreviations	v
Acknowledgments	viii
I. Abstract	1
II. Introduction	3
A. Circadian rhythms: definition, ubiquity and significance	3
B. Suprachiasmatic nucleus (SCN) as the mammalian master circadian clock	6
C. Fundamental elements of circadian timing in mammals	9
D. SCN organization and heterogeneity	13
E. Role of the calbindin subnucleus	18
F. Specific aims addressed in this thesis	21
1. To determine whether CB+ neurons within the CBSn of the hamster SCN fire action potentials in a circadian manner	21
2. To determine the microcircuitry within the CBSn of the hamster SCN which may enable a nonrhythmic population of CB+ neurons to re-establish circadian locomotion	22
III. Results	
A. Manuscript 1: Calbindin neurons in the hamster suprachiasmatic nucleus do not exhibit a circadian variation in spontaneous firing rate	24
1. Abstract	25
2. Introduction	26
3. Materials and Methods	27
4. Results	31
5. Discussion	35

B.	Manuscript 2: Intercellular communication within the calbindin subnucleus of the hamster suprachiasmatic nucleus	40
	1. Abstract	41
	2. Introduction	42
	3. Experimental Procedures	44
	4. Results	51
	5. Discussion	65
IV.	Discussion and Conclusions	75
	A. If CB+ neurons are arrhythmic, how might intercellular connectivity within the CBSn produce a rhythmic behavioral output?	77
	B. Are CB+ neurons in the CBSn truly arrhythmic?	82
	C. What's calbindin got to do with it?	85
V.	Appendix	90
VI.	References	97

List of Figures

II. Introduction

Figure 1. Schematic overview of the mammalian circadian timing system	10
Figure 2. Schematic of anatomical organization of the SCN	16
Figure 3. The calbindin subnuclei within the hamster SCN	20

III. Results

A. Manuscript 1

Figure 1. Colocalization of calbindin and Neurobiotin in an SCN neuron	32
Figure 2. Scatter plots of spontaneous firing rates of individual SCN neurons plotted against zeitgeber time	34
Figure 3. The percentage of silent cells varies with ZT and with CB phenotype	36

B. Manuscript 2

Figure 1. Reconstructions of a representative CB+ and CB- neuron within the CBSn of the hamster SCN	53
Figure 2. Schematic representing the dendritic arbor orientation for individual neurons within the CBSn	54
Figure 3. GABA in the CBSn of the hamster SCN	56
Figure 4. GAD65 within the CBSn of the hamster SCN	57
Figure 5. GABAA receptor (GABAAR) subunits in the hamster SCN	59
Figure 6. GABAAR α 2 and β 2/3 subunits within the CBSn of the hamster SCN	60
Figure 7. TGF α expression within the CBSn of the hamster SCN	61

Figure 8. Double-label immunofluorescence for CB and EGF-R in the hamster SCN	63
Figure 9. Tracer-coupling between identified neurons in the hamster CBSn	64
Figure 10. Connexin 36 expression in the hamster SCN	66
IV. Discussion and Forward Directions	
Figure 1. Schematic of anatomical organization of the hamster SCN	76
V. Appendix	
Unpublished data and data not shown	
Figure 1. CB-immunoreactive neurons in coronal sections of hamster SCN	90
Figure 2. Comparison of mean SFR of CB- and CB+ neurons recorded during the same time epoch and in the same SCN slice	91
Table 1. Comparisons between daytime and nighttime mean SFR for four populations of cells in the hamster SCN	92
Figure 3. Plot showing empirical logits versus ZT epochs for each of two phenotypes	93
Table 2. Odds ratios (based on logistic regression model) calculated at the midpoint of each time epoch	94
Figure 4. TGF α and microtubule associated protein-2 (MAP2) expression in the hamster SCN	95
Figure 5. VPAC ₂ receptor expression in the CBSn of the hamster SCN	96

List of Abbreviations

3V	3 rd ventricle
ACSF	artificial cerebrospinal fluid
AH	anterior hypothalamic area
AVP	arginine vasopressin
BST	bed nuclei stria terminalis
CB	calbindin
CB+	calbindin-immunoreactive
CB-	calbindin-nonimmunoreactive
CBsn	calbindin subnucleus/subnuclei
Cx36	connexin 36
DD	dark:dark
DM	dorsomedial
DMH	dorsomedial nucleus hypothalamus
EGF-R	epidermal growth factor receptor(s)
GABA	γ -aminobutyric acid
GABA _A R	GABA _A receptor
GAD65	glutamate decarboxylase 65
GAD67	glutamate decarboxylase 67
GHT	geniculohypothalamic tract
GRP	gastrin-releasing peptide
IF	immunofluorescent/immunofluorescence

IGL	intergeniculate leaflet
IR	infrared
IHC	immunohistochemistry
ISH	in situ hybridization
LD	light:dark
LS	lateral septal nucleus
MAP2	microtubule associated protein-2
NRSA	National Research Service Award
PB	phosphate buffer
PFA	paraformaldehyde
POA	preoptic area
PSCN	peri-suprachiasmatic area
PT	paratenial nucleus thalamus
PVH	paraventricular nucleus hypothalamus
PVT	paraventricular nucleus thalamus
RHT	retinohypothalamic tract
RT	room temperature
SAD	seasonal affective disorder
SCN	suprachiasmatic nucleus/nuclei
SCN-X	suprachiasmatic nuclei-lesioned
SD	standard deviation
SFR	spontaneous firing rate(s)
sox	supraoptic decussation

sPVZ	subparaventricular zone
TBS	Tris buffered saline
TGF α	transforming growth factor alpha
TTX	tetrodotoxin
VIP	vasoactive intestinal peptide
VPAC ₂	G protein-coupled receptor for VIP
VL	ventrolateral
VTU	ventral tuberal area
ZI	zona incerta
ZT	zeitgeber time

Acknowledgments

I struggle to remember the many people who have helped me over the years, but the list begins here. I thank: Ed McCleskey, for counseling me during a difficult time in my graduate career. Because of him, I did not quit; Charles Allen, my mentor, for providing me the opportunity to perform my graduate research in his laboratory. He gave me the freedom to learn new techniques and to start a new direction for the lab, and he unfailingly did so with a smile; Mary McKenzie, Zac Blackwood and Jonathan Britt, three generations of technicians who provided me with invaluable assistance and comic relief; Michael Andresen, (AKA “black cloud”) for always taking the time to advise, counsel and chide; Stefanie Kaech-Petrie and Bernard Sampo, for many scientific discussions and nonscientific diversions; Aurelie Snyder, confocal wizardess, for providing assistance, knowledge and humor; Michael Lasarev, for patiently educating me about statistics; David Robinson, jack of all trades, for critiquing my scientific writing and subsidizing lunch; without him, I would be a terrible and hungry writer; Dr. Valerie Densmore, for teaching me immunohistochemistry; and, to the CROET staff, for making the day-to-day experiences pleasant.

I would like to especially thank my thesis committee members: Drs. John Williams, Richard Simerly, Michael Andresen and Eliot Spindel for their advice and willingness to guide me through this process. I also wish to thank the IBMS faculty and curriculum for teaching me to be a rigorous thinker. Lastly, I would like to thank Dr. Lane Brown, who has patiently shared this crazy time with me and who actually looks forward to sharing a future lifetime of guaranteed craziness.

Abstract

Many biological functions are maintained with a periodicity of roughly 24 hours and are therefore termed circadian. The role of the suprachiasmatic nuclei (SCN) in generating circadian rhythms in behaviors and other physiological processes is well established. SCN ablation eliminates circadian rhythms, whereas transplantation of fetal SCN tissue into SCN-lesioned arrhythmic hosts restores behavioral circadian rhythmicity. To date, only one *phenotypically* identified type of SCN neuron is thought to be required in fetal SCN grafts for the restoration of circadian behaviors. Within the caudal hamster SCN, approximately 500 neurons containing the calcium binding protein, calbindin-D28K (CB), form a distinct subnucleus (CBsn). The presence of CB-immunoreactive (CB+) neurons is critical in SCN grafts for the restoration of circadian locomotion in SCN-lesioned hamsters (LeSauter and Silver, 1999). The recent identification of a distinct and critical subpopulation of SCN neurons opened the door to allow further investigation into the properties of these neurons.

In the current studies, I have investigated the functional and anatomical properties of neurons within the CBsn. In order to begin recording from these neurons, I defined the spatial coordinates for the CBsn in the coronal SCN slice and preferentially recorded from neurons within these coordinates. Since it is not possible to distinguish visually calbindin-containing neurons, I performed immunohistochemistry to determine the calbindin phenotype of each recorded cell. Using single cell recordings, I found that calbindin-immunoreactive (CB+) neurons within the CBsn surprisingly do *not* exhibit a circadian oscillation in spontaneous firing rate (SFR; Manuscript #1). On the other hand, CB- neurons from this region demonstrated a robust circadian variation in SFR.

Importantly, this study revealed that the CBSn is not a homogeneous population of CB+ cells. In fact, a small percentage of neurons in the CBSn are CB+.

Intercellular communication could be essential in integrating outputs from rhythmic (CB-) neurons and nonrhythmic (CB+) neurons to produce a circadian output in the intact animal. Thus, the second half of my thesis work (Manuscript #2) provides a neuroanatomical framework for the intercellular communication within the CBSn. Using reconstructions of previously recorded neurons, I described CB+ and CB- neuronal morphology, with an emphasis on the length and orientation of neuronal processes. Using double-label confocal microscopy, I highlighted anatomical circuitry within this subregion that may allow for the coordination or synchronization of outputs from neurons with distinct firing rates. First, I showed that CB+ neurons are GABAergic and receive GABAergic input. Second, CB+ neurons are coupled to other CBSn neurons via gap junctions. Lastly, transforming growth factor alpha (TGF α), a substance shown to inhibit locomotion in hamsters (Kramer *et al.*, 2001), is present within neurons and glia in the CBSn. In addition, CBSn neurons express the epidermal growth factor receptor (EGF-R), the only receptor for TGF α .

In summary, I have established that CB+ neurons do not demonstrate a circadian output in spontaneous firing rate. I have also provided a structural framework for synaptic communication, electrical coupling, and neuron-to-neuron or glia-neuron signaling via a growth factor within the CBSn. Although the mechanism by which CB+ neurons restore behavioral rhythmicity is still unknown, my results reveal connections that have the potential for integrating cellular communication within a subregion of the SCN that is critically involved in circadian locomotion.

II. Introduction

A. Circadian rhythms: definition, ubiquity and significance

Circadian rhythms are endogenous, self-sustained rhythms that are maintained with a period of approximately 24 hours. Many life functions, from biochemical reactions to behaviors, display circadian rhythms (Rutter *et al.*, 2002). In constant conditions (i.e. constant darkness), these rhythms ‘free-run’ with a period close to 24 h. However, circadian rhythms can be synchronized (entrained) by environmental cues so as to become exactly 24 h in duration. The most robust environmental cue is light, commonly referred to as a Zeitgeber (“time giver”). In general, circadian rhythms meet three criteria: (1) persistence in constant conditions, (2) phase resetting by light/dark cues and, (3) temperature compensation (Pittendrigh, 1993).

One of the most pervasive influences in evolution is the 24 h light:dark (LD) cycle. Therefore, it is not surprising that the circadian coordination of various life functions is evident in organisms ranging from cyanobacteria to humans. In cyanobacteria, the prokaryotic circadian clock controls all gene expression (Johnson, 2001). In mammals, circadian rhythms are expressed in behaviors (drinking, locomotion and sleep/wake cycle), endocrine functions (secretion of prolactin, melatonin, growth hormone and cortisol) and in other metabolic functions (core body temperature, blood pressure and heart rate). The ubiquity of circadian rhythms implies that the ability to anticipate regular, daily changes in the solar cycle provides a selective advantage to an organism.

Given the ubiquity of a timekeeping mechanism, it is surprising that rigorous examination of the role of the circadian clock in fitness (defined as a measure of

reproductive success) has only recently been performed in two organisms: the cyanobacterium *Synechococcus elongatus* (Ouyang *et al.*, 1998) and the fly *Drosophila melanogaster* (Beaver *et al.*, 2002). In bacteria, reproductive fitness is measured by differential growth of one strain under competition with other strains. Ouyang *et al.* (1998) demonstrated that bacterial colonies in which free-running circadian periods matched the environmental LD cycles out-competed colonies in which the endogenous clocks were not synchronized with the environmental cycle. Although the reasons for the selective advantage are unknown, the authors speculate that bacterial clocks in synchrony with the environment either utilize limiting resources more efficiently or they secrete diffusible factors that inhibit the growth of their unsynchronized counterparts. In *Drosophila*, Beaver *et al.* (2002) demonstrated that null mutations in four genes involved in the fly circadian clock (*clock*, *cycle*, *per* and *tim*) dramatically reduced fertility compared with wild-type flies. In fact, males without *per* or *tim* function had 40% less stored sperm and sired 30-50% fewer progeny than wild-type males. When circadian mutant flies were rescued by wild-type transgenes, both parameters reverted to wild-type levels. These studies provide direct evidence of the selective advantage an endogenous circadian clock has on reproductive success. Thus, early theories that the coordination of physiology and behaviors with an organism's environment has an adaptive value have been supported (Pittendrigh and Minis, 1972; Daan and Aschoff, 1982).

But, are circadian rhythms relevant to *human* health and behaviors? Humans, unlike other mammals, have created a lifestyle that does not often coincide with the solar cycle (i.e. Las Vegas). Our 24-h society has created unique opportunities for the misalignment of endogenous rhythms. Jet lag and accidents occurring during shift work

are two frequently cited examples of the potential adverse health consequences resulting from disharmony between our internal and external clocks. Night-shift workers, who comprise approximately 1 in 5 American workers (Presser, 1999), suffer from sleep disorders, reduced alertness at work, cognitive deficits, increased accidents, gastrointestinal disease, lipid intolerance and increased incidence of cardiovascular disease (U.S. Congress, 1991; Smith *et al.*, 1994; Akerstedt, 1995; Monk, 2000). Mutations or allelic variations in genes involved in the biological clock also result in human circadian disorders. This was poignantly illustrated by the discovery that a mutation in a single clock gene (*hPer2*) causes familial advanced sleep phase syndrome (Toh *et al.*, 2001), an autosomal dominant disorder characterized by a four-hour advance in the daily sleep-wake rhythm. Sufferers tend to fall asleep early in the evening (around 7:30 PM) and awaken quite early (around 4:30 AM), thus making adaptation to a “normal” family life difficult. Though not as definitively proven, it is speculated that clock gene variations might also contribute to symptoms of depression, particularly seasonal affective disorder (SAD; Bunney and Bunney, 2000). This syndrome, characterized by recurrent depression usually occurring every winter, affects over 6% of people in the United States, with a higher incidence in more northern latitudes (like Portland, OR), possibly due to decreased daylight during fall and winter (Rosenthal, 1993).

The organism’s ability to coordinate internal processes and behaviors with the ever-changing phases of the solar cycle is highly conserved. The biological clock may coordinate our internal processes and behaviors more than we previously imagined. Current investigation within the circadian field focuses on the mechanisms by which

endogenous clocks generate rhythms, entrain to the local environment and eventually, transmit timing information to the rest of the body. Understanding circadian rhythms has provided relatively simple, low-cost interventions for human disorders (i.e. phototherapy for depression and melatonin for the entrainment of blind humans). As our knowledge progresses, we can use this information to improve our mood, productivity and safety, which may even contribute to world peace.

B. Suprachiasmatic nucleus as the mammalian master circadian clock

In mammals, the master circadian clock is housed in the suprachiasmatic nuclei (SCN), two pear-shaped structures at the base of the ventral hypothalamus, on either side of the third ventricle, directly adjacent to the optic chiasm (Paxinos and Watson, 1996; Morin and Wood, 2001). The pacemaker role of the SCN has been well established. Ablation of the SCN eliminates behavioral, physiological and endocrinological circadian rhythms (Moore and Eichler, 1972; Stephan and Zucker, 1972; Rusak and Zucker, 1979). Transplantation of fetal anterior hypothalamic tissue containing the SCN into SCN-lesioned (SCN-X) recipients restores circadian behavior to arrhythmic hosts (Lehman *et al.*, 1987; LeSauter and Silver, 1998; Sollars and Pickard, 1998; Meyer-Bernstein *et al.*, 1999). In 1990, Ralph *et al.* Performed what may be considered definitive experiments establishing that *donor* SCN tissue dictates the resultant circadian rhythm of the host. Using the tau hamster, a hamster strain demonstrating a short circadian period (homozygote circadian period ≈ 20 h; Ralph and Menaker, 1988), they transplanted SCN grafts into arrhythmic SCN-X wild-type hamsters (circadian period ≈ 24 hr). The reverse experiment of implanting wild-type hamster SCN tissue into SCN-X tau hamsters was also performed. Regardless of the direction of the transplant or genotype of the host, the

restored rhythms always exhibited the period of the donor genotype. These experiments established that SCN cells are not only uniquely capable of generating circadian rhythms, but that this property can be specifically transmitted to SCN-X hosts. It is worth restating here that SCN transplants restore *behavioral* circadian rhythms. Endocrinological rhythms have never been restored after SCN ablation, supporting the hypothesis that the mechanisms mediating behavioral and endocrinological rhythms are different (Kalsbeek and Buijs, 2002).

The SCN not only drives the expression of physiological and behavioral circadian rhythms, but circadian rhythms are also present within the SCN itself. The SCN shows circadian rhythms in glucose utilization (Schwartz and Gainer, 1977; Schwartz *et al.*, 1980) and electrical activity. Studies of ensemble neuronal firing, as well as single unit firing, demonstrate a characteristic circadian oscillation in action potential firing frequency, with a peak near midday, *in vivo* (Yamazaki *et al.*, 1998) and *in vitro* in the hypothalamic slice (Inouye and Kawamura, 1979; Green and Gillette, 1982; Groos and Hendriks, 1982; Shibata *et al.*, 1982). Strong evidence that *individual* SCN neurons are competent pacemakers came from a set of seminal experiments performed in 1995 by Welsh *et al.* In recordings from cultured rat SCN neurons on fixed microelectrode arrays, they demonstrated that single SCN neurons displayed circadian rhythms in spontaneous firing rates (SFR). In addition, SCN neurons within the same culture expressed *independent* circadian rhythms in SFR. Notably, the SFR of SCN neurons were not synchronized, despite the presence of functional synapses. In fact, neurons had periods ranging from 21-26 hours, and neurons that were adjacent to each other often had firing peaks that were up to 12 h apart. The SFR of cultured SCN neurons was blocked by

tetrodotoxin (TTX) for 2.5 days, but upon removal of TTX, SFR re-emerged with the same phase observed before blockade. Using the same culture system in circadian mutant hamsters and mice, others have shown that genetic alterations determining circadian period are expressed in single SCN cells (Liu *et al.*, 1997; Herzog *et al.*, 1998).

The results of these experiments have heralded three conclusions regarding SCN function: (1) the circadian properties of the SCN are not dependent on the oscillatory properties of a complex circuit; rather, the SCN is composed of neurons which are independent circadian oscillators, (2) functional synapses are not necessary for neuronal oscillation *in vitro*, and (3) synapses may not be sufficient for synchronizing individual SCN neurons in culture (although Honma *et al.*, 2000, determined that synaptic transmission was able to synchronize neurons). Welsh *et al.*'s studies clearly discriminated rhythm generation and synchronization at the level of the cellular circadian clock. Much of the current investigation in the circadian field concentrates on expanding on the conclusions derived from these critical studies. For example, my own work addresses the questions: Are all SCN neurons equally competent clocks? How are individual SCN neurons coupled to each other to produce a single distinct physiological or behavioral output?

I have described the SCN as the *master* circadian clock in mammals. This is a deliberate designation, given a growing body of evidence for extra-SCN oscillators (Honma *et al.*, 1992; Mistlberger, 1994; Herzog and Tosini, 2001). Although this was not the focus of my research, it is important to distinguish clearly the SCN from other tissue oscillators. Using a transgenic rat with the reporter bioluminescent enzyme, luciferase, under the control of the mouse *Per1* promoter, Yamazaki *et al.* demonstrated that several

mammalian tissues display circadian rhythmicity (2000). As expected, the SCN demonstrated circadian rhythms in reporter gene activity. In addition, the lungs, liver, kidneys and skeletal muscle showed circadian rhythms in reporter gene activity. However, two features distinguish non-SCN rhythms from those of SCN rhythms. First, rhythmicity in non-SCN tissue dampens after less than 7 cycles, whereas the SCN rhythm continues for at least 32 days. (In fact, at the Society for Research on Biological Rhythms conference in May 2002, Yamazaki *et al.* reported that SCN *per1*-luciferase rhythmicity continues to cycle after more than one year!). Second, non-SCN rhythms are delayed by 3-9 h relative to the SCN rhythm. It is becoming clear that the SCN represents the top of the rhythm-generating hierarchy in the mammalian brain, coordinating the timing of other oscillators within the brain and the body.

C. Fundamental elements of circadian timing in mammals

The essential features of circadian rhythms are: (1) the presence of a pacemaker, (2) a mechanism to entrain the pacemaker to the solar cycle and, (3) communication from the pacemaker to effector systems that express rhythmicity. Figure 1 (Introduction) schematically outlines the basic elements of the mammalian circadian pacemaker.

In all organisms, time-keeping arises at the cellular level (Figure 1A Introduction), with a complex set of interlocking positive and negative transcription-translation feedback loops. Conserved “clock genes” rhythmically transcribe and translate proteins that feed back to inhibit rhythmically their own transcription. The fundamental components of the molecular clock are basic helix-loop-helix/PAS (Period-Arnt-Single-minded)-containing transcription factors. PAS domains are critical in the intracellular clock mechanism of fungi, insects and mammals (Dunlap, 1999). Although the most

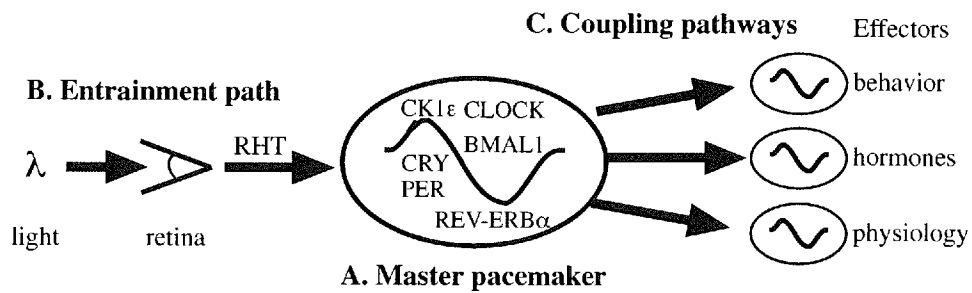


Fig 1. Schematic overview of the mammalian circadian timing system. (A) Master pacemaker. The suprachiasmatic nuclei (SCN) house the master clock in mammals. In most SCN neurons, endogenous oscillations are created by positive and negative feedback loops of clock gene transcription and translation. (B) Entrainment path. A subset of retinal ganglion neurons receive light and transmit information, via the retinohypothalamic tract (RHT) to select neurons in the SCN. This pathway mediates phase shifts at cellular and behavioral levels. (C) Coupling pathways. Endogenous rhythmic oscillations generated from the SCN are transmitted via anatomical connections and/or diffusible factors to the rest of the body to impart rhythms in physiology and behavior.

complete molecular analysis of the circadian clock mechanism has been done in *Drosophila*, homologues of most genes involved in the fly clock have been cloned in mammals. The molecular mechanisms of the mammalian clock are beginning to be rapidly unraveled.

The following is a brief summary describing the current understanding of the timing mechanism in mammals (Reppert and Weaver, 2002). In SCN neurons (and other rhythmic cells), CLOCK and BMAL1 form heterodimers that activate the rhythmic transcription of three period genes (*Per1-3*), two cryptochrome genes (*Cry1* and *Cry2*) and *Rev-Erb α* . In the cytoplasm, PER binds to CRY and casein kinase I ϵ (CKI ϵ), where the whole protein complex is phosphorylated. The phosphorylated PER/CRY/CKI ϵ complex translocates to the nucleus and binds to CLOCK-BMAL1 heterodimers. CRY proteins from the complex interact with CLOCK-BMAL1 to inhibit their transcription. In addition, CRY and PER proteins inhibit their own transcription, thus closing the negative limb of the feedback loop. The positive limb of the feedback loop is formed by BMAL1 and REV-ERB α . After CLOCK-BMAL1 activates Rev-Erb α transcription, REV-ERB α levels increase and REV-ERB α binds to the *Bmal1* promoter to inhibit its transcription. As *Bmal1* RNA levels fall, *Per* and *Cry* RNA levels rise. CRY proteins enter the nucleus and inhibit *Per*, *Cry* and *Rev-Erb α* transcription. The result of the latter is activation (by “de-repression”) of *Bmal1* transcription. In summary, CLOCK, BMAL1 and REV-ERB α form the positive limb, while CRY and PER form the negative limb of this autoregulatory feedback loop. Inherent in this outline is the necessity for a 24 h time-delay within the feedback loop. It is currently thought that patterns in RNA abundance, phosphorylation, and subcellular localization are built into this chain of events so that the loop takes 24 h

to complete (Lakin-Thomas, 2000). The exact nature and kinetics of these interactions have yet to be elucidated.

Because endogenous circadian rhythms are usually slightly longer or shorter than 24 h, the circadian clock must be regularly entrained to a 24-h day (Figure 1B Introduction). Entrainment is primarily mediated by light input. Light pulses presented during the early night phase delay the clock whereas light pulses presented during the late night phase advance the clock. Light pulses presented during the day produce no phase shift of the clock (Gillette and Tischkau, 1999). The result is stable timing shifts in behavioral and physiological rhythms on the following days. In mammals, this is accomplished by light activation of a specific subset of retinal cells conveyed directly via the retinohypothalamic tract (RHT) and also indirectly via the geniculohypothalamic tract to the SCN. Electrophysiological studies strongly suggest that synaptic transmission between the RHT and SCN neurons is mediated by NMDA and non-NMDA glutamate receptors (Kim and Dudek, 1993). The precise path from channel activation to molecular response in SCN neurons has not been identified. However, acute responses to light stimuli include induction of immediate early genes (i.e. *c-fos*) as well as genes associated with the cellular clock (i.e. *Per1* and *Per2*) in *some* SCN neurons at the same phases of the circadian cycle at which light can phase shift the circadian pacemaker (Kornhauser *et al.*, 1990; Meijer *et al.*, 1992; Hamada *et al.*, 2001). More recently, interest has shifted to understanding the role of heterogeneity in light responses among SCN neurons (Hamada *et al.*, 2001; Introduction, Section D).

A series of molecular events in SCN neurons results in rhythmic electrical activity (by mechanisms only beginning to be understood; Kuhlman *et al.*, 2003). These rhythms

can also be shifted by environmental cues (Figure 1B Introduction). Ultimately, rhythmic SCN electrical activity converts endogenously generated oscillations within clock neurons to overt rhythmic outputs (Figure 1C Introduction). How this cascade of events results in behavioral and physiological rhythms is one of the biggest missing links in the circadian field. However, it is clear that there is not a single output pathway from the SCN to all effectors. While precise anatomical connections to effectors are required for the expression of *endocrinological* rhythms such as cortisol and melatonin release (Lehman *et al.*, 1987; Meyer-Bernstein *et al.*, 1999; Kalsbeek and Buijs, 2002), diffusible substances (as yet unidentified) may be sufficient for the expression of certain circadian *behaviors*, such as locomotor activity (Silver *et al.*, 1996a; LeSauter and Silver, 1999).

D. SCN organization and heterogeneity

The SCN is composed of a heterogeneous population of approximately 16,000-20,000 neurons (van den Pol, 1980, rat; Abrahamson and Moore, 2001, mouse). Since most SCN neurons contain the inhibitory neurotransmitter, γ -aminobutyric acid (GABA; Okamura *et al.*, 1989; Moore and Speh, 1993), early descriptions of the anatomical organization within the nucleus were based on the topographic distribution of neuropeptides. In most mammalian species, the tightly-packed neurons within the dorsomedial (DM) subdivision primarily express arginine vasopressin (AVP), while the more dispersed neurons within the ventrolateral (VL) subdivision express vasoactive intestinal peptide (VIP) and/or gastrin-releasing peptide (GRP; Card and Moore, 1984, hamster; van den Pol and Tsujimoto, 1985, rat). Although this classification is commonly used, the topographic distribution of neuropeptides within the SCN may vary depending on species. For example, in the mouse SCN, AVP-immunoreactive neurons are present in

the DM, as well as the VL subdivision (Abrahamson and Moore, 2001). Likewise, in the human SCN, VIP-immunoreactive neurons are located in a central region rather than in a VL subdivision (Mai *et al.*, 1991).

To allow for comparisons across mammalian species, different designations, that of core and shell, have recently been used to describe two SCN subdivisions (Moore, 1996). To a large extent, neurons within the core and the shell tend to overlap with the previously designated VL and DM subdivisions, respectively. However, the core and shell are distinguished not only by neuropeptide phenotype, but also by neural afferent and efferent projections (Moore, 1996; Moore and Silver, 1998; Leak and Moore, 2001). The core receives visual input directly from the retina (via the RHT; Johnson *et al.*, 1988; Abrahamson and Moore, 2001) as well as indirectly from the intergeniculate leaflet (IGL) of the thalamus (via the geniculohypothalamic tract; GHT; Moore and Card, 1994). The core also receives serotonergic input from nuclei of the midbrain raphe (Ueda *et al.*, 1983; Moga and Moore, 1997). In contrast, the shell receives broad nonphotic input from hypothalamic nuclei (at least eleven), the limbic cortex, basal forebrain and the brainstem (Moga and Moore, 1997). Although earlier studies indicated that efferent projections arise as a single group from all SCN neurons (Watts and Swanson, 1987), projections from the core and shell also have a unique topography (Kalsbeek *et al.*, 1993; Leak and Moore, 2001). In general, the shell demonstrates more widespread projections to other hypothalamic and thalamic nuclei than the core. The densest projection from both regions is to the subparaventricular zone (sPVZ) of the hypothalamus, a region dorsal to the SCN (Watts and Swanson, 1987). Within this main SCN target area, SCN projections are also segregated; the core projects primarily to the lateral sPVZ and the shell projects primarily

to the medial sPVZ (Abrahamson and Moore, 2001; Leak and Moore, 2001). Reciprocal connections between the core and the shell exist, but the projections from the core to the shell are more predominant (Daikoku *et al.*, 1992; Leak *et al.*, 1999). Figure 2 (Introduction) schematically illustrates the core-shell organization of the SCN.

Neurons within the subdivisions also have functionally distinct characteristics with respect to levels of neuropeptide expression, clock gene activation and patterns of spontaneous firing. Generally, neurons in the VL subdivision have light-dependent rhythmicity (consistent with heavy retinal input to this region). Neurons in the DM subdivision have light-independent rhythmicity. For example, levels of AVP expression in DM neurons demonstrate a light-independent circadian variation (Schwartz *et al.* 1983; Schwartz and Reppert 1985), but levels of VIP, a neuropeptide in the VL region, have a light-dependent rhythm (Takahashi *et al.*, 1989; Inouye and Shibata, 1994).

Likewise, the induction of immediate early genes (i.e. *c-fos*) and several clock genes (Introduction, Section B) is regionally restricted to subpopulations of SCN neurons (Aronin *et al.*, 1990; Rusak *et al.*, 1990). In 1997, Shigeyoshi *et al.* demonstrated that expression of *mPer1* in DM neurons shows a light-independent rhythm, while expression in VL neurons demonstrates light-inducible characteristics. In mouse SCN, they found that acute light pulses during the early subjective night caused a nonuniform increase in *mPer1* expression throughout the SCN. Induced *mPer1* expression was largely confined to the VL SCN, with no significantly elevated expression in the DM region. Not only was induction of *mPer1* restricted to the VL neurons, but the induction level in adjacent cells was also varied. This was one of the first hints suggesting that the clock might be

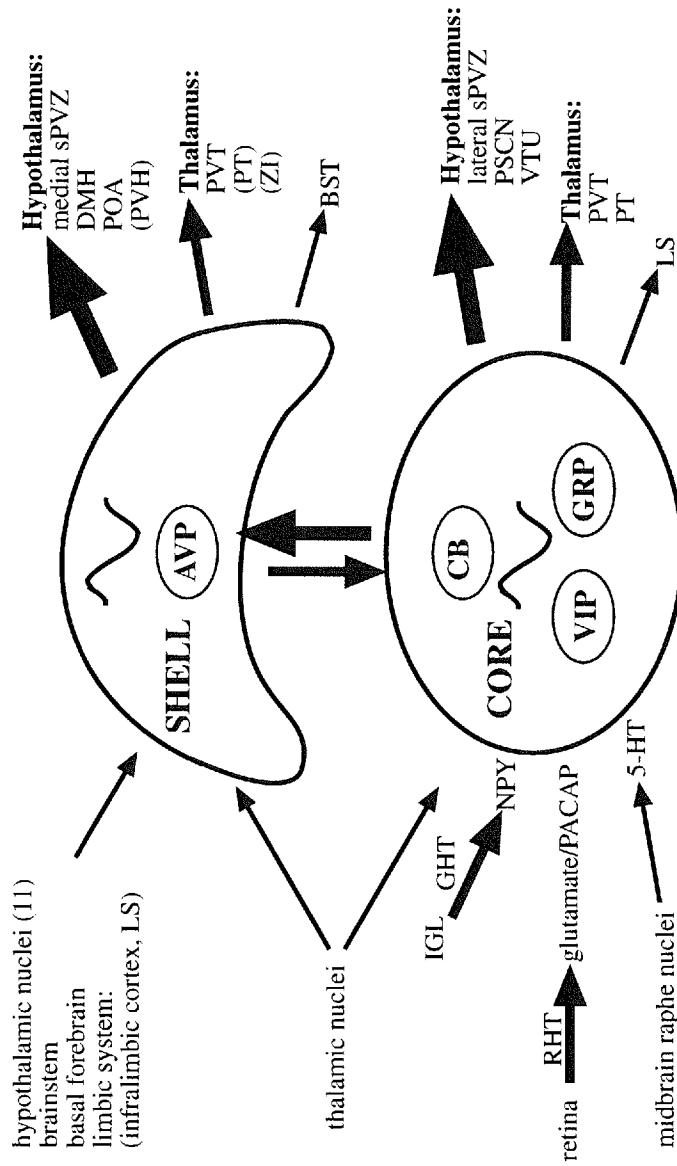


Fig 2. Schematic of anatomical organization of the SCN. This core-shell model is largely based on scheme of the rat SCN by Moore and colleagues (Moga and Moore, 1997; Leak *et al*, 1999; Leak and Moore, 2001).

reset to varying degrees in individual neurons *within* a subdivision, an idea that my research focused on and that I will expand upon in the next section.

One of the most conspicuous features of SCN neurons is a circadian rhythm in spontaneous firing rate. Whether examined by single-unit or multi-unit recordings *in vivo* or *in vitro*, the SFR of *most* SCN neurons peaks during the midday and troughs during the night (Inouye and Kawamura, 1979; Green and Gillette, 1982; Groos and Hendriks, 1982; Yamazaki *et al.*, 1998; Saeb-Parsy and Dyball, 2003). However, recent studies have highlighted the heterogeneity among SCN neurons with respect to electrical activity. Only approximately 50% to 75% of individual SCN neurons exhibit rhythmic action potential firing (Herzog *et al.*, 1997, 1998; Honma *et al.*, 1998; Liu and Reppert, 2000). Variation in electrical rhythmicity correlates with SCN anatomy. In organotypic slice cultures, 87% of neurons in the dorsal SCN fire in a circadian rhythm, while only 62% of neurons in the ventral SCN had rhythmic firing rates (Nakamura *et al.*, 2001). This decrease in electrical rhythmicity is consistent with the lack of endogenous rhythmicity in neuropeptide expression and in some clock genes in the VL subdivision (core) of the SCN.

Although evidence supports anatomical and functional differences between two broad SCN subdivisions, recognition of local subregions within these groupings is emerging. The overall goal of my research was to test whether the essential heterogeneity of the SCN exists within a defined subregion of the core subdivision of the hamster SCN.

E. Role of the calbindin subnucleus

Early lesion literature established that complete ablation of the SCN eliminated circadian rhythms. The regional extent of these lesions within the SCN was often not verified, but circadian rhythmicity persisted if as little as 25% of the SCN remained (Davis and Gorski, 1988). These results were generally interpreted to mean that there was a redundancy among SCN neurons, at least with respect to pacemaker ability. Contrary to these results, recent studies in the hamster SCN have demonstrated that small, partial lesions (representing significantly less than 75% of the SCN) led to a loss of behavioral circadian rhythmicity (LeSauter and Silver 1999; Kriegsfeld *et al.*, 2000). These lesions included a subnucleus of neurons immunoreactive for calbindin-D28K (CB). Restoration of rhythmicity appeared to be dependent upon the presence of calbindin-immunoreactive (CB+) neurons. In addition, the *strength* of rhythmicity correlated with the number of CB+ cells within the grafts (LeSauter and Silver, 1999). To date, CB+ neurons are the only *phenotypically* identified SCN neuron known to be required in fetal SCN grafts for the restoration of behavioral circadian rhythmicity.

These studies have led to two hypotheses regarding (hamster) SCN function. The first is that a small subregion of the SCN, the CB subnucleus (CBsn), is critical to the maintenance and restoration of circadian activity. Second, since fetal SCN tissue was placed within polymer-encapsulated grafts which prevented efferent outgrowth from the SCN tissue graft, rhythmicity is most likely restored via a diffusible signal(s), (Silver *et al.*, 1996a).

In the hamster, roughly 500 CB+ neurons (250 in each SCN) form bilateral subnuclei (CBsn) in the caudal portion of the SCN (Silver *et al.*, 1996b; Figure 3,

Introduction). The calbindin-D28K protein is found in select central neuronal populations within the brain and binds calcium selectively with high affinity (Celio, 1990; Leathers *et al.*, 1990; Baimbridge *et al.*, 1992). The CBSn are within the VL or core subdivision of the hamster SCN (Moore and Silver, 1998). CB+ cells receive direct, dense retinohypothalamic projections (Bryant, *et al.*, 2000). In addition, almost 80% of CB+ neurons express light-induced Fos protein at the same phases of the circadian cycle at which light can phase shift the circadian pacemaker (Kornhauser *et al.*, 1990; Meijer *et al.*, 1992). This suggests that this subpopulation of cells may participate in light entrainment of circadian rhythms.

At the time I began my research, the efferent projections of CB+ neurons were unknown. Since then, collective evidence suggests that CB+ neurons within the CBSn are intra-SCN neurons (LeSauter *et al.*, 2002; Jobst *et al.*, *Neuroscience* submission, 2003). This is in contrast to reports that core SCN neurons project outside the SCN (Leak and Moore, 2001). It is appropriate to mention here that the SCN of other species contain clusters of CB+ neurons (Mai *et al.*, human, 1991; Arvanitogiannis *et al.*, rat, 2000; Abrahamson and Moore, mouse, 2001). However, clusters of CB+ neurons in other species are not as compact as the hamster CBSn. In addition, the functional properties of CB+ neurons within the SCN of other species have not been investigated.

For many years, there was significant debate whether efferent synaptic connections from SCN grafts to the host brain were required for recovery of circadian activity (LeSauter and Silver, 1998; Sollars and Pickard, 1998). Localization of graft efferents by labeling for SCN-specific peptides revealed that the extent of peptidergic innervation of

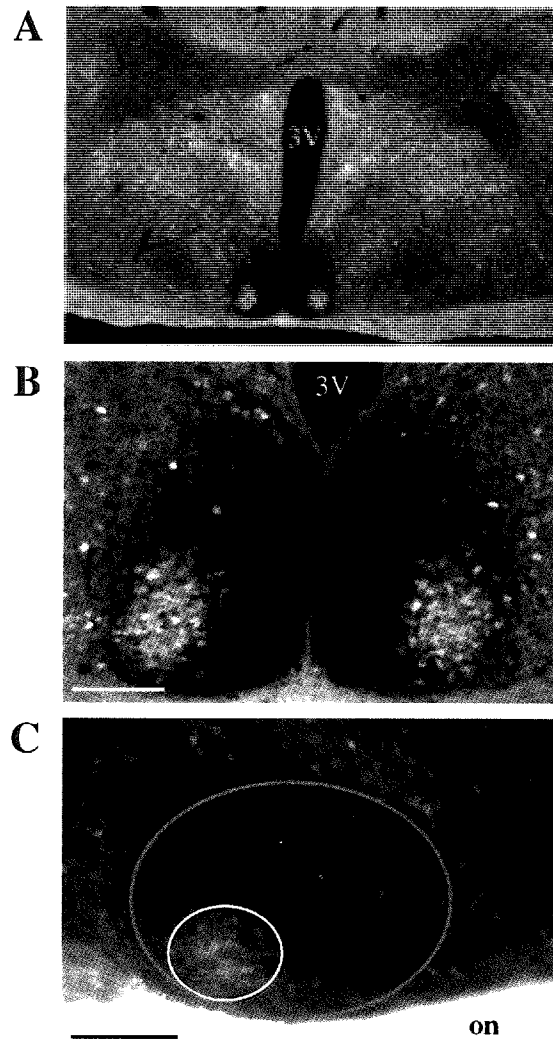


Fig 3. The calbindin subnuclei within the hamster SCN. 40 μm vibratome sections are from 6 week-old hamster perfused at ZT11. Antibodies: mouse anti-calbindin (1:8,000; Swant, Bellinzona, Switzerland); donkey anti-mouse AlexaFluor 488 (1:750; Molecular Probes, OR, USA). Images were taken on Leica DMIRBE inverted wide field epifluorescence microscope with appropriate fluorescent filter cubes. (A, B) Coronal sections. The SCN are contained within the cell-dense darkened areas on either side of the 3V. CB-immunoreactive neurons are clustered in the ventrolateral (or core) subdivision. (C) Sagittal section. Optic nerve (on) lies on bottom part of image, with the rostral SCN towards the right. Note the relative caudal position of the CBsn (white circle) within the SCN (red circle). The CBsn extend approximately 200 μm in the sagittal plane. Scale bars = 200 μm , (A); 100 μm , (B); 200 μm , (C).

host tissue varied remarkably among animals (DeCoursey and Buggy, 1989; Silver *et al.*, 1990; Li and Satinoff, 1998). However, extensive *intra-graft* peptidergic connections have been noted in all studies (Sollars and Pickard, 1998), suggesting the SCN may utilize synaptic connections *within* the graft to communicate to unidentified SCN efferents that project to the host tissue. Although the presence of the CBSn as a distinct SCN subregion is recognized as critical to the circadian rhythms of some behaviors, the nature of communication (synaptic and nonsynaptic) within and from the CBSn was entirely unknown when I began my research. The overall objective of my research has been to investigate the spontaneous electrical activity of CB+ neurons and to outline the intercellular communication between CB+ and CB- neurons within the CBSn of the hamster SCN.

F. Specific Aims addressed in this thesis

(1) To determine whether CB+ neurons within the CBSn of the hamster SCN fire action potentials in a circadian manner

Evidence suggests that CB+ neurons within the anatomically defined CBSn are a critical locus of rhythmicity in the SCN (Silver *et al.*, 1996a; LeSauter and Silver, 1999). In nocturnal rodents, SCN neurons *in vivo* and *in vitro* exhibit a circadian oscillation in firing rate, which peaks near midday. These data were obtained from single or multi-unit recordings of *unidentified* SCN neurons. Specifically, it is unknown whether CB+ neurons in the hamster CBSn exhibit a circadian variation in SFR as part of their output signal. Sodium-dependent action potentials are required for circadian drinking patterns in rats (Schwartz *et al.*, 1987; Schwartz, 1991). TTX is a blocker of sodium-dependent

action potentials. Two weeks of TTX infusion into the SCN disrupted circadian drinking rhythms *in vivo*. After halting treatment, free-running rhythms re-emerged at a phase that indicated that the pacemaker continued to function during the period of TTX administration (Schwartz *et al.*, 1987; Schwartz, 1991). Thus, rhythmic electrical activity (generated by endogenous oscillations within clock neurons) appears necessary for a rhythmic behavioral output. Similarly, since CB+ neurons are responsible for circadian locomotion, it would be expected that they fire action potentials in a circadian manner.

The null hypothesis is that CB+ neurons demonstrate a circadian oscillation in SFR, comparable to unidentified SCN neurons and consistent with their role in restoring a circadian behavior. The alternate possibility is that the SFR of CB+ neurons differs from that of previously sampled SCN neurons. The rationale is that the small number of CB+ cells in the hamster CBsn (250 in a single SCN) may not have been previously sampled, or may not have affected the average firing frequency at any single circadian time point. Manuscript 1 (Jobst and Allen, 2002) provides evidence that CB+ neurons do *not* display a circadian variation in SFR, thus rejecting the null hypothesis. Manuscript 1 discusses this surprising result, and places it within the context of new data from another lab (Hamada *et al.*, 2001) about the endogenous rhythmicity of this *functionally* distinct subpopulation of neurons.

(2) To determine the microcircuitry within the CBsn of the hamster SCN which may enable a nonrhythmic population of CB+ neurons to re-establish circadian locomotion

Although lesion experiments suggested that CB+ neurons within the CBsn were a critical “seat of pacemaking” in the SCN, accumulated data from others (Hamada *et al.*,

2001) and from my own work (Jobst and Allen, 2002) have shown that CB+ neurons are not rhythmic oscillators. Thus, an apparent paradox exists of how a nonrhythmic population of CB+ neurons is responsible for restoring a rhythmic behavior.

There are at least two distinct hypotheses to reconcile this paradox. The first is the “red herring” hypothesis: CB+ neurons are not rhythmic oscillators and their presence in fetal SCN transplants was tightly associated with another group of cells (CB-) whose presence was necessary for re-establishing circadian behaviors. A second hypothesis is that intercellular communication between CB+ and CB- neurons within the CBSn *in vivo* (or in a different slice preparation, see Discussion) is required for a circadian behavioral output.

Because SCN neurons have SFR rhythms with distinct periods from each other (Welsh *et al.*, 1995; Liu *et al.*, 1997; Herzog *et al.*, 1998; Honma *et al.*, 1998; Abe *et al.*, 2000), it is implicitly assumed that these multiple oscillators within the SCN must be integrated to produce a single circadian output in the intact animal. A lingering uncertainty in the circadian field is the nature of the intercellular mechanism(s) for synchronizing rhythms among SCN neurons. Many mechanisms, both synaptic and nonsynaptic, have been proposed to synchronize SCN neurons (van den Pol and Dudek, 1993). Manuscript 2 examines the anatomical basis of intercellular communication within the CBSn: the organization of axonal and dendritic projections; the presence of GABAergic synaptic communication; gap junctions; and, potential growth-factor mediated glial-neuronal interactions. Manuscript 2 discusses the potential role each mechanism may play in coordinating the output of neurons within the CBSn of the SCN.

III. Results

A. Manuscript 1

Calbindin neurons in the hamster suprachiasmatic nucleus do not exhibit a circadian variation in spontaneous firing rate

Erin E. Jobst and Charles N. Allen

Department of Physiology and Pharmacology and Center for Research on Occupational and Environmental Toxicology, Oregon Health & Science University,
3181 SW Sam Jackson Park Road, Portland, OR 97239, USA.

European Journal of Neuroscience, Vol 16(12), pp 2469-2474, 2002

ABSTRACT

The role of the mammalian suprachiasmatic nuclei (SCN) in generating circadian rhythms in behaviors and other physiological processes is well established. A prominent feature of SCN neurons is the circadian oscillation in action potential firing frequency, with a peak near midday. A subset of calbindin-immunoreactive (CB+) neurons forms a compact subnucleus (CBSn) in the hamster SCN. Restoration of rhythmicity using fetal SCN grafts in SCN-lesioned hamsters is critically dependent upon the presence of CB+ neurons within the transplanted grafts (LeSauter and Silver, 1999). The aim of the current study was to determine whether CB+ neurons within the CBSn of the hamster SCN fire action potentials in a circadian pattern as part of their output signal. Using patch-clamp recording, we demonstrated that CB+ neurons in the CBSn do not express a circadian rhythm in spontaneous firing frequency under diurnal conditions *in vitro*. Furthermore, the percentage of silent CB- cells varies with zeitgeber time, whereas the percentage of silent CB+ cells does not. Immunohistochemical analysis revealed that the CBSn is a nonhomogeneous nucleus, containing many more CB- than CB+ cells. Our results reveal that CB+ neurons within the CBSn represent a functionally distinct neuronal subpopulation in which rhythmic action potential output may not be necessary for the restoration of behavioral circadian rhythmicity.

INTRODUCTION

Many biological functions oscillate with a circadian period of approximately 24 hours. The role of the mammalian suprachiasmatic nuclei (SCN) in generating circadian rhythms in behaviors, endocrine functions, and other physiological processes is well established. Ablation of the SCN eliminates circadian rhythms (Moore and Eichler, 1972; Stephan and Zucker, 1972), and transplantation of fetal tissue containing the SCN into SCN-lesioned arrhythmic hosts restores behavioral circadian rhythmicity (Lehman *et al.*, 1987; LeSauter and Silver, 1998; Sollars and Pickard, 1998; Meyer-Bernstein *et al.*, 1999). Although functional grafts must contain a minimum volume of SCN tissue (Aguilar-Roblero *et al.*, 1994), the required phenotypic composition has been a matter of debate.

Silver *et al.* (1996b) have identified a subnucleus of calbindin-immunoreactive (CB+) cells in the caudal hamster SCN. In hamsters, partial SCN lesions containing the calbindin subnucleus (CBSn) lead to a loss of circadian locomotion, even when other parts of the SCN are spared (LeSauter and Silver, 1999). Circadian locomotion is restored after implantation of fetal SCN tissue with CB+ cells and fibers, into the third ventricle of previously SCN-lesioned adult hamsters (Silver *et al.*, 1996a; LeSauter and Silver, 1999). Restoration of rhythmicity was critically dependent upon the presence of CB+ neurons within the transplanted grafts. These observations have led to the hypothesis that this phenotypically identified group of SCN neurons is required for the restoration of circadian activity, though the mechanism(s) remain unknown (Silver *et al.*, 1996a).

One characteristic feature of SCN neurons is the circadian oscillation in action potential firing frequency, with a peak near midday, *in vivo* (Yamazaki *et al.*, 1998) and

in vitro in the hypothalamic slice (Inouye and Kawamura, 1979; Green and Gillette, 1982). Action potentials are necessary for circadian output, as tetrodotoxin (TTX) infusion into the SCN *in vivo* disrupts circadian drinking rhythms. After removal of TTX, free-running rhythms re-emerge in phase with the previous rhythm, indicating that the circadian pacemaker was largely unaffected by TTX (Schwartz *et al.*, 1987). These studies demonstrated that action potentials are necessary for the behavioral output of the clock, but are not required for actual timekeeping.

The aim of this study was to determine whether CB+ neurons within the CBsn of the hamster SCN fire action potentials in a circadian pattern as part of their output signal. Using patch-clamp recording, we demonstrate that CB+ neurons in the CBsn do not express a circadian rhythm in spontaneous firing frequency under diurnal conditions *in vitro*.

MATERIALS AND METHODS

Animals and housing

Adult male Syrian hamsters (*Mesocricetus auratus*; SASCO, Kingston, NY, USA) were housed under a 14 h light: 10 h dark (LD) schedule for a minimum of two weeks. Average cage light intensity was 450 lux. Times of recordings are noted as Zeitgeber time (ZT), since the primary goal of this study was to identify the neural mechanisms involved in the context of a 24-hour LD cycle. By convention, ZT12 was defined as lights off (Biello *et al.*, 1997). Food and water were available *ad libitum*. To ensure entrainment to the lighting schedule, four hamsters from each shipment were housed individually and locomotor activity was measured using an infrared sensor located above the cage. Activity was recorded continuously in 6-min epochs. The period

of locomotor activity was calculated using in-house software (Masayuki Ikeda, Advanced Research Institute for Science and Engineering, Waseda University, Tokyo, Japan). Experimental procedures involving animals were approved by the IACUC, and all efforts were made to minimize pain and the numbers of animals used.

Slice preparation

Hamsters were deeply anesthetized with halothane and decapitated. Brains were rapidly removed and placed in ice-cold ACSF solution (~310 mOsm), containing (in mM): NaCl, 138.6; KCl, 3.35; NaH₂PO₄, 0.6; MgCl₂, 1.0; CaCl₂, 2.5; glucose, 9.9; NaHCO₃, 21; saturated with 95% O₂ and 5% CO₂, pH 7.3-7.4. Coronal SCN slices (260-300 μm) were cut on a vibratome; recordings were made 1-12 h after slice preparation.

Intracellular recording

Slices were submerged in a recording chamber (0.5 ml) and continuously perfused with oxygenated 35 °C ACSF (2-3.5 ml/min). SCN neurons were identified as the dense cluster of cells immediately dorsal to the optic chiasm, extending dorsally 300 μm and laterally 200 μm from either side of the third ventricle (Morin and Wood, 2001). Electrode resistances were 5-9 MΩ when filled with an intracellular solution (290-300 mOsm), containing in mM: K-gluconate, 130; NaCl, 1; EGTA, 5; MgCl₂, 1; CaCl₂, 1; KOH, 3; Na₂ATP, 2-4, HEPES, 10 (pH 7.3-7.4), and Neurobiotin (0.4%). Spontaneous firing rates (SFR) were recorded in cell-attached patch-clamp mode, with the patch voltage clamped to 0 mV relative to the bath (Costantin and Charles, 1999). By recording the currents associated with action potentials, we avoided the cell dialysis that occurs during whole cell recording, which has been shown to affect SFR in suprachiasmatic neurons (Schaap *et al.*, 1999). SFR were recorded for 3 min, a time long enough to

determine the representative behavior of a cell's firing characteristics (Prosser and Gillette, 1989; Schaap *et al.*, 1999). After recording, whole-cell configuration was obtained and depolarizing pulses were applied to fill the cell with Neurobiotin. Data were recorded with an Axopatch 200A amplifier (Axon Instruments), low-pass filtered at 2 kHz (-3dB), and digitized at 10 kHz with an ITC-16 interface (Instrutech, Mineola, NY, USA). Pulse and PulseFit (HEKA Electronics, Lambrecht, Germany) were used for data acquisition. Off-line analysis was performed using MiniAnalysis (Synaptosoft, Version 5.3.5, Decatur, GA, USA).

Locating the calbindin subnucleus within the hamster SCN

To increase the likelihood of recording from CB+ neurons, we identified spatial coordinates for the CBSn. The CBSn is approximately 135-200 μm lateral to the third ventricle (3V), and 40-200 μm from the dorsal rim of the optic chiasm. Cells within this region were preferentially targeted for recording and precise coordinates were noted. To avoid potential mismatching between recorded and filled cells, two procedures were implemented: (1) a maximum of 3 cells was recorded from each SCN; (2) using fluorescent microscopy, the coordinates of each filled cell were measured in order to verify a match with the coordinates of each recorded cell.

Immunohistochemistry

After recordings, slices were immersion-fixed in 4% paraformaldehyde (0.1 M PB), at 4 °C for 24 h. Free-floating slices were incubated in Tris buffered saline (TBS; 50 mM Tris and 150 mM NaCl; pH 7.6) containing 0.5% Triton X-100 and 2% normal goat serum for 2 h at room temperature (RT). Slices were incubated overnight (4 °C) with a monoclonal anti-calbindin antibody (Sigma, St. Louis, MO, USA; 1:10,000). After

washes, slices were incubated in a streptavidin-fluorescein conjugate (Vector, Burlingame, CA, USA; 1:1,200) for five h (RT), and finally incubated in goat anti-mouse Alexa Fluor 568 (Molecular Probes, Eugene, OR, USA; 1:750) for 90 min (RT). Following a final wash, slices were mounted on glass slides and coverslipped with ProLong® antifade agent (Molecular Probes).

A confocal laser scanning microscope (Bio-Rad 1024 ES equipped with a krypton-argon laser mounted on an inverted fluorescent microscope) was used to collect sequential optical sections (1-2.5 μm). Single laser lines of 488 and 568 nm were used to excite fluorescein and Alexa Fluor 568, respectively. To examine colocalization of both markers (Neurobiotin and calbindin), single confocal images of Neurobiotin (pseudocolored green) or calbindin (pseudocolored red) markers were collected and combined to determine label colocalization (yellow). Assessment of CB immunoreactivity was done without knowledge of the SFR. Fluorescence bleedthrough was eliminated by using bandpass emission filters, sequential imaging and LaserSharp (BioRad ©) software.

Data Analysis

SFR are presented as means \pm standard deviations. To determine the times of peak and nadir SFR, data were grouped into 2 h bins and smoothed using a 2 h running mean with a 15 min lag. Times of highest and lowest firing rates were calculated at the middle of the 2 h bin with the highest and lowest values, respectively. Significant differences between groups ($p < 0.05$) were determined either by a Mann-Whitney U test or by an Exact Unconditional Test, which was chosen over Fisher's exact because sample sizes were not determined in advance of recording (Suissa and Shuster, 1985). The ZTs for 153

CB- and 21 CB+ cells were collapsed into 10 non-overlapping time epochs (i.e. ZT2 ≤ 4, ZT4 ≤ 6, ZT6 ≤ 8, ... ZT20 ≤ 22). Among all cells, the median firing frequency was calculated. Using this value as a threshold, cells were jointly classified according to phenotype (CB- or CB+), time epoch (ZT), and whether the firing frequency was above or below the median. Data were placed in a multi-way table and analyzed using a logistic regression model in which time and phenotype were treated as predictors of whether a cell's firing frequency would be above the median of all cells. Likelihood-based odds ratios (the odds that a CB- cell fires above the median relative to similar odds for a CB+ cell) were calculated at the midpoint for each time epoch and were based on the logistic regression model. Likelihood-based confidence intervals were used because they are more accurate than traditional logit-based intervals when sample sizes are small. p values were calculated for each time epoch and significance accepted at $p < 0.05$. We used the statistical program 'R', obtained from <http://cran.r-project.org>. (Ihaka and Gentleman, 1996).

RESULTS

We recorded the SFR of 277 neurons in the hamster SCN from ZT2-22. Individual neurons were filled with Neurobiotin and characterized on the basis of CB immunoreactivity (Fig. 1). Based on CB immunoreactivity and anatomical location, we identified four populations of neurons: (1) CB- neurons rostral to the CBSn ($n = 100$); (2) CB- neurons within the CBSn ($n = 153$); (3) CB+ neurons rostral to the CBSn ($n = 3$); and, (4) CB+ neurons within the CBSn ($n = 21$).

During the day, the mean SFR of CB- neurons within the CBSn was 4.2 ± 3.2 Hz and the mean SFR of CB- neurons rostral to the CBSn was 2.62 ± 2.64 Hz. During the

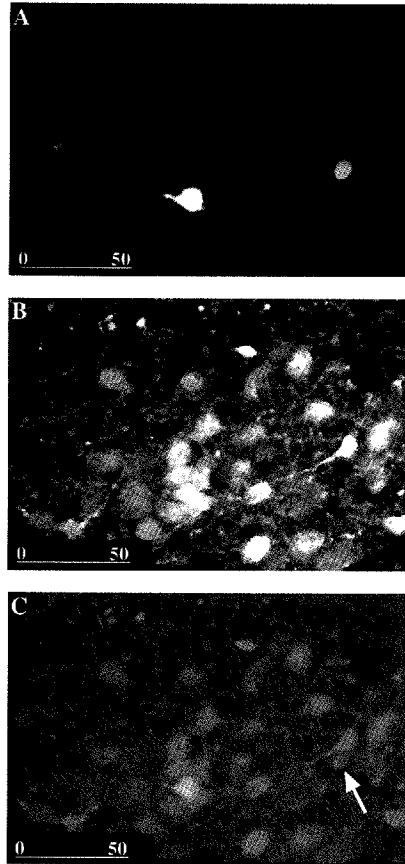


Fig 1. Colocalization of calbindin and Neurobiotin in SCN neuron. Confocal images from recorded neurons in a coronal hamster hypothalamic slice, showing: (A) two neurons filled with the intracellular marker, Neurobiotin, and visualized with a streptavidin-fluorescein conjugate. (B) Cluster of calbindin-immunoreactive (CB+) neurons. (C) Overlay image shows CB+ neurons in red. The recorded neuron on the left appears yellow, indicating colocalization of both markers. The white arrow points to the green neuron on the right, which contains only Neurobiotin and not calbindin. Scale bar is in microns.

night, the mean SFR of these cells was 1.47 ± 2.2 Hz and 1.26 ± 1.55 Hz, respectively. Comparisons between daytime and nighttime mean SFR indicate that both populations of CB- neurons exhibited a circadian variation in SFR similar to that reported in rat and hamster (Mann-Whitney U test: $U = 893;1386$; $p < 0.05$; Green and Gillette, 1982; Mason *et al.*, 1987), with the firing peak occurring at ZT6.5 and the nadir at ZT19.5 (Fig. 2A). The reduction in mean SFR at night was due to a lack of fast firing neurons as well as a larger number of silent cells (Fig. 2A). In contrast, the CB+ neurons within the CBSn lacked a circadian variation in firing rate, with a mean SFR of 0.66 ± 0.86 Hz during the day and 0.68 ± 0.88 Hz at night (Fig. 2B). The absence of fast firing neurons was evident across all time epochs: 80% of CB+ neurons within the CBSn fired at rates less than 1 Hz. In fact, during the peak epoch (ZT6-8), the mean SFR of CB- neurons within the CBSn was 5.2 ± 3.2 Hz ($n=34$), while the mean SFR of CB+ neurons within the CBSn was 0.6 ± 0.8 Hz ($n=6$). The SFR of CB- cells were significantly higher than the SFR of CB+ cells during the day (ZT2 -< 14; logistic regression model: $p < 0.01$; Fig 3, Appendix). Conversely, there was no statistical difference between CB- and CB+ cells during the night (ZT14 -< 22; logistic regression model: $p = 0.08 - 0.98$). In contrast to CB+ neurons within the CBSn, we recorded three CB+ neurons outside of the CBSn, whose mean SFR was greater than 6 Hz.

Though the recording strategy we employed facilitated recording neurons within the CBSn (174/277 neurons), our success rate for recording from CB+ neurons was still quite low (21/174=12%). This low success rate is largely because the CBSn is *not* a homogeneous population of CB+ cells. The CB subnuclei occupy a region < 200 μm long and contain only 500 CB+ neurons (Silver *et al.*, 1996b). However, the majority of cells

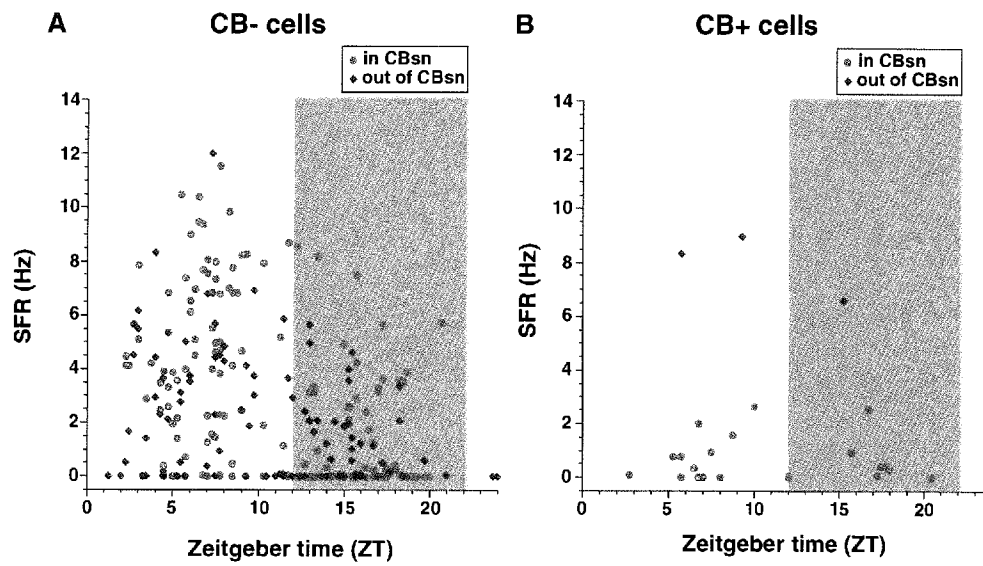


Fig 2. Scatter plots of spontaneous firing rates of individual SCN neurons plotted against zeitgeber time. (A) Firing rates of CB- neurons in the CBsn (red) and outside of the CBsn (blue) demonstrate a diurnal oscillation in firing rate. (B) Firing rates of CB+ neurons in the CBsn do not have a circadian variation in firing rate. Shading indicates lights off.

in the hamster CBsn do not express calbindin, leading to the low probability of recording from CB+ neurons.

Using the cell-attached patch technique, we were able to examine the circadian variation in the percentage of silent SCN neurons (Fig. 3A). Because the distribution of silent cells across all time epochs for CB- cells outside of the CBsn was not different from that of CB- cells within the CBsn, we grouped the two populations of CB- cells together for comparison with CB+ cells in the CBsn. Across all time points, the total percentage of silent cells was similar for CB- and CB+ cells, 27% (69/253) and 24% (5/21), respectively. However, the distribution of silent cells across the daytime and nighttime was significantly different ($p < 0.01$; Fig. 3B). During the day, 19% (28/145) of CB- neurons were silent; at night, the percentage doubled to 38% (41/108). For CB+ neurons in the CBsn, there was no significant circadian variation, as roughly equal percentages of silent neurons were recorded during the day and night, 25% (3/12) and 22% (2/9), respectively ($p = 0.991$).

DISCUSSION

Most SCN neurons exhibit a dramatic circadian variation in SFR. Even when grown in dissociated culture, some SCN neurons show phase-independent circadian firing rhythms. This finding demonstrates that circadian oscillation is not dependent on the oscillatory properties of a complex circuit (Welsh *et al.*, 1995; Honma *et al.*, 1998). Unlike most SCN neurons examined to date (Shibata *et al.*, 1982; Mason *et al.*, 1987; Herzog *et al.*, 1997), CB+ neurons within the hamster CBsn do not exhibit a circadian oscillation in firing rate under diurnal conditions.

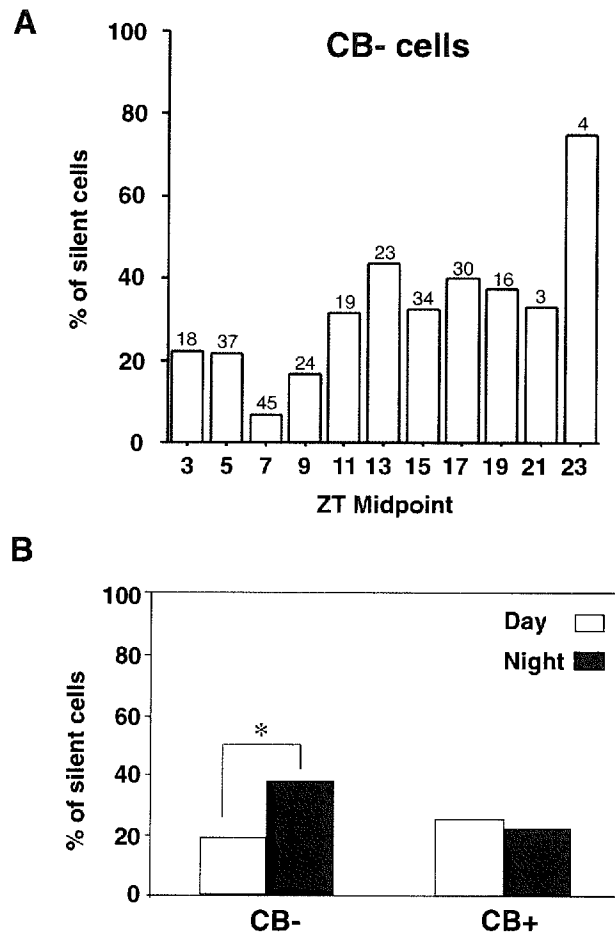


Fig 3. The percentage of silent cells varies with ZT and with CB phenotype. (A) The number of silent CB- cells (throughout the SCN) recorded vs. the midpoint of 2-h ZT epochs. Numbers above the bars indicate the total number of cells recorded during that time epoch. For example, of 45 cells recorded during ZT6-8, 7% were silent. (B) The diurnal variation in the number of silent cells based on CB phenotype. All CB- cells were compared with CB+ cells within the CBsn (*significant difference between day and night percentage of silent cells by an Exact Unconditional Test; $P = 0.001$).

Our results are consistent with studies reporting regional variation in rhythmicity among SCN neurons. In dispersed cell culture, roughly one quarter of rat SCN neurons do not display a circadian rhythm in SFR (Honma *et al.*, 1998). More recently, using organotypic slice cultures of rat SCN, Nakamura *et al.* (2001) recorded the SFR from individual SCN neurons using a multielectrode array. In the dorsal SCN, 87% of neurons demonstrated a circadian rhythm in firing rate, whereas in the ventral SCN, only 62% of neurons were rhythmic. The increased proportion of nonrhythmic cells in the ventral SCN suggests an anatomical correlation with rhythmic firing. In hamster, the CBSn is entirely contained within the ventral SCN (Silver *et al.*, 1996b). Although there is not a compact CBSn in the rat or mouse (Arvanitogiannis *et al.*, 2000; Abrahamson and Moore, 2001), the ventral pole of the SCN contains a higher percentage of CB+ cells, which may possess similar functional properties to those in the hamster CBSn. To our knowledge, the neurophysiological rhythmicity of only one other phenotypically identified neuronal type has been investigated in the SCN. Vasopressin neurons, which are primarily located in the dorsomedial region of the rat SCN, demonstrate circadian rhythmicity in spontaneous firing rate (Schaap *et al.*, 1999). Even at the level of gene expression, there is regional variation in rhythmicity. In the hamster SCN, cells outside of the CBSn express the *Period* genes, *Per1*, *Per2* and *Per3* in a rhythmic fashion. In contrast, cells within the CBSn do not rhythmically express any of the *Per* genes (Hamada *et al.*, 2001). Thus, CB+ neurons within the hamster CBSn do not exhibit two defining characteristics of many SCN neurons - circadian oscillation in SFR and *Per* gene expression.

Throughout this study and others (Celio, 1990; LeSauter and Silver, 1999), CB has been used simply as a neuroanatomical marker. However, as a neural calcium

binding protein, CB plays a functional role in cytosolic calcium buffering and transport (Baimbridge *et al.*, 1992). CB has also been reported to determine firing patterns within at least two brain regions, the frontal cortex and the supraoptic nucleus (Kawaguchi and Kubota, 1993; Li *et al.*, 1995). Precisely how CB functions to control firing rate is unknown, but altered calcium buffering is likely to affect intracellular signaling pathways that modify the properties of downstream ion channels. In the SCN, there is evidence for circadian modulation of ionic currents. Recently, Pennartz *et al.* (2002) demonstrated a diurnal modulation of the L-type calcium current in rat SCN neurons. This current occurs during the daytime and is tightly coupled to the generation of action potentials, thus contributing to the characteristic circadian pattern of high frequency firing during the day. An intriguing speculation is that CB+ neurons within the CBSn may lack a diurnal oscillation in the L-type calcium current, thus accounting for the absence of oscillation in SFR.

The lack of rhythmic action potential output from CB+ neurons seems surprising, considering the fact that restoration of a rhythmic behavioral output is dependent on the presence of CB+ neurons within fetal SCN grafts (LeSauter and Silver, 1999). In fact, CB+ cells in this region do not display any circadian property assessed thus far (Hamada *et al.*, 2001). One hypothesis that could explain this apparent paradox is that CB+ cells are not the singular critical components that are required for the restoration of circadian locomotion. The earlier identification of CB as a marker for successful grafts may have been indicative of intercellular connections between nonrhythmic CB+ cells and their rhythmic CB- counterparts that were essential for the re-establishment of circadian behavior. As we have shown in this study, the CBSn is *not* a homogeneous population of

CB+ cells, and, in fact, only 10-20% of the cells in the CBsn are immunoreactive for CB. The majority of cells in the CBsn do not contain CB, but many have been shown to express several neuropeptides (LeSauter *et al.*, 2002). These recent studies have shown that CB- neurons containing vasoactive intestinal polypeptide and gastrin releasing peptide establish connections with CB+ cells in this region. CB+ cells are also heavily weighted on the input side of the circadian system: CB+ cells receive dense input from the retina (Bryant, *et al.*, 2000), intergeniculate leaflet and the median raphe nucleus (LeSauter *et al.*, 2002). Within the CBsn, the combined presence and interaction of rhythmic CB- cells and nonrhythmic CB+ cells within the CBsn may be required to produce a meaningful output signal. The challenge for future research is to determine the intercellular communication between rhythmic and nonrhythmic neurons in this critical subregion of the hamster SCN and how this interaction produces a rhythmic output.

Acknowledgments

We would like to thank Aurelie Snyder of the OHSU-MMI Research Core Facility for her assistance with confocal microscopy and Michael R. Lasarev for help with statistical analysis. This work was supported by NINDS grant NS036607 (C.N.A.). E.E.J. was supported by pre-doctoral NRSA NS42406.

B. Manuscript 2

**Intercellular communication within the calbindin subnucleus of the hamster
suprachiasmatic nucleus**

E. E. Jobst¹, D. W. Robinson¹ and C. N. Allen^{1,2}

Department of Physiology and Pharmacology¹ and Center for Research on Occupational
and Environmental Toxicology^{1,2}, Oregon Health & Science University,
3181 SW Sam Jackson Park Road, Portland, OR 97239, USA.

Submitted to *Neuroscience*, February 2003

ABSTRACT

In mammals, the suprachiasmatic nucleus (SCN) is the master circadian pacemaker. Within the caudal hamster SCN, a cluster of neurons containing the calcium binding protein, calbindin-D28K (CB), has been implicated in circadian locomotion. However, calbindin-immunoreactive (CB+) neurons in the calbindin subnucleus (CBSn) do not display a circadian rhythm in spontaneous firing (Jobst and Allen, 2002). Previously, we proposed that intercellular communication might be essential in integrating outputs from rhythmic (CB-) neurons and nonrhythmic (CB+) neurons to produce a circadian output in the intact animal. The primary aim of this study is to provide a neuroanatomical framework to better understand intercellular communication within the CBSn. Using reconstructions of previously recorded neurons, we demonstrate that CB+ neurons have significantly more dendrites than CB- neurons. In addition, CBSn neurons have dorsally oriented dendritic arbors. Using double-label confocal microscopy, we show that GABA colocalizes with CB+ neurons and GABA_A receptor subunits make intimate contacts with neurons in the CBSn. Transforming growth factor alpha (TGF α), a substance shown to inhibit locomotion (Kramer *et al.*, 2001), is present within neurons and glia in the CBSn. In addition, neurons in the region express the epidermal growth factor receptor, the only receptor for TGF α . Lastly, we show that CB+ neurons are coupled to CB+ and CB- neurons by gap junctions. The current study provides a structural framework for synaptic communication, electrical coupling, and neuron-to-neuron or glia-neuron signaling via a growth factor within the CBSn of the hamster SCN. Our results reveal connections that have the potential for integrating cellular communication within a subregion of the SCN that is critically involved in circadian locomotion.

INTRODUCTION

In mammals, the master circadian pacemaker is the suprachiasmatic nucleus (SCN), a paired structure at the base of the hypothalamus. Comprised of roughly 16,000 neurons (van den Pol, 1980; 1991), this small region receives environmental photic information and imparts an adaptive circadian rhythm to physiological and behavioral functions. Though the SCN has been anatomically subdivided into regions based on neuropeptide content, afferent inputs and efferent projections (Card and Moore, 1984; Abrahamson and Moore, 2001; Moore *et al.*, 2002), evidence is rapidly accumulating that the SCN can be functionally subdivided into regions based on the expression of certain clock genes (Hamada *et al.*, 2001; Yan and Silver, 2002) and variations in rhythmic firing (Honma *et al.*, 1998; Nakamura *et al.*, 2001; Jobst and Allen, 2002).

Within the caudal hamster SCN, neurons containing the calcium binding protein, calbindin-D28K (CB), form a distinct cluster, or subnucleus. Partial SCN lesions containing the calbindin subnuclei (CBSn) lead to a loss of circadian behaviors, even when other parts of the SCN are spared (LeSauter and Silver, 1999). Circadian locomotion is restored after implantation of fetal SCN tissue into the third ventricle of previously SCN-lesioned adult hamsters (Silver *et al.*, 1996a; LeSauter and Silver, 1999). Restoration of rhythmicity appears to be dependent upon the presence of calbindin-immunoreactive (CB+) neurons within the transplanted grafts. These observations have led to the hypothesis that CB+ neurons within the CBSn are required for the restoration of circadian activity, though the mechanisms remain unknown (LeSauter and Silver, 1998).

In an earlier study, we demonstrated that the hamster CBSn contains CB+ neurons

as well as many more calbindin-negative (CB-) neurons. Interestingly, CB- neurons display a robust circadian rhythm in spontaneous firing, whereas their CB+ counterparts do not (Jobst and Allen, 2002). In a molecular analysis of the CBsn, many neurons presumed to be CB+ do not express a circadian oscillation in the clock genes *mPer1* and *mPer2* (Hamada *et al.*, 2001). Since CB+ neurons have not displayed any circadian properties, it has been suggested that these neurons are not pacemaker cells (Hamada *et al.*, 2001). However, the results of these studies have not been reconciled with those of earlier studies showing that the presence of (nonrhythmic) CB+ neurons is correlated with re-establishment of rhythmic locomotion (Silver *et al.*, 1996; LeSauter and Silver, 1999).

While the mechanism responsible for generating circadian rhythms is intrinsic to individual neurons in the SCN (Welsh *et al.*, 1995), it is well recognized that SCN neurons display widely varying periods in firing rhythms (Welsh *et al.*, 1995; Honma *et al.*, 1998; Nakamura *et al.*, 2001). Thus, for the intact SCN to impart a distinct circadian period to the animal, outputs from single SCN neurons must be integrated. Two of the strongest candidates proposed to synchronize SCN cells are GABA, via its action on GABA_A receptors, and gap junctions (Jiang *et al.*, 1997; Colwell, 2000; Liu and Reppert, 2000). Previously, we proposed that intercellular communication between nonrhythmic (CB+) neurons and rhythmic (CB-) neurons might be critical to produce a circadian output in the intact animal. This investigation was stimulated by the necessity for an anatomical framework on which to build an understanding of how neurons within the CBsn communicate with each other. We investigated some of the morphological properties of CB+ neurons that form the basis of intercellular communication. First, we

used neuronal reconstruction methods to examine distinct morphological characteristics of neurons in the CBSn. Second, we used double-label confocal microscopy to investigate the primary neurotransmitter and receptors of CB+ cells that may make them sensitive to potential synchronizing agents, such as GABA and transforming growth factor alpha, as well as their ability to be coupled by gap junctions.

EXPERIMENTAL PROCEDURES

Animals and housing

Adult male Syrian hamsters (*Mesocricetus auratus*; 6-11 weeks; SASCO, Kingston, NY, USA) were housed in a temperature-controlled chamber (19-21°C) under a 14:10-h light-dark cycle for a minimum of two weeks. Average cage light intensity was 450 lux. Times are noted as Zeitgeber time (ZT), since the primary goal of this study was to identify the neural mechanisms involved in the context of a 24-hour LD cycle. By convention, ZT12 was defined as lights off (Biello *et al.*, 1997). Food and water were available ad libitum. To ensure entrainment to the lighting schedule, four hamsters from each shipment were housed individually and locomotor activity was measured using an infrared sensor (Hamamatsu Pyroelectric P4488) located 30 cm above the cage. Activity was recorded continuously in 6-min epochs. The onset of locomotor activity was calculated using in-house software (Masayuki Ikeda, Advanced Research Institute for Science and Engineering, Waseda University, Tokyo, Japan). The Institutional Animal Care and Use Committee of OHSU approved all experimental procedures involving animals and all efforts were made to minimize pain and the numbers of animals used.

SCN slice preparation and intracellular labeling

Methods for brain slice preparation and electrophysiological recording of hamster SCN neurons have been previously described (Jobst and Allen, 2002). Briefly, hamsters were deeply anesthetized with halothane before decapitation. Brains were rapidly removed and placed in ice-cold ACSF (~310 mOsm), saturated with 95% O₂ and 5% CO₂, pH 7.3-7.4. Two or three coronal hypothalamic slices (260-300 μm) containing the entire rostro-caudal extent of the hamster SCN were cut on a vibratome (Leica VT1000; Germany). Individual slices were continuously perfused with oxygenated ACSF (2-3.5 ml/min) at 35°C. Recordings were made 1-12 h after slice preparation. SCN neurons were identified as the dense cluster of cells immediately dorsal to the optic chiasm, extending dorsally 300 μm and laterally 200 μm from the midline (Morin and Wood, 2001). The recording pipettes were filled with an intracellular solution, containing in mM: K-gluconate, 130; NaCl, 1; EGTA, 5; MgCl₂, 1; CaCl₂, 1; KOH, 3; Na₂ATP, 2-4, HEPES, 10 (pH 7.3-7.4), and Neurobiotin tracer (0.4%; Vector Laboratories, Burlingame, CA, USA). After recording spontaneous firing rates in cell-attached patch-clamp mode (Jobst and Allen, 2002), further negative pressure was applied to obtain whole-cell configuration and brief depolarizing pulses (20 mV steps; 0-60 mV; 200 ms) were applied to fill each recorded neuron with Neurobiotin.

Antisera used for immunohistochemistry

The following antibodies were used: mouse monoclonal anti-calbindin D-28K (1:8,000) from SWANT (Bellinzona, Switzerland); mouse monoclonal anti-calbindin D-28K (1:10,000) from Sigma (St. Louis, MO, USA); guinea pig anti-GABA (1:4,000)

from Protos Biotech Corporation (New York, New York, USA); rabbit anti-connexin 36 (1:250) from Zymed (South San Francisco, CA, USA); rabbit anti-transforming growth factor alpha (TGF α ; 1:200) from Peprotech (Rocky Hill, NJ, USA); mouse anti-microtubule associated protein 2 (MAP2; 1:400) from Sigma; rabbit anti-EGFR (1:200) from Santa Cruz Biotechnology (Santa Cruz, CA, USA); rabbit anti-calbindin D-28K (1:1,000), rabbit anti-glutamate decarboxylase (GAD)65 (1:200), rabbit anti-glutamate decarboxylase (GAD)67 (1:1,000), rabbit anti-GABA_A receptor α 1 subunit (against residues 1-16 of α 1 mature mouse or rat peptide; 1:500), rabbit anti-GABA_A receptor α 2 subunit (against carboxy terminus of rat peptide; 1:500) and mouse monoclonal anti-GABA_A receptor β -chain (against β 2 and β 3 subunits; 1:100) from Chemicon International (Temecula, CA, USA).

Immunohistochemistry on recorded cells

Slices were immersion-fixed in 4% paraformaldehyde (PFA; 0.1 M phosphate buffer, pH 7.4), at 4°C for at least 24 h. After fixation, free-floating slices were rinsed in Tris buffered saline (TBS; 50 mM Tris buffer and 150 mM NaCl; pH 7.6) containing 0.5% Triton X-100. To block non-specific binding, slices were incubated in 2% normal goat serum in TBS for 2 h at room temperature (RT) and washed as before. Slices were incubated overnight at 4°C with a monoclonal anti-calbindin antibody. After rinsing in TBS, slices were incubated in a streptavidin-fluorescein conjugate (1:1,200; Vector Laboratories) for 5 h at RT, washed in TBS, and finally incubated in goat anti-mouse Alexa Fluor 568 (1:750; Molecular Probes, Eugene, OR, USA) for 90 min at RT.

Following a final wash in TBS, slices were mounted on glass slides and coverslipped with ProLong® antifade agent (Molecular Probes).

Morphological reconstruction and statistical analysis

Each Neurobiotin-filled neuron was reconstructed using NeuroLucida (MicroBrightField, Williston, VT, USA), a neuron reconstruction program, and analyzed with NeuroExplorer (MicroBrightField) to evaluate cell body perimeter, number of dendrites and nodes (branch points), mean dendritic length and axon length. A process was defined as an axon only if an axon terminal was clearly present, or if it was a very thin structure originating from either the soma or from a proximal dendrite (van den Pol, 1980). Dendritic areas were calculated using the area of a complex polygon that encompasses the ends of the dendrites. The software application ImageJ (<http://rsb.info.nih.gov/ij/>) was used to calculate the area of this polygon.

The relative effectiveness of dendritic synapses depends on type and distribution, as well as on dendritic geometry and resting membrane properties. Since the distribution of receptors along the dendrites in the CBsn is unknown, we analyzed the extent and orientation of the total possible synaptic surface area of the dendritic arbor. Dendritic extent and dendritic arbor orientation were determined using methods previously described by Warren *et al.* (2003). Briefly, a two-dimensional representation of each neuron was plotted on polar coordinates using the center of the soma as the origin (0,0). The dendritic extent was determined by summing the lengths of the longest dendrites in symmetrically opposite 30° ($\pi/6$ radians) regions of the dendritic field.

The dendritic arbor orientation was determined by converting each pixel comprising the dendritic tree into a vector, with a distance relative to the center of the soma. The vector angle was defined as the angle formed between a line connecting a point in the dendritic tree with the center of the soma and an axis oriented with respect to specific SCN landmarks: dorsal (toward the subparaventricular zone), 0°; ventral (toward the supraoptic decussation), 180°; medial (toward the 3V), 90°; and, lateral: (toward the anterior hypothalamic area), 270°. Vector analysis was then used to calculate the resultant vector length and angle. The resultant vector length indicates the *extent* of dendritic arbor polarization and the resultant angle indicates the *direction* of the polarization. Resultant vector lengths were normalized to compare the degree of arbor polarization across cells with different sizes of dendritic arbors. Thus, a neuron with a symmetrical dendritic tree would have an orientation index close to 0, whereas a very polarized cell would have an orientation index closer to 1. By comparing resultant vector angles between CB+ and CB- neurons within the Cbsn, it was possible to determine whether the *direction* of their projections differed.

Data are presented as mean \pm standard deviations. Morphological comparisons were made using an unpaired two-population Student's *t* test or an exact permutation test (Ramsey and Schafer, 1997). Comparisons between day and night tracer coupling were made using a two-sided Exact Unconditional Test. The probability level at which the null hypothesis was rejected was $p < 0.05$.

Immunohistochemistry

Between ZT3-10 (lights on), hamsters were anesthetized with isoflurane and perfused intracardially through the ascending aorta with 5-10 ml of heparin (1,000 units/ml) followed by 150 ml of 4% PFA in 0.1 M sodium phosphate buffer (PB; pH 7.4). Brains were removed, blocked and post-fixed for 1-4 h. Sectioning for GABA, EGF-R, and TGF α was done on a vibrating blade microtome. For other antibodies, brains were cryoprotected in 20% sucrose overnight at 4°C. They were subsequently quick-frozen in Tissue-Tek OCT compound (Ft. Washington, PA, USA) on crushed dry ice and coronally sectioned at a thickness of 40 μ m. Slices were processed similarly to recorded slices, except that the blocking solution contained 3% normal goat serum and TBS contained 0.2% Triton X-100 (Triton was excluded for one set of experiments with TGF α). Slices were incubated in primary antibodies from 18-45 h at 4°C. Following washes, slices were incubated in the appropriate secondary antibodies conjugated to an Alexa fluorophore (Alexa 488 or Alexa 568 at 1:750; Molecular Probes). For GABA immunohistochemistry, intracardial perfusions were done with 4% PFA in 0.1 M borate buffer (pH 9.5; Gu *et al.*, 1999) and detergent was not used in washes or incubations. For GABA_A receptor subunits, we used an antigen retrieval method (Jiao *et al.*, 1999) to unmask epitope antigens because conventional staining for ionotropic receptors often results in considerable diffuse intracellular staining (Fritschy and Mohler, 1995; Fritschy *et al.*, 1998). Briefly, free-floating sections were incubated in 10 mM sodium citrate (pH 8.5) at 80°C in a water-bath for 30 min. Following washes, sections were incubated in primary antibodies and the standard IHC procedure was followed. Each staining combination was analyzed in sections from at least two or three animals. Selective

labeling, resembling that acquired with the specific antibodies, could not be detected when primary antibodies were omitted. The absence of cross-reactivity between the secondary antibodies was verified by omitting one of the primary antibodies during the overnight incubation. When the peptide immunogen was available (EGF-R), antibody binding to antigen was blocked by pre-absorption with a ten-fold excess of the corresponding blocking peptide.

Confocal microscopy

A confocal laser scanning microscope (Bio-Rad 1024 ES) equipped with a krypton-argon laser mounted on a Nikon Eclipse TE300 inverted fluorescent microscope was used to examine sections. Sequential optical sections (0.5-2.0 μm) were collected using single laser lines of 488 and 568 nm. Unambiguous identification of double-immunofluorescent neurons was achieved by sequential examination of several confocal planes through the same cell. Fluorescence bleed-through was eliminated by using bandpass emission filters, sequential imaging and LaserSharp (BioRad ©) software. A series of optical sections was collected for each fluorophore and stored separately as a series of 512 X 512 (or 1024 X 1024) pixel images. Images were processed with LaserSharp software. Brightness and contrast of the digital images were adjusted in Photoshop (Adobe Systems, San Jose, CA USA). Confocal images are presented as either a stack of optical sections, or as single optical sections.

RESULTS

Cytoarchitecture and dendritic arbor orientation of CB+ and CB- cells in the CBsn

To determine whether there are morphological differences between CB+ and CB- neurons in the CBsn, we made three-dimensional representations of 27 neurons (13 CB+; 14 CB-) from the CBsn, obtained following intracellular staining with Neurobiotin and reconstruction using Neurolucida. In 14 cells (6 CB+; 8 CB-), we were able to clearly identify the axon (see Methods). Table 1 summarizes the morphological properties of CB+ and CB- neurons in the CBsn. Although cell body perimeter, mean length of axons and dendrites and number of nodes were not significantly different, CB+ neurons had significantly more dendrites than CB- neurons (3.1 ± 1.0 vs. 2.1 ± 0.5 , $p = 0.00645$: two-population unpaired Student's t test). Due to the small sample size and discrete nature of the data, we confirmed this result with a permutation test ($p = 0.0073$: exact, Ramsey and Schafer, 1997). The difference in the distribution of the number of dendrites between the two phenotypes was evident: 21% (3/14) of CB- neurons had 3 dendrites, while the remaining 79% had one or two dendrites. In contrast, 69% (9/13) of CB+ neurons had 3 or more dendrites: 15% had 5 dendrites; 8% had 4 dendrites; 46% had 3 dendrites and the remaining 31% had 2 dendrites.

Figure 1 shows the morphology and orientation of a representative CB+ neuron and a CB- neuron. The tracer-filled neurons were visualized under fluorescence microscopy (Panel A), reconstructed using Neurolucida (Panel B) and arranged on a polar plot with SCN coordinates, in accordance with how each neuron was oriented *in situ* (Panel C). Figure 2 is a schematic illustration of the dendritic arbor orientations for all reconstructed cells. More than 75% of the reconstructed cells had dendritic arbors

	CB-	CB+
Cell body perimeter	35.15 ± 5.67	35.59 ± 3.73
Number of dendrites	2.14 ± 0.53*	3.08 ± 1.04*
Total dendritic length	356.65 ± 165.86	388.33 ± 168.26
Number of nodes	1.43 ± 0.85	1.15 ± 1.07
Mean dendritic length	170 ± 78.47	141.2 ± 88.52
Mean axonal length	59.84 ± 35.85	32.73 ± 33.85
Normalized vector length[∇]	0.7 ± 0.3	0.6 ± 0.3
Orientation of dendritic arbor (degrees relative to dorsal)	3.1 ± 68.1	5.4 ± 70.4

Values are in microns (except for vector length and orientation) ± s.d.

[∇]Values are unitless

* Indicates a significant difference ($p < 0.05$)

Table 1. Morphological characteristics and dendritic arbor orientation of CB+ and CB- neurons in the hamster CBSn. Values are in μm (except for orientation of dendritic arbors, which is in degrees; and, normalized vector length, which is unitless; see Methods) ± s.d.

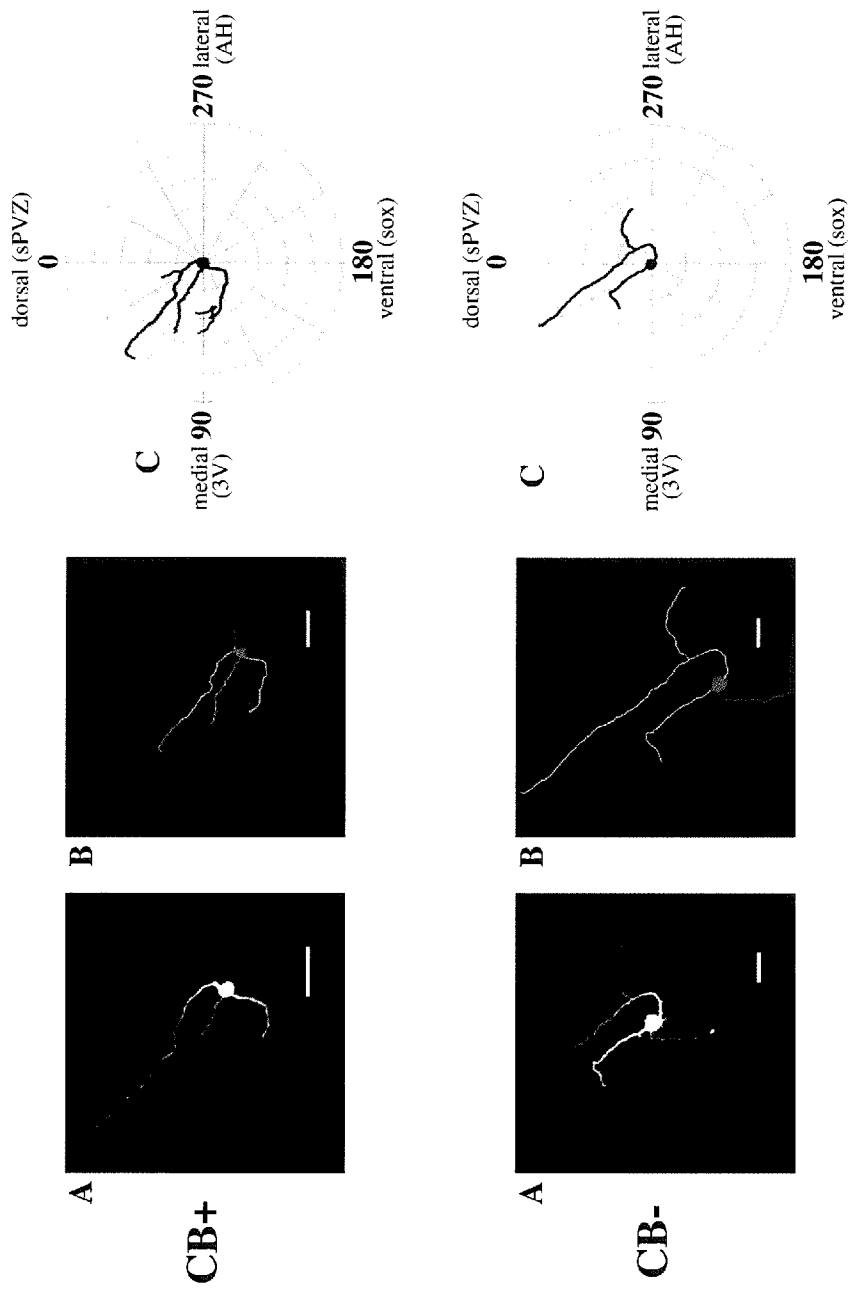


Fig 1. Reconstructions of a representative CB+ and CB- neuron within the CBsn of the hamster SCN. (A) Recorded Neurobiotin-filled neurons were visualized with streptavidin fluorescein. (B) Filled neuronal somas (red), dendrites (yellow) and axon (pink) were reconstructed using Neurobiotin. (C) Dendritic arbors were placed on a polar plot to calculate the polar coordinates for each black pixel that comprised the soma and dendrites. The CB+ neuron has 3 dendrites and the CB- neuron has 2 dendrites. SCN landmarks designate the orientation of each neuron within the slice preparation. Numbers indicate degrees. Scale bars = 25 μ m (CB+), 15 μ m (CB-).

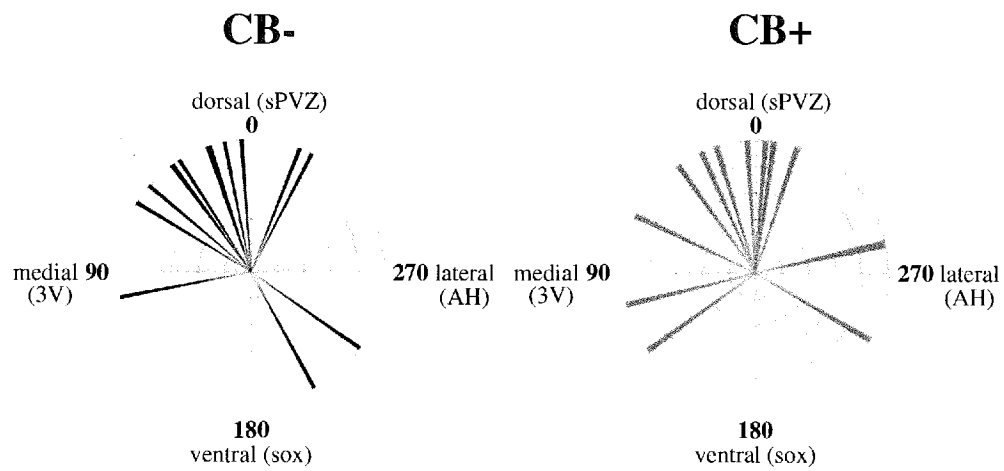


Fig 2. Schematic representing the dendritic arbor orientation for individual neurons within the CBSn. Each line on the polar plot illustrates the orientation of the dendritic arbor of a single reconstructed neuron.

oriented slightly lateral or medial of dorsal, and a smaller proportion (6/27; 22%) were oriented ventrally, toward the supraoptic decussation. There were no significant differences in the orientation of the dendritic arbors ($5.4^\circ \pm 70.4^\circ$ vs. $3.1^\circ \pm 68.1^\circ$; $p = 0.932$, two-population Student's *t* test) or the normalized vector lengths (0.6 ± 0.3 vs. 0.7 ± 0.3 ; $p = 0.682$, two-population Student's *t* test) between CB+ and CB- cells, respectively. These results indicate that both CB+ and CB- neurons in the CBSn had fairly polarized dendritic arbors (normalized vector lengths closer to 1 than 0) that were mostly oriented dorsally toward the subparaventricular zone (sPVZ; Fig. 2).

CB+ neurons in the CBSn are GABAergic and receive GABAergic input

Double-label immunofluorescence (IF) for CB and GABA demonstrated that the majority of CB-IF neurons also contained GABA-IF (Fig. 3; single white arrowheads). In 3 SCNs, individual CB-IF neurons were counted for colocalization with GABA. Roughly 94% of CB-IF neurons also contain GABA-IF (493/524). Of note, most of the cellular profiles in the CBSn contained GABA-IF, although many GABA-IF neurons in the CBSn did not demonstrate CB-IF (Fig. 3; double white arrowheads). In addition to CB and GABA colocalization in the CBSn, immunoreactivity for glutamate decarboxylase 67 (GAD67), one of two related isoforms of the synthetic enzyme for GABA, was detected in CB-IF somas (data not shown).

To investigate whether CB neurons receive GABAergic input, we used two strategies. First, we used an antibody directed against GAD65, an isoform of GAD exclusively located within synaptic terminals (Erlander *et al.*, 1991). Low power images revealed GAD65-IF in a punctate pattern throughout the SCN, including the CBSn (Fig. 4A). Analysis of a single optical slice at higher magnification showed GAD65-IF puncta

CB/GABA

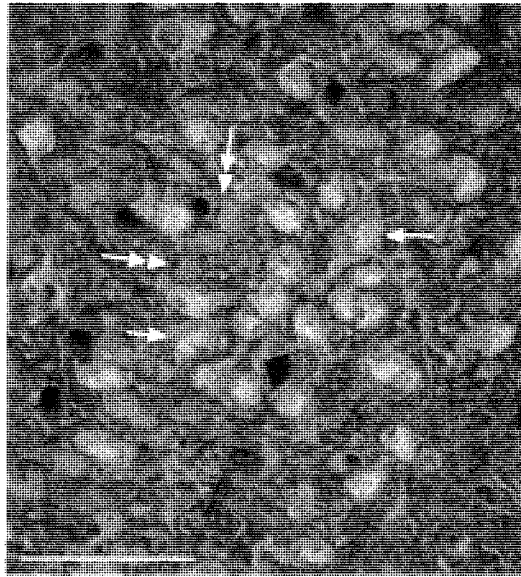


Fig 3. GABA in the CBsn of the hamster SCN. Figure represents color confocal digital image (1.0 μm resolution) of double-label immunofluorescence for CB (red) and GABA (green). Most neuronal profiles have GABA labeling. The single white arrowheads indicate neurons displaying colocalization of CB and GABA. Double white arrowheads indicate GABA-IF neurons that do not display CB-IF. Brain was from a hamster perfused at ZT8. Scale bar = 50 μm .

CB/GAD65

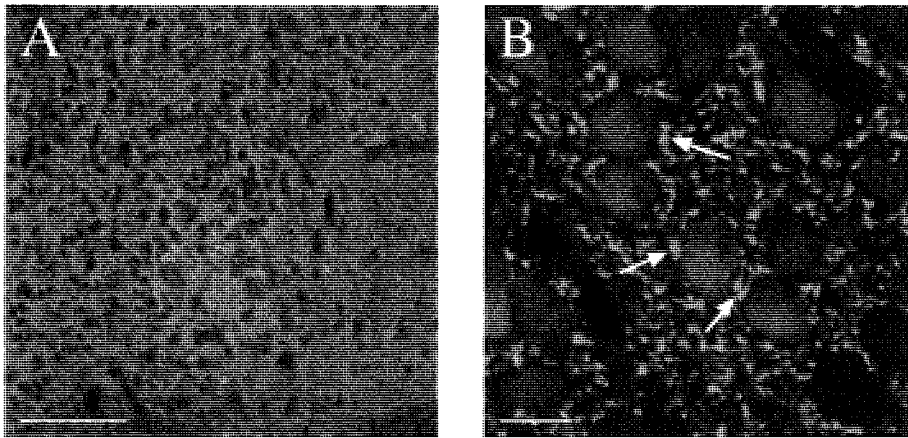


Fig 4. GAD65 within the CBsn of the hamster SCN. (A) GAD65 is seen in punctate profiles densely localized within the SCN. (B) In a single 0.5 μm confocal section, GAD65-IF (green) is dense in punctate profiles (white arrowheads) coming in close contact with CB-IF neurons (red). Brain was from a hamster perfused at ZT10. Scale bars = 100 μm (A), 10 μm (B).

(white arrows) coming into close apposition with CB-IF somas (Fig. 4B). To provide further support for the hypothesis that CB-IF neurons receive GABAergic input, we assessed the presence of GABA_A receptor (GABA_AR) subunits in the CBsn (Fig. 5). Figure 5 illustrates the expression of GABA_AR α 1, α 2 and β 2/3 subunits in the hamster SCN. Although a high level of α 1-IF was present in the anterior hypothalamic area lateral to the SCN, no significant α 1-IF was present within the SCN (Fig. 5A). Conversely, immunoreactivity for the GABA_AR α 2 and β 2/3 subunits was prominent in the SCN (Fig. 5B, C). Distribution of β 2/3-IF and α 2-IF within the CBsn is summarized in Figure 6. Confocal microscopic analysis demonstrated that β 2/3-IF and α 2-IF did not colocalize with CB-IF profiles and appeared to be excluded from all neuronal somas (Fig. 6A, B). Labeling for the β 2/3 subunits was diffusely distributed around CB+ neurons, whereas labeling for the α 2 subunit appeared as discrete puncta (Fig. 6A, B, insets). Our data indicate that α 2 and β 2/3 subunits contribute to the composition of GABA_ARs in the CBsn.

TGF α and its receptor, EGF-R, are expressed within the CBsn

Transforming growth factor alpha (TGF α), a 50 amino-acid polypeptide member of the epidermal growth factor (EGF) family, has recently been identified as a potential diffusible SCN output factor that inhibits locomotion (Kramer *et al.*, 2001). Because of the association of TGF α in locomotor inhibition and the role of the CBsn in circadian locomotion, we investigated the expression of TGF α in this region. The cellular expression of TGF α within the SCN was dependent on conditions of immunohistochemical processing (Fig. 7). Under detergent-free conditions, TGF α -IF was abundantly detected in neuronal profiles throughout the SCN (Fig. 7A, left column).

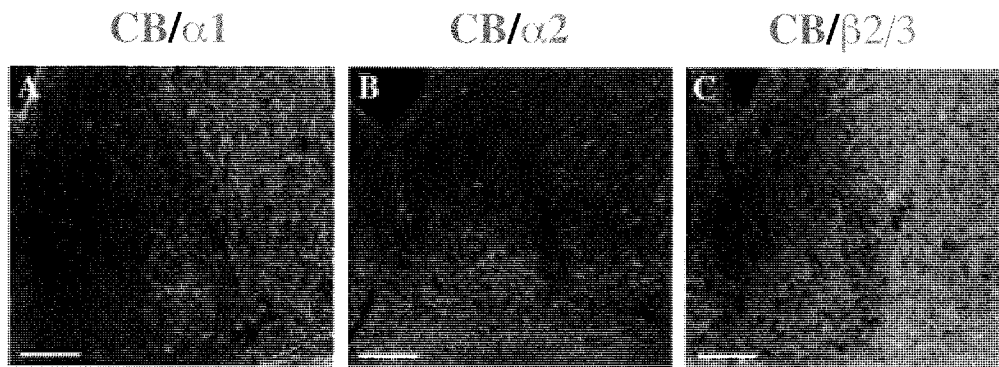


Fig 5. GABA_A receptor (GABAAR) subunits in the hamster SCN. Figures represent color confocal digital images of double-label immunofluorescence for CB (red) and GABAAR subunits (green). (A-C., 2.0 μ m resolution). (A) GABAAR α 1-IF is mostly absent from the SCN, but is moderately expressed in the adjacent anterior hypothalamic area. (B) GABAAR α 2-IF is densest in the ventral SCN. (C) GABAAR β 2/3-IF is present primarily in the ventrolateral SCN. Scale bar = 100 μ m.

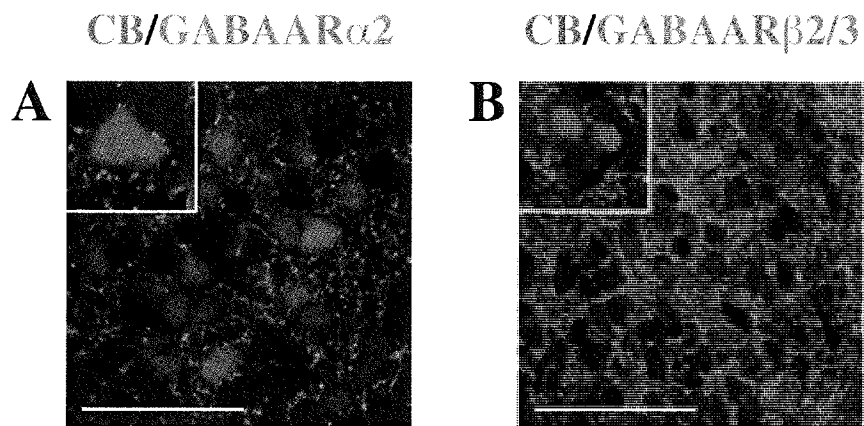


Fig 6. GABAAR α 2 and β 2/3 subunits within the CBsn of the hamster SCN. Figures represent single confocal sections (1.0 μ m resolution) of double-label immunofluorescence for CB (red) and GABAAR subunits (green). (A) α 2-IF is dense in punctate profiles surrounding CB-IF somas. (B) β 2/3-IF is expressed as more diffuse labeling around SCN somas. Scale bar = 50 μ m. Inset images in the upper left corners are higher magnifications (single optical slices, 0.5 μ m resolution) illustrating α 2-IF as discrete puncta surrounding a CB-IF neuron, whereas β 2/3-IF is more diffuse around CB-IF somas.

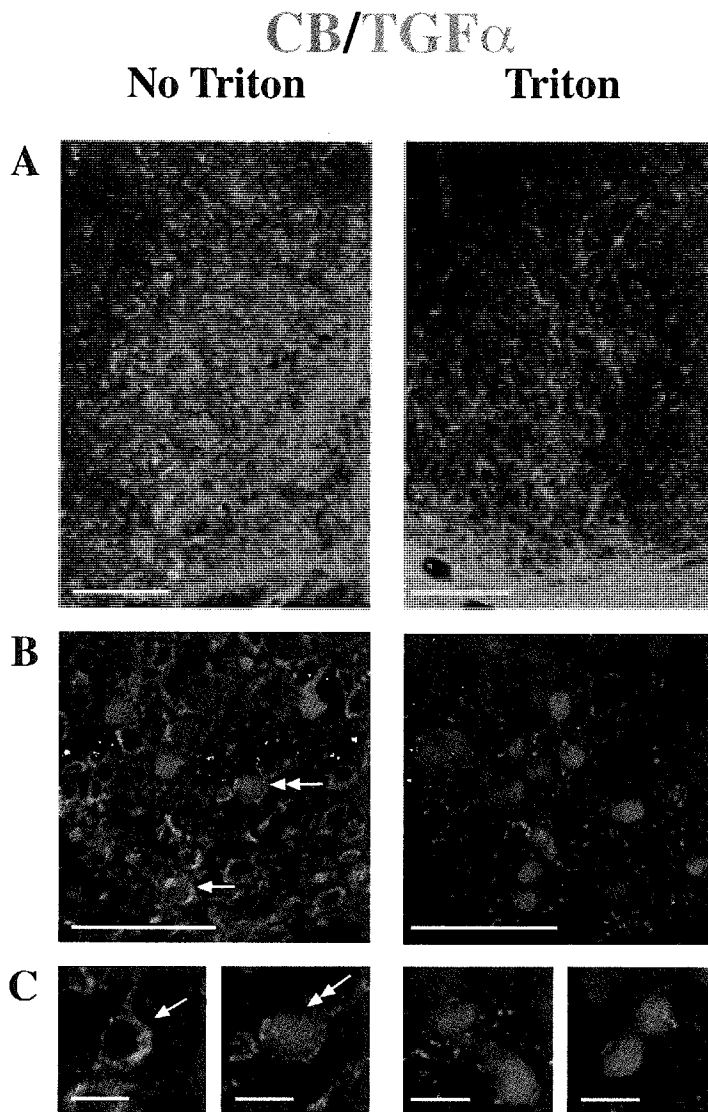


Fig 7. TGF α expression within the CBsn of the hamster SCN. Figures represent single confocal sections of double-label immunofluorescence for CB (red) and TGF α (green). The left column demonstrates TGF α labeling under detergent-free conditions and the right column illustrates TGF α labeling when Triton X-100, a non-ionic detergent, was used during the blocking incubation. (A) No Triton: TGF α -IF is predominantly localized in neuronal profiles within the SCN. (A) Triton: TGF α -IF is more diffusely labeled, and primarily localized in glia. (B) No Triton: TGF α and CB colocalization in the CBsn. Single white arrowhead indicates a neuron with CB-IF and TGF α -IF colocalized in the cytoplasm; double white arrowhead indicates a neuron with CB-IF in the nucleus and TGF α -IF in the cytoplasm. (B) Triton: TGF α -IF is dense in punctate profiles surrounding CB-IF somas, but does not colocalize with CB-IF somas. (C) Higher power magnifications of single neurons in B (0.5 μ m resolution). Scale bars = 100 μ m (A), 50 μ m (B), 10 μ m (C).

Within the CBsn, TGF α -IF was present in the cytoplasm of scattered neurons, including several CB-IF somas (Fig. 7B, C: left column, white arrows). In contrast, incubation with a detergent prior to the primary antibodies revealed TGF α -IF predominantly within fibers (Fig. 7A, B: right column) that did not colocalize with microtubule associated protein-2 (MAP2), a stringent neuronal marker (data not shown). Discrete TGF α -IF puncta made close appositions around CB-IF somas, but never colocalized with CB-IF somas (Fig. 7B, C: right column). Together, the data provide evidence for TGF α expression in neurons as well as non-neural structures within the hamster SCN.

SCN distribution of the only receptor for TGF α , the EGF receptor (EGF-R or erbB1), is shown in Figure 8A. Although (EGF-R)-IF was present in scattered neurons throughout the dorsomedial subdivision, the highest expression was detected in the ventrolateral SCN. At higher magnification, (EGF-R)-IF was mainly associated with the cytoplasm and somal membrane, whereas CB-IF was nuclear and cytoplasmic (Fig. 8A, inset). Preincubation of the rabbit EGF-R antibody with the immunizing peptide resulted in the complete loss of specific staining (Fig. 8B), demonstrating the specificity of this antibody in the hamster SCN.

CB+ neurons are coupled to other SCN neurons within the CBsn via gap junctions

Gap junctions allow the transfer of ions and small molecules between cells. Evidence for the presence of gap junctions in CB+ neurons came from physiological and anatomical experiments. During intracellular recordings, injected Neurobiotin tracer spread to other neurons that were not recorded (Fig. 9). This tracer coupling is a hallmark feature of cells linked by gap junctions (Peinado *et al.*, 1993; Trexler *et al.*, 2001). During the day, no tracer coupling was observed for the twelve CB+ neurons recorded. In

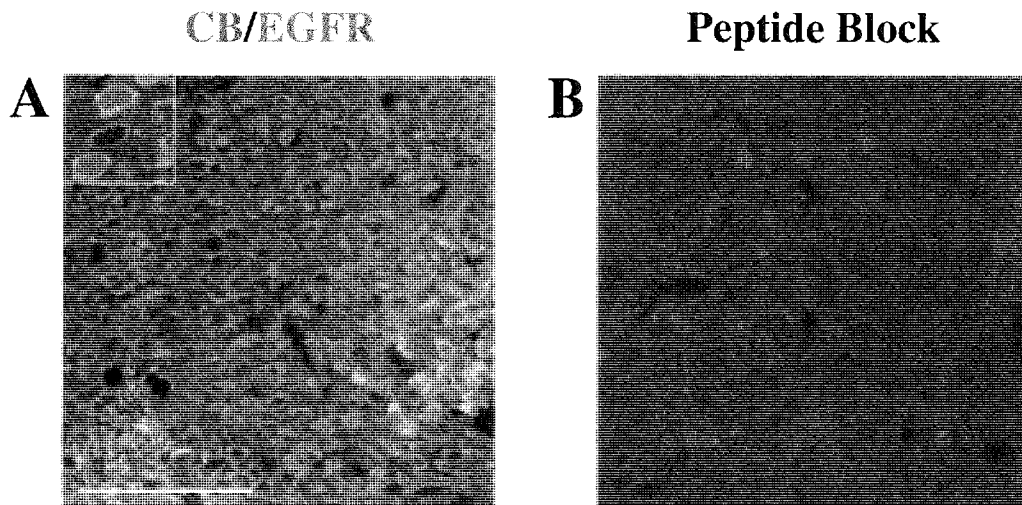


Fig 8. Double-label immunofluorescence for CB (red) and EGF-R (green) in the hamster SCN. Figures represent a stack of 15 confocal digital images (2.0 μm resolution). (A) EGF-R labeled neurons are scattered throughout the SCN, although the highest concentration of labeled neurons is in the ventrolateral subdivision. Many neurons display colocalization of EGF-R and CB (yellow). Image in the upper left inset is a higher magnification of a single confocal section (0.5 μm resolution). Neurons colocalize CB and EGF-R. EGF-R labeling is expressed in the cytoplasm, whereas CB labeling is in the cytoplasm and nuclei. (B) EGF-R binding is absent after pre-absorption with the immunizing peptide, demonstrating the specificity of EGF-R antibody in the hamster SCN. Scale bar = 100 μm .

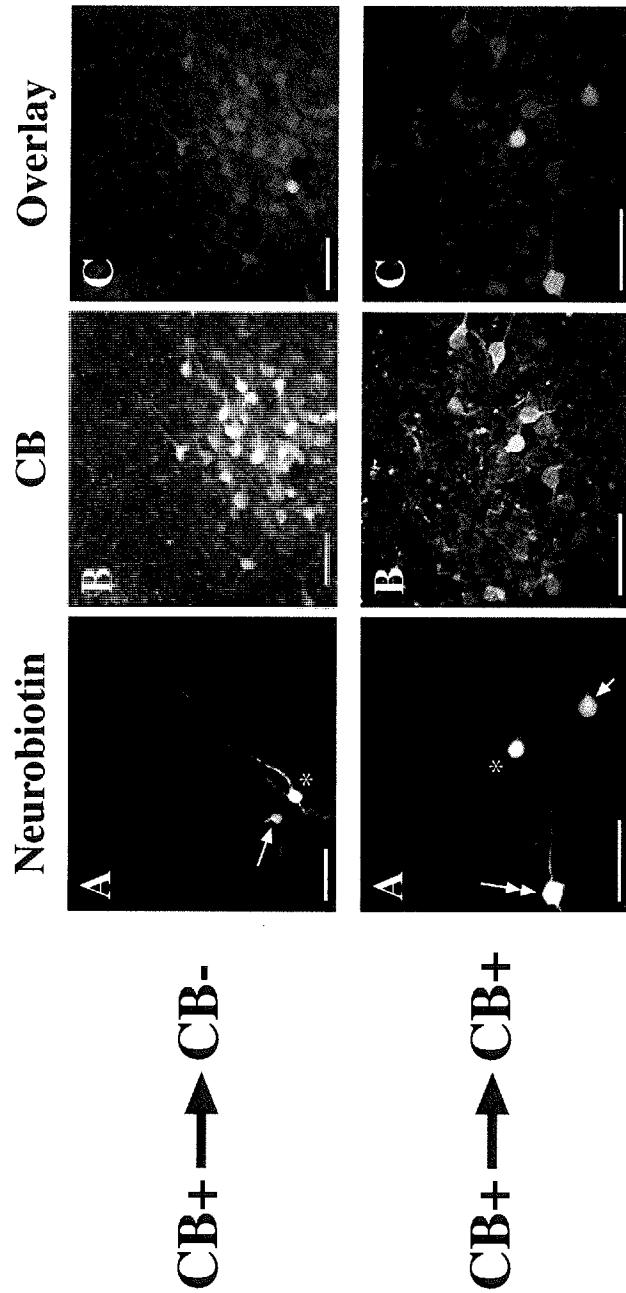


Fig 9. Tracer-coupling between identified neurons in the hamster CBsn. (A) Neurobiotin-filled neurons visualized with streptavidin fluorescein. The cells directly filled were identified by coordinates measured during recording. Recorded neurons are indicated by an asterisk (*). Tracer-coupled neurons are indicated by arrows. (B) CB-IF neurons visualized with Alexa 568. (C) Overlay images of A and B. Neurons that appear yellow contain both Neurobiotin and calbindin. The top 3 panels show tracer coupling between a recorded CB+ neuron (*) and a CB- neuron (arrow) at ZT18. In Panel A (top), it is possible to see the processes of the two neurons contact. The bottom 3 panels show a recorded CB+ neuron (*) coupled to one CB+ neuron (double arrow) and one CB- neuron (single arrow) at ZT17. In Panel A (bottom), the contact sites of the processes are out of the plane of section. Scale bars = 50 μ m.

contrast, two of nine CB+ neurons recorded during the night were tracer coupled to either CB+ or CB- neurons (Fig. 9). Although the data are suggestive of a diurnal difference in tracer coupling, this trend did not reach significance (Exact Unconditional Test: $p = 0.098$).

Immunolocalization of connexin 36 (Cx36), a transmembrane gap junction protein that has been specifically localized to neuronal membranes (Rash *et al.*, 2001), provided anatomical evidence for gap junctions in the CBSn. Cx36-IF was fairly evenly distributed throughout the entire SCN (Fig. 10A), appearing as scattered puncta within the CBSn (Fig. 10B). At higher magnification, Cx36-IF was detected in the somas of both CB+ and CB- neurons (Fig. 10C), strengthening the findings of tracer-coupling between both neuronal phenotypes.

DISCUSSION

The current study provides information about the anatomic basis of intercellular communication within the CBSn. Our findings support synaptic communication via GABA, neuron-to-neuron or glia-to-neuron communication via TGF α , and electrical communication via gap junctions. In a previous study, we proposed that intercellular communication is essential to integrate outputs from rhythmic (CB-) neurons and nonrhythmic (CB+) neurons for the production of a circadian output in the intact animal. Consistent with this suggestion, evidence has shown that GABA and TGF α are two potential synchronizing agents in the SCN (Liu and Reppert, 2000; Kramer *et al.*, 2001). In addition, the orientation of dendritic arbors within the CBSn tends to be dorsal, providing insight as to the origin of inputs. CB+ neurons have more dendrites, suggesting

CB/Cx36

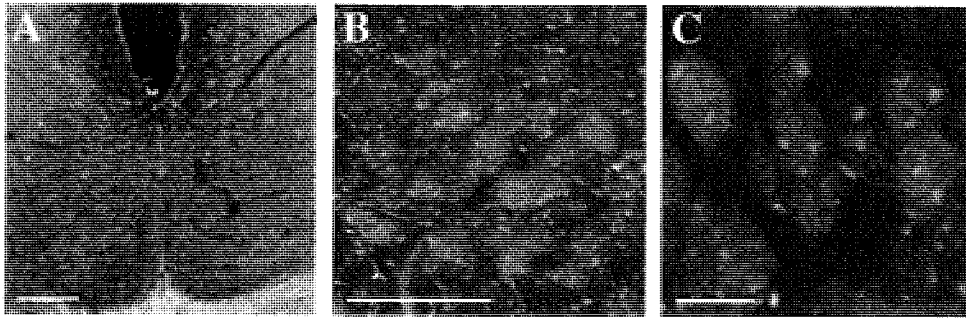


Fig 10. Cx36 expression in the hamster SCN. Figures represent single confocal digital images of double-label immunofluorescence for CB (red) and Cx36 (green). (A) Cx36 is densely distributed throughout the SCN. (B) Cx36 is seen primarily in punctate profiles throughout the CBSn (1.0 μm resolution). (C) At higher magnification, Cx36-IF is seen in CB-IF somas and unlabeled somas (0.5 μm resolution). Scale bars = 100 μm (A), 50 μm (B), 10 μm (C).

that they play a more integrative role in this region. The present results provide the anatomical framework necessary to gain a better understanding of intercellular communication within the CBsn.

Neuronal cytoarchitecture within the CBsn

Based on our analysis of filled cells, we have described several morphological properties of neurons within the CBsn (Table 1). The most important finding of our study was that CB+ neurons have significantly more dendrites than their CB- counterparts within the CBsn. While only 21% of CB- neurons had more than 2 dendrites, 69% of CB+ neurons had 3 or more dendrites. Based on van den Pol's morphological classification (van den Pol, 1980), CB+ neurons would most closely be classified as radial multipolar, whereas CB- neurons would be simple bipolar or monopolar. These results suggest that CB+ neurons have a large capacity for dendritic integration of synaptic inputs or that they may segregate inputs differently. Our data are consistent with evidence that CB+ neurons receive multiple intra-SCN inputs (LeSauter *et al.*, 2002).

The dendritic arbors of both CB+ and CB- neurons were primarily oriented dorsally, indicating that neurons in the CBsn receive synaptic input from dorsal regions. Of note, LeSauter *et al.* (2002) demonstrated a lack of reciprocal communication between CB+ neurons (located in the ventrolateral subdivision) and vasopressinergic neurons, which are densely packed in the dorsomedial subdivision of the hamster SCN (Card and Moore, 1984). However, this study only investigated somal appositions within the CBsn and most synaptic interaction in the SCN is axo-dendritic (van den Pol, 1980, 1986; Bosler, 1989). Our evidence shows that dendrites from neurons within the CBsn are

appropriately situated to receive input from neurons within the dorsomedial subdivision of the SCN, though the neuropeptide phenotype of these neurons remains unknown.

To our knowledge, the morphology of only one other phenotypically identified neuron has been studied in the SCN. After intracellular recording, Pennartz *et al.* (1998) investigated the morphological properties of 24 vasopressin (VP) neurons in the rat SCN. With few dendrites and axons with multiple collaterals coursing into target structures, VP neurons were identified as SCN projection neurons. In contrast, axons of neurons within the CBSn were neither as long as those reported by Jiang *et al.* (1997), nor did they demonstrate the collateral branching of VP or other SCN neurons (van den Pol, 1980; Jiang *et al.*, 1997; Pennartz *et al.*, 1998). Although it is possible that parts of processes leaving the section were not measured, more than seventy percent of the processes we identified as axons had clear axon terminals, strengthening our identification of a process as an axon as well as its termination point. It is more likely that the markedly shorter axons we report in the hamster CBSn represent true differences from those previously reported in the rat SCN. Consistent with another report (LeSauter *et al.*, 2002), CB+ neurons, as well as CB- neurons in this region, are likely to be intra-SCN projection neurons.

GABA in the CBSn

Although GABA has been identified in most neurons and terminals in the SCN (van den Pol, 1985; Moore and Speh, 1993; Morin and Blanchard, 2001), the GABAergic nature of neurons within the CBSn had not previously been examined. Our results show that most CB+ neurons colocalize GABA, indicating that CB+ cells are likely to use GABA as a neurotransmitter. The present study also demonstrates that CB+ cells receive

GABAergic input. The close apposition of punctate GAD65-IF and CB-IF somas suggests that GABAergic terminals are appropriately situated to provide GABAergic synaptic input. This is also consistent with the presence of $\alpha 2$ and $\beta 2/3$ GABA_AR subunits in close contact with CB+ somas.

Cell-to-cell communication within the SCN clearly utilizes GABA. In addition, GABA may be involved in synchronizing firing rhythms through GABA_ARs. Though it is not yet known how this cellular synchronization occurs, GABA application synchronizes SCN cells in culture (Liu and Reppert, 2000). The authors proposed that GABA is an important endogenous synchronizer *in vivo*, rationalizing that the level of released GABA in culture was below threshold for synchronization. In the intact animal, GABA also alters behavioral rhythms (Ralph and Menaker, 1989; Gillespie *et al.*, 1997; Mintz *et al.*, 2002), presumably by changing the output of SCN neurons. While it remains unknown whether GABA *in vivo* synchronizes the firing rates of CB- and CB+ cells, we have demonstrated that the neurons in this SCN subregion have the anatomic capability to respond to GABA.

Our data demonstrate a high level of $\alpha 2$ and $\beta 2/3$ subunit expression within the hamster SCN, but no significant $\alpha 1$ subunit expression. These findings are consistent with previous studies exploring the GABA_AR subunit composition in the SCN (Araki and Tohyama, 1992; O'Hara *et al.*, 1995). Only one study assessed the distribution of GABA_AR subunit proteins in the hamster SCN, detecting $\alpha 2$, $\alpha 5$, $\beta 1$ and $\beta 3$ subunits (Naum *et al.*, 2001). However, this study was limited by the inability to determine the cellular localization of these subunits. Based on analysis of subunit expression in the rat central nervous system, $\alpha 2$ and $\beta 3$ mRNAs tend to have similar expression patterns,

suggesting that these are functional subunit combinations forming GABA_ARs (Wisden *et al.*, 1992). Our data are consistent with GABA_ARs in the hamster CBsn having the $\alpha 2/\beta 3$ composition. Since the subunit make-up of the GABA_AR, particularly its alpha-subunit content, determines its pharmacological characteristics, these results may have implications for the pharmacological properties of this region (Mehta and Ticku, 1999). A limitation of this study is that we did not localize the GABA_AR subunits to either a perisynaptic (postsynaptic) or presynaptic arrangement on the somas. Further study using ultrastructural techniques is needed to confirm this localization.

The role of TGF α in the CBsn

Early studies established that the transplanted SCN can restore circadian rhythms of locomotion via a diffusible output signal (Silver *et al.*, 1996a). In addition, the strength of rhythmicity was correlated with the presence of CB+ neurons within the transplants (LeSauter and Silver, 1999). Taken together, these results suggest that a diffusible messenger may either be released from or acted upon CB+ cells in the CBsn of the hamster SCN. Recently, it was shown that TGF α , a candidate diffusible SCN output factor, inhibited locomotion in hamsters during constant infusion into the third ventricle (Kramer *et al.*, 2001). The above findings prompted our investigation of TGF α expression in the CBsn. Although a recent study has shown that glial cells are the primary source of TGF α within the hamster SCN (Li *et al.*, 2002), we found that the differential expression of TGF α in neurons and non-neuronal cells was dependent on detergent conditions during immunohistochemical processing. Under detergent-free conditions, TGF α was predominantly expressed in neurons, but it could also be detected in processes and fibers that are presumably of glial origin (Fig. 7A, B; Li *et al.*, 2002). Our prediction

is that detergent causes TGF α to dialyze out of neurons, but not out of non-neural cells. It is critical to emphasize that the presence of TGF α in neurons may reflect ligand uptake and not synthesis. To determine whether neurons or glia are the source of TGF α , in situ hybridization studies should be done.

Regardless of whether TGF α is synaptically released by neurons or trans-synaptically released by astrocytes, all of TGF α 's actions are mediated by the EGF-R (ErbB1), a member of a family of receptor tyrosine kinases. Although Kramer *et al.* (2001) demonstrated EGF-R expression only in the sPVZ, a primary efferent target of the SCN, our results demonstrate EGF-R expression in many SCN neurons (Fig. 8). Previous reports have localized EGF-R mRNA in discrete regions of the rat brain (Kaser *et al.*, 1992; Seroogy *et al.*, 1994) and neuronal expression of EGF-R has been shown in GABAergic neurons within the rat striatum (Kornblum *et al.*, 1995). To our knowledge, this is the first demonstration of EGF-R specifically within SCN neurons.

Although little is known about the signaling functions of EGF-R in neurons, evidence indicates that ion channels are among the targets of tyrosine kinases (Siegelbaum, 1994; Jonas and Kaczmarek, 1996). In a human cell line overexpressing EGF-R, protein phosphorylation at tyrosine residues activates calcium channels, which in turn open calcium-activated potassium channels, causing neuronal hyperpolarization (Peppelenbosch *et al.*, 1991). However, if calcium influx is strongly buffered by an endogenous calcium buffer, calcium-activated potassium channels may not be activated, and the result of EGF-R activation could be depolarization. Hence, the functional consequences expected from activation of EGF-R may be modulated by the presence of the endogenous calcium buffer calbindin. Future studies need to examine the effects of

TGF α on CB+ and CB- neurons within the CBsn. Our results demonstrate that TGF α and its receptor are expressed within the CBsn, consistent with the role both TGF α and the CBsn play in locomotor behavior in hamsters.

Gap junctions within the CBsn

Using physiological tracer coupling and anatomical immunolocalization of a neural gap junction protein, we identified gap junctions in neurons within the CBsn. Although neuronal coupling was not found in cultured SCN cells (Welsh and Reppert, 1996), gap junctions between neurons are present in SCN slices (Jiang *et al.*, 1997; Colwell, 2000). We found roughly 20% of CB+ neurons were tracer-coupled at night while none were coupled during the day. Although this observation did not reach statistical significance, it is suggestive of a trend in nocturnal coupling of CB+ neurons. These findings are in contrast to those of others, in which more tracer coupling occurred during the day in SCN neurons (Jiang *et al.*, 1997; Colwell, 2000). Colwell reported three times more tracer coupling during the day, suggesting that this may be due to more electrical activity during this period. This is consistent with the fact that tetrodotoxin and muscimol, agents that decrease spontaneous activity in the SCN, decrease coupling (Colwell, 2000; Shinohara *et al.*, 2000). Since CB+ cells demonstrate no diurnal peak in spontaneous firing activity (Jobst and Allen, 2002), this could contribute to the lack of tracer coupling we observed during the day in this population. An intriguing speculation is that functional gap junctions are rhythmically regulated in the CBsn. If CB+ cells are not electrically coupled to CB- cells during the day, CB- cells may not impart rhythmic oscillations to CB+ cells.

Anatomic evidence for neuronal gap junctions in the CBSn was derived from the immunolocalization of Cx36, a connexin protein identified by freeze-fracture replica immunogold labeling as a neuronal gap junction partner (Rash *et al.*, 2001). Although our tracer-coupling data demonstrate tracer coupling involving neuronal processes (Fig. 9), the strong punctate labeling in the somas (Fig. 10) is characteristic of that previously reported for Cx36 (Belluardo *et al.*, 2000; Rash *et al.*, 2001). This may be due to the fact that the amount of connexin protein at physiological points of contact is below the resolution of light microscopy. The fact that nonrhythmic CB+ neurons are coupled to rhythmic CB- neurons suggests that this may be one possible mechanism of intercellular synchronization used within the CBSn.

Functional implications of the morphological properties of SCN neurons within the CBSn

Evidence to date suggests that CB+ neurons within the hamster CBSn are a nonrhythmic population (Hamada *et al.*, 2001; Jobst and Allen, 2002). How is this reconciled with evidence that the presence of CB+ neurons is correlated with the restoration of circadian locomotion (LeSauter and Silver, 1999)? It is possible that CB+ cells within the CBSn are lacking the intrinsic mechanism to be circadian oscillators. Alternatively, synaptic input provided to CB+ neurons *in vivo* (or in a different *in vitro* slice orientation) may allow their output to be integrated with that of rhythmically firing neurons. The current results provide a neuroanatomical framework for synaptic communication, electrical coupling, and neuron-to-neuron or glia-neuron signaling via a growth factor within the CBSn of the hamster SCN. Synaptic release of GABA and electrical coupling via gap junctions may act to synchronize the output of CB+ neurons and CB- neurons. In addition, actions of the paracrine factor TGF α may have differential

actions on CB+ and CB- neurons, ultimately imparting different downstream signal cascades that may be relevant for output signals to locomotor effectors. Whether these mechanisms represent possible mediators of interneuronal rhythm synchrony in the CBsn remains to be tested. While it is difficult to draw a circuit diagram, our anatomical study provides testable hypotheses for how the structural characteristics of CB+ and CB- neurons in the CBsn can be related to their electrophysiological function within the SCN.

Acknowledgments

We would like to thank Aurelie Snyder of the OHSU-MMI Research Core Facility for her assistance with confocal microscopy and Michael Lasarev for statistical assistance. This work was supported by NINDS grants NS036607 (C.N.A.) and NS42406 (E.E.J.).

IV. Discussion and Conclusions

At the outset of this project, almost nothing was known about the CBSn, except that CB+ cells were considered critical for the maintenance and restoration of behavioral rhythmicity. Over the past four years, remarkable progress has been made in detailing the functional and anatomical organization within this subregion of the hamster SCN. In Figure 1 (Discussion), I have incorporated my data (red), as well as those of others (blue) that have made significant contributions to understanding this critical SCN subregion.

Using single cell recordings from an *in vitro* slice preparation, my data (Manuscript #1) demonstrate that CB+ neurons, surprisingly do not exhibit a circadian oscillation in spontaneous firing rate. On the other hand, CB- neurons from this region have a circadian output in SFR. Significantly, this study also revealed that the CBSn is *not* a homogeneous population of CB+ cells, and, in fact, only a small percentage of neurons in the CBSn are immunoreactive for CB.

From neuronal reconstructions, I defined CB+ and CB- neuronal morphology. Contrary to data demonstrating that core SCN neurons are projection neurons (Figure 2, Introduction; Moga and Moore, 1997; Leak and Moore, 2001), my axonal measurements illustrate that CB+ and CB- neurons project relatively short intra-SCN distances. My results are consistent with those of LeSauter *et al.* (2002). Using injections of biotinylated dextran amine into the CBSn, they identified no *reciprocal* connections from CB+ neurons to AVP neurons within the shell subregion. However, my evidence shows that dendrites of CB+ neurons are appropriately situated to receive input from neurons within the shell subdivision. Further studies need to be done to determine the connectivity between core CBSn neurons and neurons within the shell.

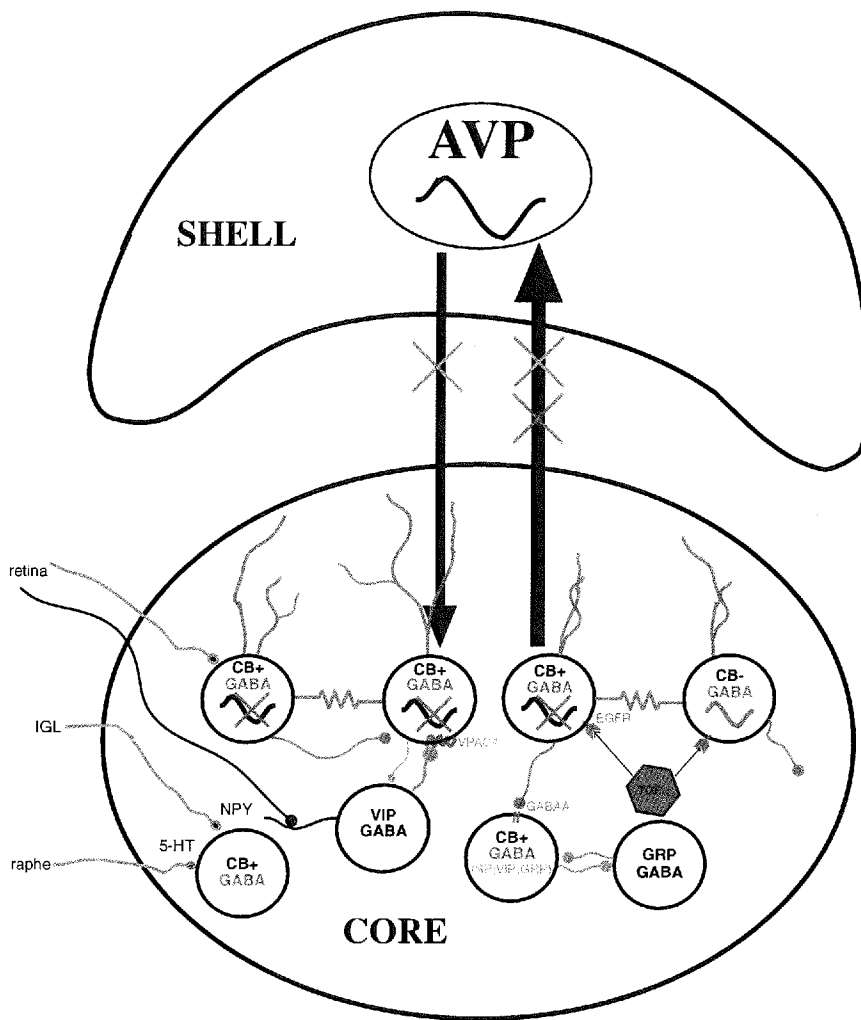


Fig 1. Schematic of anatomical organization of the hamster SCN. This revised core-shell model (see Fig 2, Introduction) contains recent data from my research (highlighted in red), as well as those of others (highlighted in blue; Bryant *et al.*, 2000; LeSauter *et al.*, 2002) since my investigation began. Thickness of axons indicates strength of projections. X's between Shell and Core indicate a lack of connectivity between CB+ neurons and AVP+ neurons (based on LeSauter *et al.*, 2002; Jobst *et al.*, 2003). See Discussion for details.

Lastly, my research (Manuscript #2) has highlighted anatomical circuitry within this subregion that may allow for the coordination or synchronization of outputs from neurons with distinct firing rates. My work has shown that CB+ neurons use GABA as a main neurotransmitter and that they receive GABAergic input. CB+ neurons may communicate with other CBSn neurons via gap junctions, in a manner that may be diurnally regulated. My identification of TGF α and its receptor, EGF-R, within the CBSn are especially interesting in light of the recent description of the role of this growth factor in controlling locomotion in the hamster (Kramer *et al.*, 2001).

My thesis work has provided the only functional information about the electrical activity of CB+ neurons in the CBSn. In addition, my work has defined the CBSn as a heterogeneous subregion of the SCN, with neurons interconnected by GABAergic synapses, gap junctions and at least one growth factor. My findings have raised many interesting questions about how this complex network is responsible for circadian behaviors. In the remainder of this discussion, I present a synopsis of several speculations and potential future studies, as well as a few caveats.

(A) If CB+ neurons are arrhythmic, how might intercellular connectivity within the CBSn produce a rhythmic behavioral output?

Original studies demonstrated the importance of the CBSn to locomotor rhythmicity based on the following data: (1) smaller lesions than previously used, which were centered on the CBSn, resulted in loss of circadian rhythmicity; (2) transplanted grafts were successful in restoring behavioral rhythmicity, probably via a diffusible factor, only when CB+ neurons were present; and, (3) the absolute power of locomotor

rhythmicity was significantly correlated with the number of CB+ neurons in the graft (LeSauter and Silver, 1999). The current interpretation of these data is that CB+ neurons *alone* are responsible for the restored rhythms. There are, of course, alternative conclusions that can be drawn.

One possibility is that another population of unidentified pacemaker cells lies within or near the CBSn, and this population is responsible for the maintenance and restoration of behavioral rhythmicity. Thus, identification of CB+ neurons as the key cells may be a red herring, diverting our attention from the ‘real’ pacemakers. However, there is no evidence to date to suggest that an additional group of cells is responsible.

An alternative possibility is that intercellular interactions between CB+ and CB- cells within the CBSn are the “key” to restoration of behavioral rhythmicity. Since the free-running period of individual oscillators differ within the SCN (Welsh *et al.*, 1995; Honma *et al.*, 1998), it has been implicitly assumed that intercellular communication must maintain synchrony within a population of SCN neurons. The results presented in Manuscript #2 provide an anatomic foundation upon which future physiological investigations into the communication between CB+ neurons and CB- neurons can be performed.

GABA and gap junctions

Neurons interconnected by electrical and GABAergic synapses have been well studied in many regions of the brain (Galarreta and Hestrin, 2001a). Physiological and modeling studies have suggested that gap junctions between GABAergic interneurons often generate and facilitate synchronous activity as an emergent property of their interconnections (Bragin *et al.*, 1995; Bartos *et al.*, 2001).

Despite previous demonstrations of dye coupling between adult SCN neurons and proposals that gap junctions may form a critical component of intercellular communication (van den Pol and Dudek, 1993; Jiang *et al.*, 1997; Colwell, 2000), simultaneous recordings from pairs of electrotonically-coupled neurons have not been performed in the SCN. Using dual-cell recordings, direct evidence for electrotonic coupling between two neurons can be obtained by injecting current into one cell and observing a potential change in a second (coupled) cell. Though dual-cell recordings have been technically difficult in other regions due to the preselection necessary to finding a connected cell, the CBN of the hamster SCN may be an ideal location for this type of investigation because it is a small, well-defined subregion of the SCN known to contain gap junctions. My studies have provided morphological and immunohistochemical evidence of electrotonic coupling between GABAergic CB+ and CB- neurons. Future studies should address several aspects of the nature of electrotonic coupling between neurons with identified CB phenotypes within the CBN.

Perhaps the most obvious question to answer is whether electrically coupled neurons (for example, a CB+ and a CB- neuron) show synchronous action potentials. In the locus ceruleus, this is not the case (Christie *et al.*, 1989). Rather, electrical coupling acts as a low pass filter, synchronizing slow spontaneous subthreshold membrane potential oscillations (MacVicar and Dudek, 1981; Galarreta and Hestrin, 2001b). Instead of an action potential being transmitted from one neuron to a second neuron, a train of presynaptic spikes can result in a postsynaptic *hyperpolarization* due to the electrical transmission of the afterhyperpolarization (Galarreta and Hestrin, 2002). How then might CB+ and CB- neurons be synchronized? In the SCN, neurons demonstrate spontaneous

(TTX-insensitive) oscillations in membrane potential which occur selectively during the daytime (Pennartz *et al.*, 2002). The oscillations, primarily generated by a diurnal rhythm in the L-type calcium current, provide an excitatory drive for the high daytime SFR characteristic of most SCN neurons. Although CB+ neurons do not fire action potentials at high frequency during the day, daytime oscillations in subthreshold depolarization could still be transmitted from CB+ neurons to both CB+ (nonrhythmic) and CB- (rhythmic) electrically coupled neurons. Electrical transmission of subthreshold depolarizations through CB+ neurons may contribute to the firing rate of other neurons, and thus be critical to synchronizing neuronal activity throughout the nucleus.

The strength of electrical coupling between identified neurons in the CBsn should be determined by measuring the coupling coefficient (the ratio between the voltage change observed in the noninjected and the injected neuron). Although the average range of coupling coefficients in the literature is roughly 3-10%, the strength of coupling between individual neurons varies from less than 0.5% to 40% (Galarreta and Hestrin, 2001a). Given that there is evidence that subthreshold rhythmic oscillations between coupled cells are dependent on extracellular calcium (Christie *et al.*, 1989), and that gap junction permeability is strongly affected by intracellular calcium concentration (Bennett *et al.*, 1991), it might be anticipated that coupling strength varies, depending on whether neurons contain CB, a high affinity calcium buffer.

It is also likely that there is an interaction between electrical and GABAergic synapses within the CBsn. In organotypic slice cultures of rat SCN, GABA_A receptor activation inhibited gap junction propagation of an evoked depolarization (Shinohara *et al.*, 2000). With dual-cell recordings, the interplay between GABA_A receptors and gap

junctions could be directly investigated. In the neocortex, when electrical and GABAergic synapses coexist between two neurons, a presynaptic action potential produces a complex response in the postsynaptic neuron. Initially, there is a (biphasic) voltage-independent electrical component and a voltage-dependent GABA_A receptor-mediated component (Galarreta and Hestrin, 2001b). Although the latter is normally hyperpolarizing, this is dependent on the resting membrane potential of the postsynaptic neuron, which is determined by its intrinsic activity as well as synaptic influences. Thus, a situation can be envisaged in which combined electrical and GABAergic signaling could promote synchronous spiking in the SCN. For example, almost synchronous excitatory retinal inputs onto different neurons in the CBSn would promote a mutual depolarizing phase of the electrical response, possibly inducing a group of coupled CBSn neurons to fire synchronously. This response is dependent on nearly synchronous excitatory input, for if the input is delayed, then the GABA_A receptor-mediated component will predominate. In the SCN, this latter voltage-dependent response is likely dependent on circadian cycle, as the membrane potential of daytime neurons is more depolarized than nighttime neurons (de Jeu *et al.*, 1998; Pennartz *et al.*, 2002). In summary, coincident retinal input in the intact animal could be the excitatory stimulus that allows a group of electrotonically-coupled interneurons to fire in synchrony and contribute to the overt (rhythmic) output from the SCN.

Lastly, future studies should also address additional anatomical questions about gap junctions between CBSn neurons. First, it should be determined whether there is a “microdomain” for electrotonic coupling within the CBSn. For example, is coupling spatially restricted to neurons within the CBSn? In terms of anatomical SCN organization,

is coupling restricted to neurons within the core? Or, does coupling extend from neurons in the core (CBsn) to neurons in the shell? Electron-microscopy studies could be done to assess the precise location of gap junctions in this region because the cellular location of gap junctions has functional implications. For example, coupling in dendritic segments proximal to the soma would decrease the time for signal transduction, whereas coupling in distal segments would be subject to dendritic filtering properties. From my reconstructed cells, tracer-coupling occurred at neuronal processes. Most often, gap junctions are found between two dendrites (Fukuda and Kosaka, 2000; Tamas *et al.*, 2000); no study to date has demonstrated gap junctions between two axons (Galarreta and Hestrin, 2001a).

My thesis research has provided morphological and immunohistochemical evidence of electrotonic coupling between GABAergic CB+ and CB- neurons within the CBsn. Although results from these proposed studies would not directly address the mechanism by which SCN grafts (with CB+ neurons) restore circadian behaviors, they would provide valuable data about how extensive the interconnected network of electrical and chemical synapses is in the CBsn and how these may be affected by CB phenotype and circadian time.

(B) Are CB+ neurons in the CBsn truly arrhythmic?

During the course of my investigation of the SFR of CB+ cells, Hamada *et al.* (2001) demonstrated that *Per1* and *Per2* mRNA do not rhythmically oscillate in the CBsn. They concluded that *all* neurons within the CBsn are not functional pacemakers. These data, along with my findings that CB+ neurons do not express a circadian variation

in SFR, are consistent with the possibility that CB+ neurons are not rhythmic oscillators. However, some additional experiments could strengthen this assertion before a definitive conclusion is made.

First, Hamada *et al.* did not perform combined in situ hybridization (ISH) and immunohistochemistry (IHC) to determine definitively whether CB+ neurons lack rhythmic *Per* expression. Given that the CBSn is not a homogenous population of CB+ neurons (Manuscript #1), it remains possible that CB+ neurons may rhythmically express *Per* mRNA, but that the signal was missed in the gross ISH signal. Future studies using combined ISH/IHC should be performed to conclude definitively whether CB+ neurons, which form a small proportion of the CBSn, lack rhythmic clock gene expression.

Second, the conclusion drawn from my electrophysiological study is that under *diurnal* conditions, CB+ neurons in a *coronal slice preparation* do not exhibit a rhythmic variation in SFR. This set of conditions represents a particular situation in which multiple variables (or a combination of them) may affect the result. It must be considered that the failure of CB+ neurons to fire rhythmic action potentials could be an artifact of the conditions under which they were studied. Future studies should assess each of these variables for their possible contribution to the outcome of the study. Briefly, I will address each of these variables and the potential impact on SCN electrical activity.

I recorded from slices obtained from animals housed in LD conditions because my initial interest was the electrophysiological activity of CB+ neurons in the context of a normal 24-h LD cycle. However, it is possible that the rhythmicity of CB+ neurons could have been masked by prior visual input. For example, VIP gene expression in the SCN shows a clear diurnal rhythm, but shows no circadian fluctuation under constant

dark (DD) conditions in the adult animal (Introduction, Section D). A few investigators have hypothesized that VIP mRNA has an endogenous rhythm, but that it is masked by neural inputs from outside the SCN, including primary and secondary visual afferents. This theory is based upon evidence describing an endogenous rhythm in VIP expression under DD conditions either during early developmental stages (Ban *et al.* 1997) or in adult serotonergic afferent-lesioned rats (Okamura *et al.* 1995). As CB+ neurons in the CBsn receive dense retinal innervation (Bryant *et al.*, 2000), it is possible that prior visual input may have masked endogenous rhythmicity. Future studies should examine the circadian pattern of SFR of CB+ neurons from hamsters housed in DD conditions.

Slice orientation is another variable to consider in the interpretation of rhythmicity data. Although coronal, sagittal and horizontal slices have all been used in electrophysiological recordings in the SCN (Kim and Dudek, 1993; Thomson and West, 1990; Schaap *et al.*, 1999), each orientation results in the selective preservation and destruction of connections. As discussed above, the removal of certain synaptic connections (or the presence of others) could liberate or promote endogenous rhythms. Jagota *et al.* demonstrated that slice orientation has functional consequences (2000). The circadian rhythm of SFR, recorded as a single daytime peak in coronal SCN slices, showed two distinct peaks when slices are cut in the horizontal plane. However, it is unknown whether both activity peaks originated in single cells or whether they were produced by distinct cell populations. While CB+ neurons do not demonstrate rhythmic firing in the coronal slice, this population of SCN neurons should be studied in different slice orientations to evaluate the impact of the presence (or loss) of connections.

Regardless of slice orientation, the slice preparation always results in loss of connectivity to and from the region under study. Ultimately, to understand the role of CBsn in the intact animal, the electrical activity of CB+ neurons should be assessed *in vivo* in the hamster SCN. Extracellular recording from single SCN neurons could be performed in anesthetized hamsters, using the coordinates of LeSauter and Silver for the CBsn (1999). To increase the probability of recording from CB+ neurons, SFR recordings should preferentially be performed on neurons with optic nerve input. CB+ neurons receive dense retinal input, with retinal terminals making primarily axo-somatic contacts with CB+ perikarya (Bryant *et al.*, 2000). Optic nerve input to a cell under study could be determined by whether the cell responded to electrical stimulation of the optic nerve or changes in ambient light intensity (Saeb-Parsy and Dyball, 2003). After SFR recordings, neurons could be filled with biotinamide, using a juxtacellular labeling method (Pinault, 1996; Aicher *et al.*, 2001) and subsequently phenotypically characterized by IHC. Though this procedure would be labor-intensive, there is evidence that subpopulations of SCN neurons have different SFR, dependent on efferent and afferent connections *in vivo* (Saeb-Parsy and Dyball, 2003).

(C) What's calbindin got to do with it?

This discussion would be incomplete without addressing a seemingly overlooked question: does calbindin itself play a role in restoring or maintaining behavioral circadian rhythmicity? Or is CB simply a marker for an SCN subregion that is critical? Throughout my research and that of others, CB has been used as a neuroanatomical marker to define distinct subpopulations of neurons. However, CB is a major calcium-binding protein in

the nervous system, with well-described calcium-buffering properties. In addition, new roles for CB as a “trigger” protein, which changes conformation after binding calcium and modulates the activity of enzymes, have recently been described. I will review direct and indirect evidence for some physiological roles of CB, as well as my speculations of what CB’s role may be in the SCN.

One of the physiological functions described for CB is its ability to regulate patterns of action-potential firing within at least two brain regions, the frontal cortex and the supraoptic nucleus (Kawaguchi and Kubota, 1993; Li *et al.*, 1995). In the SCN, two difficulties presented themselves as insurmountable in the direct assessment of whether CB controlled neuronal firing patterns. First, in order to eject CB or an antibody against CB from the recording patch electrode into the neuron, whole-cell patch-clamp mode would be required. In the SCN, spontaneous firing dramatically decreases in whole-cell mode within minutes – a time considerably shorter than that for diffusion of CB or anti-CB from the pipette to the neuron (Schaap *et al.*, 1999; Li *et al.* 1995). Second, with the ejection of either substance, it would be impossible to discriminate the presence of endogenous CB. Of note, I recorded from three CB+ neurons, outside of the CBsn, but still within the SCN. The average firing rate of these neurons was significantly higher (mean SFR > 6 Hz; Appendix, Table 1) than that of CB+ neurons within the CBsn. These data are suggestive that, within the SCN, CB may not control spontaneous firing rates.

If CB were involved in the maintenance of behavioral rhythmicity, it might be expected that transgenic calbindin-deficient mice demonstrate atypical or absent circadian rhythms. Although calbindin null mutant mice have been generated (Airaksinen *et al.*, 1997), their circadian phenotype has not yet been reported. Even if these transgenic

animals demonstrate aberrant circadian rhythms, caution should be taken in the interpretation of this finding. First, CB is present in select populations of neurons throughout the brain. CB plays many roles in development and physiology, independent of its role in circadian rhythms. In addition, compensatory mechanisms often occur in knock-out animals and these must be considered when interpreting results. In addition, the role of CB+ neurons in circadian rhythms has only been characterized in the hamster. It is possible that CB's potential role in the SCN may be a species-specific phenomenon.

On the other hand, the results of a more direct investigation suggest that CB might *not* be involved in circadian rhythmicity. Hamada *et al.* recently reported that circadian rhythms were unaffected after injection of antisense oligonucleotides for CB into the 3V of hamsters (Society for Research on Biological Rhythms, 2002). Instead, antisense treatment changed the effect of light-induced phase shifts and gene expression. In normal hamsters, light pulses during the night phase cause phase shifts in circadian rhythms and induction of *Per1* mRNA in select SCN neurons. Conversely, light pulses during the day have no effect. In contrast, antisense-treated hamsters lacked the normal responses to light pulses at night, but responded to light pulses during the day with phase shifts and *Per1* induction. The investigators interpreted these findings to mean that CB acts as a photic "gate" in the SCN. In other words, CB may signal the SCN when light is a relevant input and when it is not. Interestingly, this finding of differential sensitivity to light is consistent with a report that the number of CB+ neurons in the rat SCN is increased significantly during the dark phase (Arvanitogiannis *et al.*, 2000).

Although calbindin's physiological roles in other regions of the brain have been attributed to its function as a high affinity calcium buffer, recent evidence suggests that

CB may also serve as a calcium sensor or “trigger” protein, similar to calmodulin (Baimbridge *et al.*, 1992). Using spectroscopic and fluorescence methods, Berggard *et al.* demonstrated that CB undergoes a conformational change during calcium binding (2002a). In addition, they have identified myo-inositol-1 (or 4)-monophosphatase (IMPase) as a potential target of CB (Berggard *et al.*, 2002b). IMPase is a key enzyme in the regulation of the phosphatidylinositol-signaling pathway. It catalyzes the hydrolysis of myo-inositol-1 (or 4)-monophosphate to form free myo-inositol, thus maintaining a supply that represents the precursor for inositol phospholipid second messenger systems. During cell stress conditions of low pH and substrate concentration, a situation in which CB gene expression is upregulated (Lowenstein *et al.*, 1991), CB activates IMPase up to 250-fold. Thus, CB’s physiological role could be attributed to its effects on PI-linked signal transduction. Future experiments in slice recordings could assess whether differences in signaling cascades exist between CB+ and CB- neurons in the SCN.

Of special interest to a potential role in the SCN, a second function has recently been attributed to CB. Since calmodulin is required to activate nitric oxide synthase (NOS) in the brain (Stamler *et al.*, 1992), investigators evaluated whether such a role could exist for CB. Tao *et al.* used spectroscopic methods to assess directly whether cysteine residues in CB react with thiol groups of cysteines to form S-nitroso compounds (2002). S-nitroso compounds can donate nitric oxide (NO) to other proteins, effectively prolonging the life of this labile free radical. Their results demonstrated that CB can be nitrosated, concluding that CB could act as a NO buffer or reservoir in the brain. In the SCN, very little NOS has been detected in the SCN by diaphorase staining, although biochemical assays have shown that the SCN has high NOS activity (Chen *et al.*, 1997).

In vivo and *in vitro* application of NOS inhibitors block the nighttime light (or glutamate)-induced resetting of behavioral rhythms and peak of SFR, respectively (Ding *et al.*, 1994; Gillette and Tischkau, 1999). Given the similarity of these results to those of the CB antisense injections in hamsters (Hamada *et al.*, 2002), a link between CB and its potential role as a NO reservoir in light-induced phase shifts should be more directly assessed. In the earlier experiments (LeSauter and Silver, 1999), lesions of the CBsn could represent the loss of a crucial NO reservoir in the SCN. Moreover, the grafts with CB+ neurons that restored behavioral rhythmicity may have done so by releasing NO, a diffusible signal that would be able to permeate the encapsulated grafts.

In conclusion, my thesis research has answered questions about the functional output of CB+ neurons and provided a cellular anatomical framework within the CBsn of the hamster SCN. My *in vitro* experimental design can be used to test my anatomic observations as well as my current speculations. The results will shed more light on how the CBsn is involved in behavioral rhythmicity and phase shifts.

V. Appendix

Unpublished results and data not shown

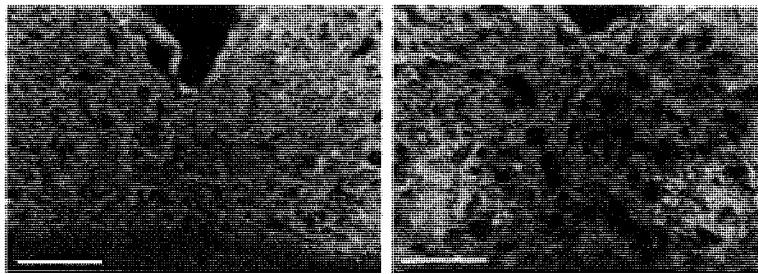


Fig 1. CB-immunoreactive neurons in coronal sections of hamster SCN. Confocal images of 50 μm coronal sections of hamster SCN (projection image of 10 individual 2.0 μm optical sections). Neurons are stained for glutamate decarboxylase (GAD)65 (red), one of the synthetic enzymes for GABA, which clearly outlines the borders of the SCN, and for calbindin (green). (A) Scattered CB+ neurons lie in the dorsolateral region of the rostral SCN. (B) More tightly packed subnuclei of CB+ neurons in mid-caudal SCN, (section B is 150 μm caudal to A). Scale bar = 100 μm .

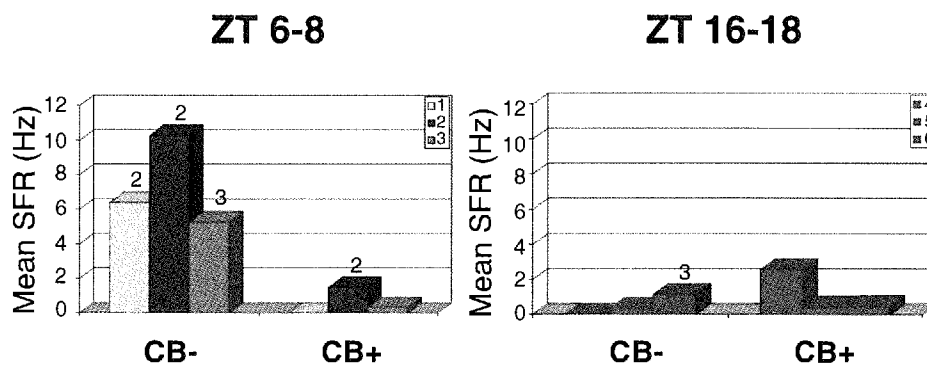


Fig 2. Comparison of mean SFR of CB- and CB+ neurons recorded during the same time epoch and in the same SCN slice. Bar colors indicate neurons from the same slice. Numbers above each bar indicate the number of cells recorded. Those without numbers indicate that only one cell was recorded.

Zeitgeber Time (ZT)	CB- in CBsn*	CB- out of CBsn*	CB+ in CBsn	CB+ out of CBsn
Daytime (ZT22-12)	4.2 ± 3.2 Hz (n = 88)	2.62 ± 2.64 Hz (n = 59)	0.66 ± 0.86 Hz (n = 14)	8.64 ± 0.46 Hz (n = 2)
Nighttime (ZT12-22)	1.47 ± 2.2 Hz (n = 65)	1.26 ± 1.55 Hz (n = 41)	0.68 ± 0.88 Hz (n = 7)	6.6 Hz (n = 1)

Table 1. Comparisons between daytime and nighttime mean SFR for four populations of cells in the hamster SCN. Columns with asterisks indicate that Mann-Whitney U tests revealed a significant difference between daytime and nighttime SFR ($p < 0.05$).

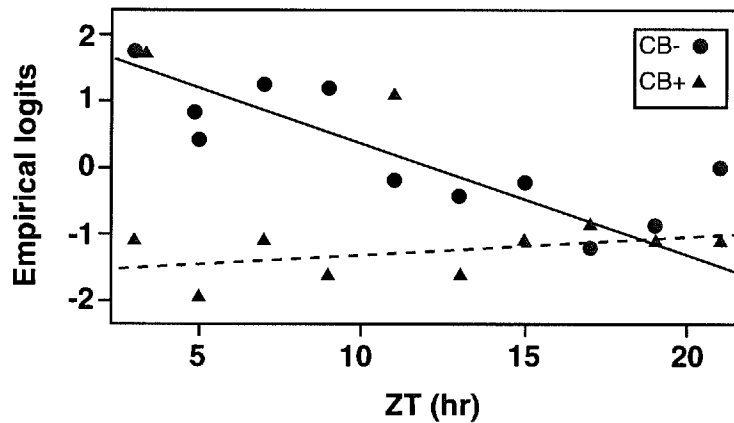


Fig 3. Plot showing empirical logits versus ZT epochs for each of two phenotypes. Spontaneous firing rates of CB- cells were significantly higher than SFR for CB+ cells during the day, but not during the night. Plot shows empirical logits (log_e (odds)) versus ZT epoch for CB+ and CB- cell phenotypes (see Manuscript 1: Methods, data analysis). Lines show the linear trend estimated from a logistic regression model (line through circles indicates trend for CB- cells; line through triangles indicates trend for CB+ cells). The downward slope of the linear trend for the CB- cells indicates that these cells are likely to fire above the median frequency during the day (ZT2 -< 14), and below the median frequency during the night (ZT14 -< 21). The linear trend for the CB+ cells is nearly flat, indicating that CB+ cells tend to fire below the median split, regardless of ZT.

Midpoint	Odds Ratio	95% CI
3	34.60	(4.24-636.9)
5	23.43	(4.10-281.7)
7	15.86	(3.80-126.6)
9	10.74	(3.17-60.2)
11	7.27	(2.35-32.5)
13	4.92	(1.50-23.6)
15	3.33	(0.87-21.6)
17	2.25	(0.46-22.0)
19	1.53	(0.22-22.8)
21	1.03	(0.10-25.2)

Table 2. Based on the logistic regression model (Fig 3, Appendix), odds ratios were calculated at the midpoint of each time epoch. Odds ratios are the odds that a CB- cell will fire above the median (1.8 Hz) relative to similar odds for a CB+ cell, together with 95% likelihood-based confidence intervals (CI). Confidence intervals that do not include one imply a significant difference exists; those that include one indicate no real change between the two odds. For example, during the ZT6-8 epoch, the odds a CB- cell will have a SFR above 1.8 Hz is estimated to be 15.86 times higher than the odds of a CB+ cell firing above 1.8 Hz (with a 95% CI from 3.80-126.6 times higher).

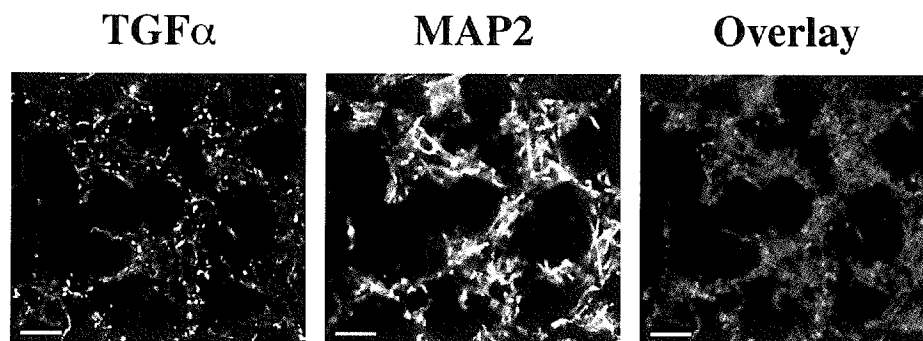


Fig 4. TGF α and microtubule associated protein-2 (MAP2) expression in the hamster SCN. Figure represents color confocal digital image (0.5 μ m resolution) of double-label immunofluorescence for TGF α (green) and MAP2 (red). Immunostaining for TGF α (rabbit anti-TGF α , 1:200; Peprotech, Rocky Hill, NJ) and MAP2 (mouse anti-MAP2, 1:400; Sigma, St. Louis, MO) are shown at the level of the CBSn. IHC was done with 0.2% Triton X-100 during the blocking incubation. Note lack of TGF α colocalization with MAP2, a stringent neuronal marker. Brain was from animal perfused at ZT 10. Scale bar = 10 μ m.

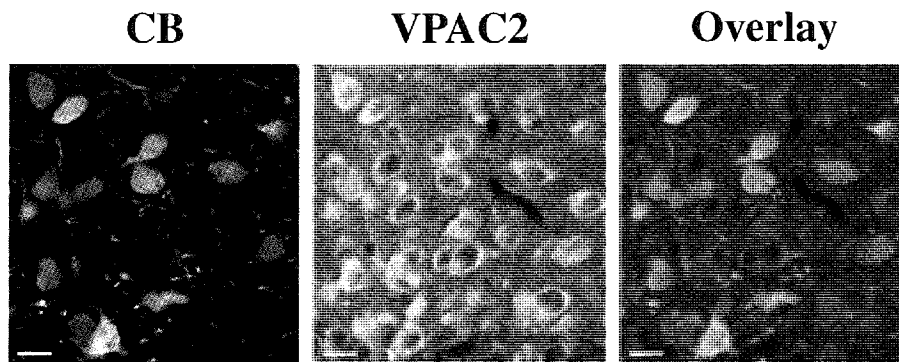


Fig 5. VPAC2 receptor expression in the CBsn of the hamster SCN. Figure represents color confocal digital image (2 μm resolution) of double-label immunofluorescence for CB (red) and VPAC2 receptor (red). Immunostaining for the VPAC2R (Mouse anti-VPAC2R, 1:100; Antibody Solutions, Palo Alto, CA) is shown at the level of the CBsn. Many neurons colocalized CB and the VPAC2R protein. Notably, VPAC2R labeling is only expressed in the cytoplasm (yellow), whereas CB labeling (Rabbit anti-calbindin, 1:1,000; Chemicon International, Temecula, CA) is in cytoplasm and nuclei. Scale bar = 10 μm . Brain was from animal perfused at ZT 14. 0.2% Triton was used during 2h blocking incubation.

VI. References

- Abe, M., Herzog, E.D. and Block, G.D. (2000) Lithium lengthens the circadian period of individual suprachiasmatic nucleus neurons. *Neuroreport* **11**, 3261-3264.
- Abrahamson, E.E. and Moore, R.Y. (2001) Suprachiasmatic nucleus in the mouse: retinal innervation, intrinsic organization and efferent projections. *Brain Res* **916**, 172-191.
- Aguilar-Roblero, R., Morin, L.P. and Moore, R.Y. (1994) Morphological correlates of circadian rhythm restoration induced by transplantation of the suprachiasmatic nucleus in hamsters. *Exp Neurol* **130**, 250-260.
- Aicher, S.A., Schreihof, A.M., Kraus, J.A., Sharma, S., Milner, T.A. and Guyenet, P.G. (2001) Mu-opioid receptors are present in functionally identified sympathoexcitatory neurons in the rat rostral ventrolateral medulla. *J Comp Neurol* **433**, 34-47.
- Airaksinen, M.S., Thoenen, H. and Meyer, M. (1997) Vulnerability of midbrain dopaminergic neurons in calbindin-D28k- deficient mice: lack of evidence for a neuroprotective role of endogenous calbindin in MPTP-treated and weaver mice. *Eur J Neurosci* **9**, 120-127.
- Akerstedt, T. (1995) Work hours, sleepiness and the underlying mechanisms. *J Sleep Res* **4**, 15-22.
- Araki, T. and Tohyama, M. (1992) Region-specific expression of GABAA receptor alpha 3 and alpha 4 subunits mRNAs in the rat brain. *Brain Res Mol Brain Res* **12**, 293-314.
- Aronin, N., Sagar, S.M., Sharp, F.R. and Schwartz, W.J. (1990) Light regulates expression of a Fos-related protein in rat suprachiasmatic nuclei. *Proc Natl Acad Sci U S A* **87**, 5959-5962.
- Arvanitogiannis, A., Robinson, B., Beaulieu, C. and Amir, S. (2000) Calbindin-D28k immunoreactivity in the suprachiasmatic nucleus and the circadian response to constant light in the rat. *Neuroscience* **99** (3):397-401.
- Baimbridge, K.G., Celio, M.R. and Rogers, J.H. (1992) Calcium-binding proteins in the nervous system. *Trends Neurosci* **15**, 303-308.
- Ban, Y., Shigeyoshi, Y. and Okamura, H. (1997) Development of vasoactive intestinal peptide mRNA rhythm in the rat suprachiasmatic nucleus. *J Neurosci* **17**, 3920-3931.
- Bartos, M., Vida, I., Frotscher, M., Geiger, J.R. and Jonas, P. (2001) Rapid signaling at inhibitory synapses in a dentate gyrus interneuron network. *J Neurosci* **21**, 2687-2698.

- Beaver, L.M., Gvakharia, B.O., Vollintine, T.S., Hege, D.M., Stanewsky, R. and Giebultowicz, J.M. (2002) Loss of circadian clock function decreases reproductive fitness in males of *Drosophila melanogaster*. *Proc Natl Acad Sci U S A* **99**, 2134-2139.
- Belluardo, N., Mud inverted question mark, G., Trovato-Salinaro, A., Le Gurun, S., Charollais, A., Serre-Beinier, V., Amato, G., Haefliger, J.A., Meda, P. and Condorelli, D.F. (2000) Expression of connexin36 in the adult and developing rat brain. *Brain Res* **865**, 121-138.
- Bennett, M.V., Barrio, L.C., Bargiello, T.A., Spray, D.C., Hertzberg, E. and Saez, J.C. (1991) Gap junctions: new tools, new answers, new questions. *Neuron* **6**, 305-320.
- Berggard, T., Miron, S., Onnerfjord, P., Thulin, E., Akerfeldt, K.S., Enghild, J.J., Akke, M. and Linse, S. (2002a) Calbindin D28k exhibits properties characteristic of a Ca²⁺ sensor. *J Biol Chem* **277**, 16662-16672.
- Berggard, T., Szczepankiewicz, O., Thulin, E. and Linse, S. (2002b) Myo-inositol monophosphatase is an activated target of calbindin D28k. *J Biol Chem* **277**, 41954-41959.
- Biello, S.M., Golombek, D.A., Schak, K.M. and Harrington, M.E. (1997) Circadian phase shifts to neuropeptide Y In vitro: cellular communication and signal transduction. *J Neurosci* **17**, 8468-8475.
- Bosler, O. (1989) Ultrastructural relationships of serotonin and GABA terminals in the rat suprachiasmatic nucleus. Evidence for a close interconnection between the two afferent systems. *J Neurocytol* **18**, 105-113.
- Bragin, A., Jando, G., Nadasdy, Z., Hetke, J., Wise, K. and Buzsaki, G. (1995) Gamma (40-100 Hz) oscillation in the hippocampus of the behaving rat. *J Neurosci* **15**, 47-60.
- Bryant, D.N., LeSauter, J., Silver, R. and Romero, M.T. (2000) Retinal innervation of calbindin-D28K cells in the hamster suprachiasmatic nucleus: ultrastructural characterization. *J Biol Rhythms* **15**, 103-111.
- Bunney, W.E. and Bunney, B.G. (2000) Molecular clock genes in man and lower animals: possible implications for circadian abnormalities in depression. *Neuropsychopharmacology* **22**, 335-345.
- Card, J.P. and Moore, R.Y. (1984) The suprachiasmatic nucleus of the golden hamster: immunohistochemical analysis of cell and fiber distribution. *Neuroscience* **13**, 415-431.
- Celio, M.R. (1990) Calbindin D-28k and parvalbumin in the rat nervous system. *Neuroscience* **35** (2):375-475.

- Chen, D., Hurst, W.J., Ding, J.M., Faiman, L.E., Mayer, B. and Gillette, M.U. (1997) Localization and characterization of nitric oxide synthase in the suprachiasmatic nucleus: evidence for a nitergic plexus in the biological clock. *J Neurochem* **68**, 855-861.
- Christie, M.J., Williams, J.T. and North, R.A. (1989) Electrical coupling synchronizes subthreshold activity in locus coeruleus neurons in vitro from neonatal rats. *J Neurosci* **9**, 3584-3589.
- Colwell, C.S. (2000) Rhythmic coupling among cells in the suprachiasmatic nucleus. *J Neurobiol* **43**, 379-388.
- Costantin, J.L. and Charles, A.C. (1999) Spontaneous action potentials initiate rhythmic intercellular calcium waves in immortalized hypothalamic (GT1-1) neurons. *J Neurophysiol* **82**, 429-435.
- Daan, S. and Aschoff, J. (1982) Circadian contributions to survival. In: Aschoff, J., Daan, S. and Groos, G., (Eds.) *Vertebrate Circadian Systems*, pp. 305-321. Berlin: Springer Verlag.
- Daikoku, S., Hisano, S. and Kagotani, Y. (1992) Neuronal associations in the rat suprachiasmatic nucleus demonstrated by immunoelectron microscopy. *J Comp Neurol* **325**, 559-571.
- Davis, F.C. and Gorski, R.A. (1988) Development of hamster circadian rhythms: role of the maternal suprachiasmatic nucleus. *J Comp Physiol* **162**, 601-610.
- de Jeu, M., Hermes, M. and Pennartz, C. (1998) Circadian modulation of membrane properties in slices of rat suprachiasmatic nucleus. *Neuroreport* **9**, 3725-3729.
- DeCoursey, P.J. and Buggy, J. (1989) Circadian rhythmicity after neural transplant to hamster third ventricle: specificity of suprachiasmatic nuclei. *Brain Res* **500**, 263-275.
- Ding, J.M., Chen, D., Weber, E.T., Faiman, L.E., Rea, M.A. and Gillette, M.U. (1994) Resetting the biological clock: mediation of nocturnal circadian shifts by glutamate and NO. *Science* **266**, 1713-1717.
- Dunlap, J.C. (1999) Molecular bases for circadian clocks. *Cell* **96**, 271-290.
- Erlander, M.G., Tillakaratne, N.J., Feldblum, S., Patel, N. and Tobin, A.J. (1991) Two genes encode distinct glutamate decarboxylases. *Neuron* **7**, 91-100.
- Fritschy, J.M. and Mohler, H. (1995) GABAA-receptor heterogeneity in the adult rat brain: differential regional and cellular distribution of seven major subunits. *J Comp Neurol* **359**, 154-194.

- Fritschy, J.M., Weinmann, O., Wenzel, A. and Benke, D. (1998) Synapse-specific localization of NMDA and GABA(A) receptor subunits revealed by antigen-retrieval immunohistochemistry. *J Comp Neurol* **390**, 194-210.
- Fukuda, T. and Kosaka, T. (2000) Gap junctions linking the dendritic network of GABAergic interneurons in the hippocampus. *J Neurosci* **20**, 1519-1528.
- Galarreta, M. and Hestrin, S. (2002) Electrical and chemical synapses among parvalbumin fast-spiking GABAergic interneurons in adult mouse neocortex. *Proc Natl Acad Sci U S A* **99**, 12438-12443.
- Galarreta, M. and Hestrin, S. (2001a) Electrical synapses between GABA-releasing interneurons. *Nat Rev Neurosci* **2**, 425-433.
- Galarreta, M. and Hestrin, S. (2001b) Spike transmission and synchrony detection in networks of GABAergic interneurons. *Science* **292**, 2295-2299.
- Gillespie, C.F., Mintz, E.M., Marvel, C.L., Huhman, K.L. and Albers, H.E. (1997) GABA(A) and GABA(B) agonists and antagonists alter the phase-shifting effects of light when microinjected into the suprachiasmatic region. *Brain Res* **759**, 181-189.
- Gillette, M.U. and Tischkau, S.A. (1999) Suprachiasmatic nucleus: the brain's circadian clock. *Recent Prog Horm Res* **54**, 33-58; discussion 58-9.
- Green, D.J. and Gillette, R. (1982) Circadian rhythm of firing rate recorded from single cells in the rat suprachiasmatic brain slice. *Brain Res* **245**, 198-200.
- Groos, G. and Hendriks, J. (1982) Circadian rhythms in electrical discharge of rat suprachiasmatic neurones recorded in vitro. *Neurosci Lett* **34**, 283-288.
- Gu, G., Varoqueaux, F. and Simerly, R.B. (1999) Hormonal regulation of glutamate receptor gene expression in the anteroventral periventricular nucleus of the hypothalamus. *J Neurosci* **19**, 3213-3222.
- Hamada, T., LeSauter, J., Venuti, J.M. and Silver, R. (2001) Expression of Period genes: rhythmic and nonrhythmic compartments of the suprachiasmatic nucleus pacemaker. *J Neurosci* **21**, 7742-7750.
- Hamada, T., LeSauter, J., Lokshin, M., Romero, M.T., Yan L.Y., Venuti, J.M. and Silver, R. (2002) Identification of a circadian mechanism for gating sensory input. *Society for Research on Biological Rhythms Abstract*, Program No. 29.
- Herzog, E.D., Geusz, M.E., Khalsa, S.B., Straume, M. and Block, G.D. (1997) Circadian rhythms in mouse suprachiasmatic nucleus explants on multimicroelectrode plates. *Brain Res* **757** (2):285-290.

- Herzog, E.D., Takahashi, J.S. and Block, G.D. (1998) Clock controls circadian period in isolated suprachiasmatic nucleus neurons. *Nat Neurosci* **1**, 708-713.
- Herzog, E.D. and Tosini, G. (2001) The mammalian circadian clock shop. *Semin Cell Dev Biol* **12**, 295-303.
- Honma, S., Kanematsu, N. and Honma, K. (1992) Entrainment of methamphetamine-induced locomotor activity rhythm to feeding cycles in SCN-lesioned rats. *Physiol Behav* **52**, 843-850.
- Honma, S., Shirakawa, T., Katsuno, Y., Namihira, M. and Honma, K. (1998) Circadian periods of single suprachiasmatic neurons in rats. *Neurosci Lett* **250**, 157-160.
- Honma, S., Shirakawa, T., Nakamura, W. and Honma, K. (2000) Synaptic communication of cellular oscillations in the rat suprachiasmatic neurons. *Neurosci Lett* **294**, 113-116.
- Ihaka, R. and Gentleman, R. (1999) R: A language for data analysis and graphics. *J Comp and Graphical Statistics* **5**, 299-314.
- Inouye, S.T. and Kawamura, H. (1979) Persistence of circadian rhythmicity in a mammalian hypothalamic "island" containing the suprachiasmatic nucleus. *Proc Natl Acad Sci U S A* **76**, 5962-5966.
- Jagota, A., de la Iglesia, H.O. and Schwartz, W.J. (2000) Morning and evening circadian oscillations in the suprachiasmatic nucleus in vitro. *Nat Neurosci* **3**, 372-376.
- Jiang, Z.G., Yang, Y.Q. and Allen, C.N. (1997) Tracer and electrical coupling of rat suprachiasmatic nucleus neurons. *Neuroscience* **77**, 1059-1066.
- Jiao, Y., Sun, Z., Lee, T., Fusco, F.R., Kimble, T.D., Meade, C.A., Cuthbertson, S. and Reiner, A. (1999) A simple and sensitive antigen retrieval method for free-floating and slide-mounted tissue sections. *J Neurosci Methods* **93**, 149-162.
- Jobst, E.E. and Allen, C.N. (2002) Calbindin neurons in the hamster suprachiasmatic nucleus do not exhibit a circadian variation in spontaneous firing rate. *Eur J Neurosci* **16**, 2469-2474.
- Jobst, E.E., Robinson, D.W. and Allen, C.N. (2003) Intercellular communication within the calbindin subnucleus of the hamster suprachiasmatic nucleus. Submitted to *Neuroscience*
- Johnson, C.H. (2001) Endogenous timekeepers in photosynthetic organisms. *Annu Rev Physiol* **63**, 695-728.
- Johnson, R.F., Morin, L.P. and Moore, R.Y. (1988) Retinohypothalamic projections in the hamster and rat demonstrated using cholera toxin. *Brain Res* **462**, 301-312.

- Jonas, E.A. and Kaczmarek, L.K. (1996) Regulation of potassium channels by protein kinases. *Curr Opin Neurobiol* **6**, 318-323.
- Kalsbeek, A. and Buijs, R.M. (2002) Output pathways of the mammalian suprachiasmatic nucleus: coding circadian time by transmitter selection and specific targeting. *Cell Tissue Res* **309**, 109-118.
- Kalsbeek, A., Teclemariam-Mesbah, R. and Pevet, P. (1993) Efferent projections of the suprachiasmatic nucleus in the golden hamster (*Mesocricetus auratus*). *J Comp Neurol* **332**, 293-314.
- Kaser, M.R., Lakshmanan, J. and Fisher, D.A. (1992) Comparison between epidermal growth factor, transforming growth factor- alpha and EGF receptor levels in regions of adult rat brain. *Brain Res Mol Brain Res* **16**, 316-322.
- Kawaguchi, Y. and Kubota, Y. (1993) Correlation of physiological subgroupings of nonpyramidal cells with parvalbumin- and calbindinD28k-immunoreactive neurons in layer V of rat frontal cortex. *J Neurophysiol* **70**, 387-396.
- Kim, Y.I. and Dudek, F.E. (1993) Membrane properties of rat suprachiasmatic nucleus neurons receiving optic nerve input. *J Physiol* **464**, 229-243.
- Kornblum, H.I., Gall, C.M., Seroogy, K.B. and Lauterborn, J.C. (1995) A subpopulation of striatal gabaergic neurons expresses the epidermal growth factor receptor. *Neuroscience* **69**, 1025-1029.
- Kornhauser, J.M., Nelson, D.E., Mayo, K.E. and Takahashi, J.S. (1990) Photic and circadian regulation of c-fos gene expression in the hamster suprachiasmatic nucleus. *Neuron* **5**, 127-134.
- Kramer, A., Yang, F.C., Snodgrass, P., Li, X., Scammell, T.E., Davis, F.C. and Weitz, C.J. (2001) Regulation of daily locomotor activity and sleep by hypothalamic EGF receptor signaling. *Science* **294**, 2511-2515.
- Kriegsfeld, L.J., LeSauter, J. and Silver, R. (2000) Regulation of circadian rhythms by a suprachiasmatic nucleus subregion. *Society for Neuroscience Abstract Program No.* **76.10**.
- Kuhlman, S.J., Silver, R., Le Sauter, J., Bult-Ito, A. and McMahon, D.G. (2003) Phase resetting light pulses induce Per1 and persistent spike activity in a subpopulation of biological clock neurons. *J Neurosci* **23**, 1441-1450.
- Lakin-Thomas, P.L. (2000) Circadian rhythms: new functions for old clock genes. *Trends Genet* **16**, 135-142.
- Leak, R.K., Card, J.P. and Moore, R.Y. (1999) Suprachiasmatic pacemaker organization analyzed by viral transsynaptic transport. *Brain Res* **819** (1-2):23-32.

- Leak, R.K. and Moore, R.Y. (2001) Topographic organization of suprachiasmatic nucleus projection neurons. *J Comp Neurol* **433**, 312-334.
- Leathers, V.L., Linse, S., Forsen, S. and Norman, A.W. (1990) Calbindin-D28K, a 1 alpha,25-dihydroxyvitamin D3-induced calcium-binding protein, binds five or six Ca²⁺ ions with high affinity. *J Biol Chem* **265**, 9838-9841.
- Lehman, M.N., Silver, R., Gladstone, W.R., Kahn, R.M., Gibson, M. and Bittman, E.L. (1987) Circadian rhythmicity restored by neural transplant. Immunocytochemical characterization of the graft and its integration with the host brain. *J Neurosci* **7**, 1626-1638.
- LeSauter, J., Kriegsfeld, L.J., Hon, J. and Silver, R. (2002) Calbindin-D(28K) cells selectively contact intra-SCN neurons. *Neuroscience* **111**, 575-585.
- LeSauter, J. and Silver, R. (1999) Localization of a suprachiasmatic nucleus subregion regulating locomotor rhythmicity. *J Neurosci* **19**, 5574-5585.
- LeSauter, J. and Silver, R. (1998) Output signals of the SCN. *Chronobiol Int* **15**, 535-550.
- Li, H. and Satinoff, E. (1998) Fetal tissue containing the suprachiasmatic nucleus restores multiple circadian rhythms in old rats. *Am J Physiol* **275**, R1735-1744.
- Li, X., Sankrithi, N. and Davis, F.C. (2002) Transforming growth factor-alpha is expressed in astrocytes of the suprachiasmatic nucleus in hamster: role of glial cells in circadian clocks. *Neuroreport* **13**, 2143-2147.
- Li, Z., Decavel, C. and Hatton, G.I. (1995) Calbindin-D28k: role in determining intrinsically generated firing patterns in rat supraoptic neurones. *J Physiol* **488** (Pt 3), 601-608.
- Liu, C. and Reppert, S.M. (2000) GABA synchronizes clock cells within the suprachiasmatic circadian clock. *Neuron* **25**, 123-128.
- Liu, C., Weaver, D.R., Strogatz, S.H. and Reppert, S.M. (1997) Cellular construction of a circadian clock: period determination in the suprachiasmatic nuclei. *Cell* **91**, 855-860.
- Lowenstein, D.H., Miles, M.F., Hatam, F. and McCabe, T. (1991) Up regulation of calbindin-D28K mRNA in the rat hippocampus following focal stimulation of the perforant path. *Neuron* **6**, 627-633.
- MacVicar, B.A. and Dudek, F.E. (1981) Electrotonic coupling between pyramidal cells: a direct demonstration in rat hippocampal slices. *Science* **213**, 782-785.

- Mai, J.K., Kedziora, O., Teckhaus, L. and Sofroniew, M.V. (1991) Evidence for subdivisions in the human suprachiasmatic nucleus. *J Comp Neurol* **305**, 508-525.
- Mason, R., Harrington, M.E. and Rusak, B. (1987) Electrophysiological responses of hamster suprachiasmatic neurones to neuropeptide Y in the hypothalamic slice preparation. *Neurosci Lett* **80** (2):173-179.
- Mehta, A.K. and Ticku, M.K. (1999) An update on GABAA receptors. *Brain Res Brain Res Rev* **29**, 196-217.
- Meijer, J.H., Rusak, B. and Ganshirt, G. (1992) The relation between light-induced discharge in the suprachiasmatic nucleus and phase shifts of hamster circadian rhythms. *Brain Res* **598**, 257-263.
- Meyer-Bernstein, E.L., Jetton, A.E., Matsumoto, S.I., Markuns, J.F., Lehman, M.N. and Bittman, E.L. (1999) Effects of suprachiasmatic transplants on circadian rhythms of neuroendocrine function in golden hamsters. *Endocrinology* **140**, 207-218.
- Mintz, E.M., Jasnow, A.M., Gillespie, C.F., Huhman, K.L. and Albers, H.E. (2002) GABA interacts with photic signaling in the suprachiasmatic nucleus to regulate circadian phase shifts. *Neuroscience* **109**, 773-778.
- Mistlberger, R.E. (1994) Circadian food-anticipatory activity: formal models and physiological mechanisms. *Neurosci Biobehav Rev* **18**, 171-195.
- Moga, M.M. and Moore, R.Y. (1997) Organization of neural inputs to the suprachiasmatic nucleus in the rat. *J Comp Neurol* **389**, 508-534.
- Monk, T.H. (2000) What can the chronobiologist do to help the shift worker? *J Biol Rhythms* **15**, 86-94.
- Moore, R.Y. (1996) Entrainment pathways and the functional organization of the circadian system. *Prog Brain Res* **111**, 103-119.
- Moore, R.Y. and Card, J.P. (1994) Intergeniculate leaflet: an anatomically and functionally distinct subdivision of the lateral geniculate complex. *J Comp Neurol* **344**, 403-430.
- Moore, R.Y. and Eichler, V.B. (1972) Loss of a circadian adrenal corticosterone rhythm following suprachiasmatic lesions in the rat. *Brain Res* **42**, 201-206.
- Moore, R.Y. and Silver, R. (1998) Suprachiasmatic nucleus organization. *Chronobiol Int* **15** (5):475-487.
- Moore, R.Y. and Speh, J.C. (1993) GABA is the principal neurotransmitter of the circadian system. *Neurosci Lett* **150**, 112-116.

- Moore, R.Y., Speth, J.C. and Leak, R.K. (2002) Suprachiasmatic nucleus organization. *Cell Tissue Res* **309**, 89-98.
- Morin, L.P. and Blanchard, J.H. (2001) Neuromodulator content of hamster intergeniculate leaflet neurons and their projection to the suprachiasmatic nucleus or visual midbrain. *J Comp Neurol* **437**, 79-90.
- Morin, L.P. and Wood, R.I. (2001) *A stereotaxic atlas of the golden hamster brain*, First ed. San Diego: Academic Press.
- Nakamura, W., Honma, S., Shirakawa, T. and Honma, K. (2001) Regional pacemakers composed of multiple oscillator neurons in the rat suprachiasmatic nucleus. *Eur J Neurosci* **14**, 666-674.
- Naum, O. G, Fernanda Rubio, M. and Golombek, D.A. (2001) Rhythmic variation in gamma-aminobutyric acid(A)-receptor subunit composition in the circadian system and median eminence of Syrian hamsters. *Neurosci Lett* **310**, 178-182.
- O'Hara, B.F., Andretic, R., Heller, H.C., Carter, D.B. and Kilduff, T.S. (1995) GABAA, GABAC, and NMDA receptor subunit expression in the suprachiasmatic nucleus and other brain regions. *Brain Res Mol Brain Res* **28**, 239-250.
- Obrietan, K., Impey, S. and Storm, D.R. (1998) Light and circadian rhythmicity regulate MAP kinase activation in the suprachiasmatic nuclei. *Nat Neurosci* **1**, 693-700.
- Okamura, H., Berod, A., Julien, J.F., Geffard, M., Kitahama, K., Mallet, J. and Bobillier, P. (1989) Demonstration of GABAergic cell bodies in the suprachiasmatic nucleus: in situ hybridization of glutamic acid decarboxylase (GAD) mRNA and immunocytochemistry of GAD and GABA. *Neurosci Lett* **102**, 131-136.
- Okamura, H., Kawakami, F., Tamada, Y., Geffard, M., Nishiwaki, T., Ibata, Y. and Inouye, S.T. (1995) Circadian change of VIP mRNA in the rat suprachiasmatic nucleus following p-chlorophenylalanine (PCPA) treatment in constant darkness. *Brain Res Mol Brain Res* **29**, 358-364.
- Ouyang, Y., Andersson, C.R., Kondo, T., Golden, S.S. and Johnson, C.H. (1998) Resonating circadian clocks enhance fitness in cyanobacteria. *Proc Natl Acad Sci U S A* **95**, 8660-8664.
- Paxinos, G. and Watson, C. (1996) *The rat brain in stereotaxic coordinates*, Third ed. New York : Academic Press.
- Peinado, A., Yuste, R. and Katz, L.C. (1993) Extensive dye coupling between rat neocortical neurons during the period of circuit formation. *Neuron* **10**, 103-114.
- Pennartz, C.M., Bos, N.P., Jeu, M.T., Geurtsen, A.M., Mirmiran, M., Sluiter, A.A. and Buijs, R.M. (1998) Membrane properties and morphology of vasopressin neurons in slices of rat suprachiasmatic nucleus. *J Neurophysiol* **80**, 2710-2717.

- Pennartz, C.M., de Jeu, M.T., Bos, N.P., Schaap, J. and Geurtsen, A.M. (2002) Diurnal modulation of pacemaker potentials and calcium current in the mammalian circadian clock. *Nature* **416**, 286-290.
- Peppelenbosch, M.P., Tertoolen, L.G. and de Laat, S.W. (1991) Epidermal growth factor-activated calcium and potassium channels. *J Biol Chem* **266**, 19938-19944.
- Pinault, D. (1996) A novel single-cell staining procedure performed in vivo under electrophysiological control: morpho-functional features of juxtacellularly labeled thalamic cells and other central neurons with biocytin or Neurobiotin. *J Neurosci Methods* **65**, 113-136.
- Pittendrigh, C.S. (1993) Temporal organization: reflections of a Darwinian clock-watcher. *Annu Rev Physiol* **55**, 16-54.
- Pittendrigh, C.S. and Minis, D.H. (1972) Circadian systems: longevity as a function of circadian resonance. *Proceedings of Nat. Acad. Sci. USA* **69**, 1537-1539.
- Presser, H. (1999) Toward a 24-hr economy. *Science* **284**, 1778-1779.
- Prosser, R.A. and Gillette, M.U. (1989) The mammalian circadian clock in the suprachiasmatic nuclei is reset in vitro by cAMP. *J Neurosci* **9**, 1073-1081.
- Ralph, M.R., Foster, R.G., Davis, F.C. and Menaker, M. (1990) Transplanted suprachiasmatic nucleus determines circadian period. *Science* **247**, 975-978.
- Ralph, M.R. and Menaker, M. (1989) GABA regulation of circadian responses to light. I. Involvement of GABAA-benzodiazepine and GABAB receptors. *J Neurosci* **9**, 2858-2865.
- Ralph, M.R. and Menaker, M. (1988) A mutation of the circadian system in golden hamsters. *Science* **241**, 1225-1227.
- Ramsey, F. and Schafer, D. (1997) *The Statistical Sleuth: a course in methods of data analysis*, Belmont, CA: Wadsworth Publishing Company.
- Rash, J.E., Yasumura, T., Dudek, F.E. and Nagy, J.I. (2001) Cell-specific expression of connexins and evidence of restricted gap junctional coupling between glial cells and between neurons. *J Neurosci* **21**, 1983-2000.
- Reppert, S.M. and Weaver, D.R. (2002) Coordination of circadian timing in mammals. *Nature* **418**, 935-941.
- Rosenthal, N.E. (1993) *Winter Blues: Seasonal Affective Disorder*, New York, USA: Guilford Press.

- Rusak, B., Robertson, H.A., Wisden, W. and Hunt, S.P. (1990) Light pulses that shift rhythms induce gene expression in the suprachiasmatic nucleus. *Science* **248**, 1237-1240.
- Rusak, B. and Zucker, I. (1979) Neural regulation of circadian rhythms. *Physiol Rev* **59**, 449-526.
- Rutter, J., Reick, M. and McKnight, S.L. (2002) Metabolism and the control of circadian rhythms. *Annu Rev Biochem* **71**, 307-331.
- Saeb-Parsy, K. and Dyball, R.E. (2003) Defined cell groups in the rat suprachiasmatic nucleus have different day/night rhythms of single-unit activity in vivo. *J Biol Rhythms* **18**, 26-42.
- Schaap, J., Bos, N.P., de Jeu, M.T., Geurtsen, A.M., Meijer, J.H. and Pennartz, C.M. (1999) Neurons of the rat suprachiasmatic nucleus show a circadian rhythm in membrane properties that is lost during prolonged whole-cell recording. *Brain Res* **815**, 154-166.
- Schwartz, W.J. (1991) Further evaluation of the tetrodotoxin-resistant circadian pacemaker in the suprachiasmatic nuclei. *J Biol Rhythms* **6**, 149-158.
- Schwartz, W.J., Coleman, R.J. and Reppert, S.M. (1983) A daily vasopressin rhythm in rat cerebrospinal fluid. *Brain Res* **263**, 105-112.
- Schwartz, W.J., Davidsen, L.C. and Smith, C.B. (1980) In vivo metabolic activity of a putative circadian oscillator, the rat suprachiasmatic nucleus. *J Comp Neurol* **189**, 157-167.
- Schwartz, W.J. and Gainer, H. (1977) Suprachiasmatic nucleus: use of ¹⁴C-labeled deoxyglucose uptake as a functional marker. *Science* **197**, 1089-1091.
- Schwartz, W.J., Gross, R.A. and Morton, M.T. (1987) The suprachiasmatic nuclei contain a tetrodotoxin-resistant circadian pacemaker. *Proc Natl Acad Sci U S A* **84**, 1694-1698.
- Schwartz, W.J. and Reppert, S.M. (1985) Neural regulation of the circadian vasopressin rhythm in cerebrospinal fluid: a pre-eminent role for the suprachiasmatic nuclei. *J Neurosci* **5**, 2771-2778.
- Seroogy, K.B., Numan, S., Gall, C.M., Lee, D.C. and Kornblum, H.I. (1994) Expression of EGF receptor mRNA in rat nigrostriatal system. *Neuroreport* **6**, 105-108.
- Shibata, S., Oomura, Y., Kita, H. and Hattori, K. (1982) Circadian rhythmic changes of neuronal activity in the suprachiasmatic nucleus of the rat hypothalamic slice. *Brain Res* **247** (1):154-158.

- Shigeyoshi, Y., Taguchi, K., Yamamoto, S., Takekida, S., Yan, L., Tei, H., Moriya, T., Shibata, S., Loros, J.J., Dunlap, J.C. and Okamura, H. (1997) Light-induced resetting of a mammalian circadian clock is associated with rapid induction of the mPer1 transcript. *Cell* **91**, 1043-1053.
- Shinohara, K., Hiruma, H., Funabashi, T. and Kimura, F. (2000) GABAergic modulation of gap junction communication in slice cultures of the rat suprachiasmatic nucleus. *Neuroscience* **96**, 591-596.
- Siegelbaum, S.A. (1994) Channel regulation. Ion channel control by tyrosine phosphorylation. *Curr Biol* **4**, 242-245.
- Silver, R., Lehman, M.N., Gibson, M., Gladstone, W.R. and Bittman, E.L. (1990) Dispersed cell suspensions of fetal SCN restore circadian rhythmicity in SCN-lesioned adult hamsters. *Brain Res* **525**, 45-58.
- Silver, R., LeSauter, J., Tresco, P.A. and Lehman, M.N. (1996a) A diffusible coupling signal from the transplanted suprachiasmatic nucleus controlling circadian locomotor rhythms. *Nature* **382**, 810-813.
- Silver, R., Romero, M.T., Besmer, H.R., Leak, R., Nunez, J.M. and LeSauter, J. (1996b) Calbindin-D28K cells in the hamster SCN express light-induced Fos. *Neuroreport* **7**, 1224-1228.
- Smith, L., Folkard, S. and Poole, C.J. (1994) Increased injuries on night shift. *Lancet* **344**, 1137-1139.
- Sollars, P.J. and Pickard, G.E. (1998) Restoration of circadian behavior by anterior hypothalamic grafts containing the suprachiasmatic nucleus: graft/host interconnections. *Chronobiol Int* **15**, 513-533.
- Stamler, J.S., Simon, D.I., Osborne, J.A., Mullins, M.E., Jarak, O., Michel, T., Singel, D.J. and Loscalzo, J. (1992) S-nitrosylation of proteins with nitric oxide: synthesis and characterization of biologically active compounds. *Proc Natl Acad Sci U S A* **89**, 444-448.
- Stephan, F.K. and Zucker, I. (1972) Circadian rhythms in drinking behavior and locomotor activity of rats are eliminated by hypothalamic lesions. *Proc Natl Acad Sci U S A* **69**, 1583-1586.
- Suissa, S. and Shuster, J. (1985) Exact Unconditional Test. Sample sizes for the 2 X 2 binomial trial. *Journal of Royal Statistical Society* **148**, 317-327.
- Takahashi, Y., Okamura, H., Yanaihara, N., Hamada, S., Fujita, S. and Ibata, Y. (1989) Vasoactive intestinal peptide immunoreactive neurons in the rat suprachiasmatic nucleus demonstrate diurnal variation. *Brain Res* **497**, 374-377.

- Tamas, G., Buhl, E.H., Lorincz, A. and Somogyi, P. (2000) Proximally targeted GABAergic synapses and gap junctions synchronize cortical interneurons. *Nat Neurosci* **3**, 366-371.
- Tao, L., Murphy, M.E. and English, A.M. (2002) S-nitrosation of Ca(2+)-loaded and Ca(2+)-free recombinant calbindin D(28K) from human brain. *Biochemistry* **41**, 6185-6192.
- Thomson, A.M. and West, D.C. (1990) Factors affecting slow regular firing in the suprachiasmatic nucleus in vitro. *J Biol Rhythms* **5**, 59-75.
- Toh, K.L., Jones, C.R., He, Y., Eide, E.J., Hinz, W.A., Virshup, D.M., Ptacek, L.J. and Fu, Y.H. (2001) An hPer2 phosphorylation site mutation in familial advanced sleep phase syndrome. *Science* **291**, 1040-1043.
- Trexler, E.B., Li, W., Mills, S.L. and Massey, S.C. (2001) Coupling from AII amacrine cells to ON cone bipolar cells is bidirectional. *J Comp Neurol* **437**, 408-422.
- Ueda, S., Kawata, M. and Sano, Y. (1983) Identification of serotonin- and vasopressin immunoreactivities in the suprachiasmatic nucleus of four mammalian species. *Cell Tissue Res* **234**, 237-248.
- United States of America Congress. (1991) *Biological Rhythms: Implications for the worker*. Washington, D.C.: U.S. Government Printing Office.
- van den Pol, A.N. (1980) The hypothalamic suprachiasmatic nucleus of rat: intrinsic anatomy. *J Comp Neurol* **191**, 661-702.
- van den Pol, A.N. and Dudek, F.E. (1993) Cellular communication in the circadian clock, the suprachiasmatic nucleus. *Neuroscience* **56**, 793-811.
- van den Pol, A.N. and Tsujimoto, K.L. (1985) Neurotransmitters of the hypothalamic suprachiasmatic nucleus: immunocytochemical analysis of 25 neuronal antigens. *Neuroscience* **15**, 1049-1086.
- van den Pol, A. (1991) The suprachiasmatic nucleus: morphological and cytochemical substrates for cellular interaction. In: Klein, D., Moore, R. and Reppert, S., (Eds.) *Suprachiasmatic Nucleus: The Mind's Clock*, New York: Oxford University Press.
- Warren, E., Allen, C., Brown, R. and Robinson, D. (2003) Intrinsic light responses of retinal ganglion cells projecting to the circadian system. *Eur J Neurosci*, in press.
- Watts, A.G. and Swanson, L.W. (1987) Efferent projections of the suprachiasmatic nucleus: II. Studies using retrograde transport of fluorescent dyes and simultaneous peptide immunohistochemistry in the rat. *J Comp Neurol* **258**, 230-252.

- Welsh, D.K., Logothetis, D.E., Meister, M. and Reppert, S.M. (1995) Individual neurons dissociated from rat suprachiasmatic nucleus express independently phased circadian firing rhythms. *Neuron* **14**, 697-706.
- Welsh, D.K. and Reppert, S.M. (1996) Gap junctions couple astrocytes but not neurons in dissociated cultures of rat suprachiasmatic nucleus. *Brain Res* **706**, 30-36.
- Wisden, W., Laurie, D.J., Monyer, H. and Seeburg, P.H. (1992) The distribution of 13 GABAA receptor subunit mRNAs in the rat brain. I. Telencephalon, diencephalon, mesencephalon. *J Neurosci* **12**, 1040-1062.
- Yamazaki, S., Kerbeshian, M.C., Hocker, C.G., Block, G.D. and Menaker, M. (1998) Rhythmic properties of the hamster suprachiasmatic nucleus in vivo. *J Neurosci* **18** (24):10709-10723.
- Yamazaki, S., Numano, R., Abe, M., Hida, A., Takahashi, R., Ueda, M., Block, G.D., Sakaki, Y., Menaker, M. and Tei, H. (2000) Resetting central and peripheral circadian oscillators in transgenic rats. *Science* **288**, 682-685.
- Yan, L. and Silver, R. (2002) Differential induction and localization of mPer1 and mPer2 during advancing and delaying phase shifts. *Eur J Neurosci* **16**, 1531-1540.